General Disclaimer

One or more of the Following Statements may affect this Document

- This document has been reproduced from the best copy furnished by the organizational source. It is being released in the interest of making available as much information as possible.

- This document may contain data, which exceeds the sheet parameters. It was furnished in this condition by the organizational source and is the best copy available.

- This document may contain tone-on-tone or color graphs, charts and/or pictures, which have been reproduced in black and white.

- This document is paginated as submitted by the original source.

- Portions of this document are not fully legible due to the historical nature of some of the material. However, it is the best reproduction available from the original submission.

School of
ENGINEERING
DUKE UNIVERSITY

DESIGN OF ENERGY STORAGE REACTORS
FOR DC-TO-DC CONVERTERS

by

De Yu Chen

DESIGN OF ENERGY STORAGE REACTORS
FOR DC-TO-DC CONVERTERS

by

De Yu Chen

August 18, 1975

for

NATIONAL AERONAUTICS AND SPACE ADMINISTRATION

DESIGN OF ENERGY STORAGE REACTORS
FOR DC-TO-DC CONVERTERS

BY

De Yu Chen

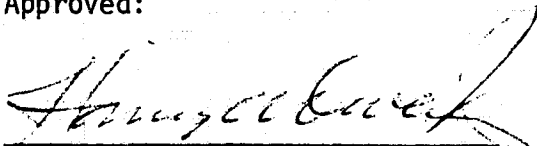Department of Electrical Engineering
Duke University

Date: _Cccgcct /t, /675_

Approved:

Harry A. Owen, Supervisor

A dissertation submitted in partial fulfillment of
the requirements for the degree of Doctor of
Philosophy in the Department of Electrical
Engineering in the Graduate School of
Arts and Sciences of Duke University

1975

ABSTRACT

(Electrical Engineering)

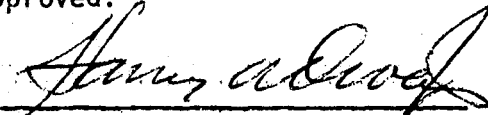DESIGN OF ENERGY STORAGE REACTORS
FOR DC-TO-DC CONVERTERS

by

De Yu Chen

Department of Electrical Engineering
Duke University

Date: *August 18, 1975*

Approved:

Harry A. Owen

Harry A. Owen, Jr. Supervisor

Thomas G Wilson

W. T. Joines

C. R. S.

ABSTRACT

In recent years, energy-storage dc-to-dc converters have been widely used in power-conditioning applications. These converters usually employ energy-storage reactors to store and transfer energy in some controlled manner. The design of these reactors is a crucial step in the design of the converter as a whole, however, these designs usually are performed on a trial-and-error basis with little analytical guidance available. This dissertation presents two methodical approaches to the design of energy-storage reactors for a group of widely used dc-to-dc converters.

One of these approaches is based on a steady-state time-domain analysis of piecewise-linearized circuit models of the converters, while the other approach is based on an analysis of the same circuit models, but from an energy point of view. The design procedure developed from the first approach includes a search through a stored data file of magnetic core characteristics and results in a list of usable reactor designs which meet a particular converter's requirements. Because of the complexity of this procedure, a digital computer usually is used to implement the design algorithm. The second approach, based on a study of the storage and transfer of energy in the magnetic reactors, leads to a relatively simple and straightforward design procedure which can be implemented rather quickly with hand calculations. The heart of this procedure is a specially constructed table of magnetic core characteristics. This procedure does not provide the designer

(iii)

with as much information as the first approach does, but it does provide an easy way to quickly reach a workable design and is particularly useful when the design has to be done by hand calculations or with a small calculator. In short, both of these approaches have individual merits and can serve as complements to each other.

In addition to the design procedures described above, an equation which can be easily used to quickly determine the lower-bound volume of workable cores for given converter design specifications is derived. Using this computed lower-bound volume, a comparative evaluation of various converter configurations is presented. This comparison provides some guidance for choosing a particular converter configuration from among the various configurations available. It is believed that this analytical guidance in conjunction with design procedures presented in this dissertation can significantly reduce the time, and hence the cost, of designing energy-storage reactors in dc-to-dc converters.

ACKNOWLEDGEMENTS

I would like to express my deepest appreciation to Dr. Harry A. Owen, Jr., and Dr. Thomas G. Wilson, both my professors, for their guidance and encouragement throughout the course of my graduate study. Their advice and efforts have been most important in the development and in the writing of this dissertation.

I would also like to thank Mr. Trey Burns, my colleague, for his proofreadings of this dissertation; Mr. Jimmy Hartley, laboratory assistant, for his drafting work, and to Mrs. Joyce Pate for her typing.

Finally, I would like to express my gratitude to my wife and my parents for their help, understanding, and encouragement during the course of my graduate study.

De Yu Chen

(v)

CONTENTS

LIST OF FIGURES

LIST OF TABLES

LIST OF TABLES CONT.

DESIGN OF ENERGY-STORAGE REACTORS
FOR DC-TO-DC CONVERTERS

Chapter I

INTRODUCTION

Magnetic-energy-storage static dc-to-dc converters have been widely used in regulated dc-to-dc power conversion applications. Because of their small size, light weight, and high efficiency, they are particularly well-suited for aerospace applications. These converters usually can be classified in one of four basic categories: (A) single-winding voltage step-up converters which are capable of stepping up the input voltage; (B) single-winding current step-up converters which are capable of stepping up the input current; (C) single-winding voltage step-up/current step-up converters which are capable of stepping up either the input voltage or the input current; and (D) two-winding voltage step-up/current step-up converters. Any one of three different types of controllers-- constant frequency, constant on-time and constant off-time-- can be used to regulate the output voltage of these various types of converter. One of the most important elements in each of these converter configurations is a magnetic reactor which is used for energy storage and transfer. These reactors usually are a major portion of the total weight and volume of the converters and consequently minimizing the size is often an important consideration in many applications. In the past, reactors for dc-to-dc converters usually have been designed on a trial-and-error basis where experience and intuition are the primary design tool, with little analytical guidance available except for a few particular

(2)

converter types [1,2]. This dissertation, motivated by Ref. [2], presents an analysis-based systematic approach to the design of energy-storage reactors for a group of widely used dc-to-dc converters.

The purpose of this dissertation is three-fold:

(1) to establish analytical relationships between various converter parameters which lead to design procedures for the energy-storage reactors in dc-to-dc converters.

(2) to demonstrate the feasibility of computer-aided procedures for designing reactors in dc-to-dc converters.

(3) to present a simple and direct method for designing these energy-storage reactors, which can be used when the design has to be made by hand calculations.

This dissertation is based on material presented in a series of publications [3,4,5,6, and 7] of which the writer is the principal author.

Chapter II presents the derivation of design equations which lead to systematic procedures for designing the energy-storage reactors for nine controller-converter combinations. These equations and the subsequent procedures are based on a time-domain analysis of each of the converter configurations. A similar approach is followed in Chapter III to develop procedures for designing the reactors for three two-winding controller-converter combinations. The presence of two windings on the reactors of these converters not only makes it possible to achieve input-output conductive isolation but it also provides additional flexibility in the reactor design which is not available in single-winding converters. By utilizing the extra freedom provided by the additional winding, ten converter design or performance constraints are presented which enable incorporating additional design objectives into the procedure.

The design procedures presented in Chapters II and III can be implemented by hand calculations, but because of the complexity of the procedure, a digital computer is usually used to implement the design algorithm. These design procedures include searching through a stored data file of magnetic core specifications to yield a list of designs which meet a particular converter specification. This search process usually begins with the smallest available core size and proceeds toward the largest size in the catalog. For a given converter specification, no knowledge of the required size of workable cores is immediately available. Thus, the search process can be very time-consuming when the procedure is followed with hand calculations.

In Chapter IV, a constraint relationship on the converter core volume is established. This constraint relationship is expressed in terms of a lower-bound condition on core volume, and is derived from an analysis of the various converters from an energy point of view. The lower-bound condition enables the designer to quickly screen the population of available reactor cores to determine those cores which are candidates for a particular design specification, thereby greatly simplifying the search process. Using this lower bound condition and some results obtained in Chapters II and III, a new procedure for designing the energy-storage reactors for dc-to-dc converters is developed in Chapter V. The heart of this procedure is a special table of core parameters which are calculated from data provided by magnetic core manufacturers.

By utilizing this special table and the lower-bound condition developed in Chapter IV, the core search process is reduced to a methodical table search. This procedure does not require repetitive trial designs and thus can be carried out rather quickly with hand calculations.

Conclusions which can be drawn from this work are presented in

Chapter VI with suggestions for future research. The derivations of some
of the more important analytical expressions presented in the text are
outlined in the Appendices. The International System of Units (SI) is
used throughout, and a glossary of symbols and their associated units
is placed at the end of this dissertation.

Chapter II

DESIGN OF ENERGY-STORAGE REACTORS FOR
SINGLE-WINDING DC-TO-DC CONVERTERS

2.1 Introduction

The three single-winding converters considered in the dissertation
are shown in Fig. 2.1 [8]. The circuit in Fig. 2.1(A) is the voltage step-up
configuration, which has an average output voltage V_0 higher than the dc
input voltage V_I, and is designated as VU. Fig. 2.1(B) shows the current
step-up configuration designated as CU which has an output current I_0 higher
than the average input current I_I and an output voltage V_0 lower than the
input voltage V_I. The voltage step-up/current step-up configuration in
Fig. 2.1(C) can either step up or step down the output voltage while simul-
taneously supplying an output current that is lower or higher, respectively,
than the average source input current. This configuration is identified by
UD, standing for up-down. Each converter consists of an energy-storage re-
actor, a filter capacitor, a power transistor switch, a free wheeling-diode,
and a controller which controls the duty cycle of the power transistor.
Three type of controllers -- constant frequency, constant on-time, and con-
stant off-time -- are often used to pulse modulate the power transistor to
achieve output voltage regulation. The constant frequency controller pro-
duces a pulse of appropriate width and constant frequency to drive the power
transistor; the constant on-time controller and constant off-time controller

(6)
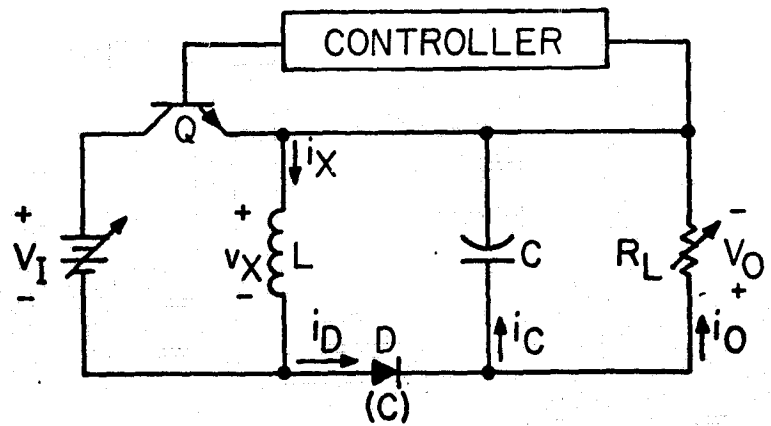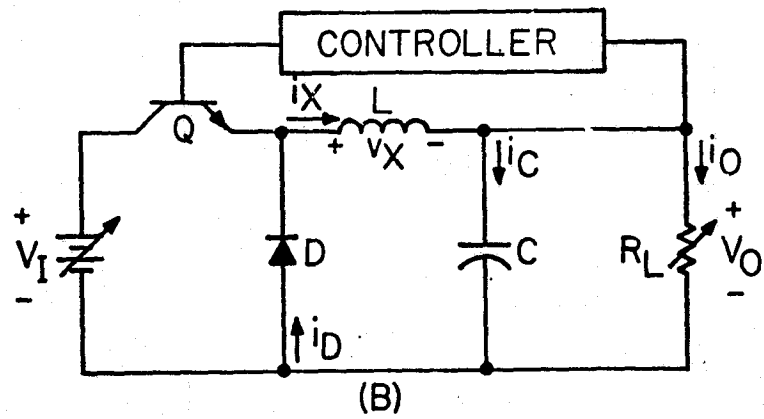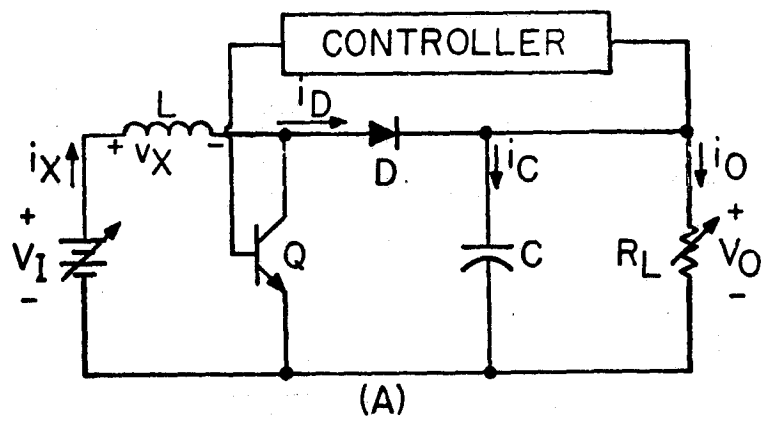
Figure 2.1(A) Single-winding voltage step-up converter (VU)

(B) Single-winding current step-up converter (CU)

(C) Single-winding voltage step-up/current step-up converter (UD)

produce pulses to drive the power transistor, respectively, for fixed transistor on-time and fixed transistor off-time.

The primary objective in the design of energy storage reactors for dc-to-dc converters is to select a suitable magnetic core, determine the number of turns and size of the winding wire such that the converter is capable of providing a regulated output voltage over a specified range of input voltage and output power.

This chapter, based heavily on Ref. [3], presents equations and procedures for designing the reactors for the three single-winding converters in conjunction with the three controller types.

2.2 Circuit Analysis

The design procedures are developed from time-domain analyses of piecewise-linearized models of the power section of the three converter types. The power transistor and diode in each of these converters operate as switches. When the transistor is conducting, the diode is cut off, and the energy supplied by the input source is stored in the reactor core. The energy stored in the core during the transistor on-time is released through the diodes to supply the load during the time when the transistor is cut off. The flux density in the magnetic core cycles between the values B_A and B_B, the minimum and the maximun values of the excursion in steady state for a given set of operating conditions. Analysis of each of the three converter types yields equations for B_A and B_B according to the type of controller employed in the feedback path of the closed-loop regulated converter. These two sets of equations form the bases of design algorithms from which the number of turns N is computed and from which the various currents are found.

2.2.1 Modes of Operation

Two modes of operation are possible for each of the three circuit configurations, depending on the nature of the cyclic excursion of core flux density. The core material for the inductor is assumed to have a linear B versus H characteristic, such as shown in Fig. 2.2, where B_S is the saturation flux density, B_R the residual flux density, and B_A and B_B represent, respectively, the minimum and maximum values of the cyclic flux-density excursion of the core at any particular set of circuit operating conditions. In Mode 1 operation, the flux in the core is, at all times, moving either upward toward B_S during a time interval t_{on} or downward toward B_R during time interval t'_{off}; in other words, $B_A \geq B_R$ and $B_B \leq B_S$. In Mode 2 operation, the flux in the core resides for a finite period of time t''_{off} at the residual value; in other words, $B_A = B_R$ for a time t''_{off} during each cycle. Mode 1 is often referred as the continuous conduction mode and Mode 2 as the discontinuous conduction mode.

2.2.2 Assumptions

The three circuit configurations are analyzed under the following six assumptions. 1) The transistors and diodes act as switches with constant forward voltage drops of V_Q and V_D, respectively, and infinite reverse resistances. 2) The magnetic cores of inductors L are operated in the linear range with constant permeability $\mu = \Delta B / \Delta H$. 3) The filter capacitors C are so large that the output voltage has negligible ripple. 4) The controller controlling the duty cycle of the transistors are perfect, drawing zero current from the load and operating with zero time delay. 5) The unregulated input voltages V_I are always larger than transistor saturation voltage drops V_Q. 6) The resistances of the windings are neglected during the design process.
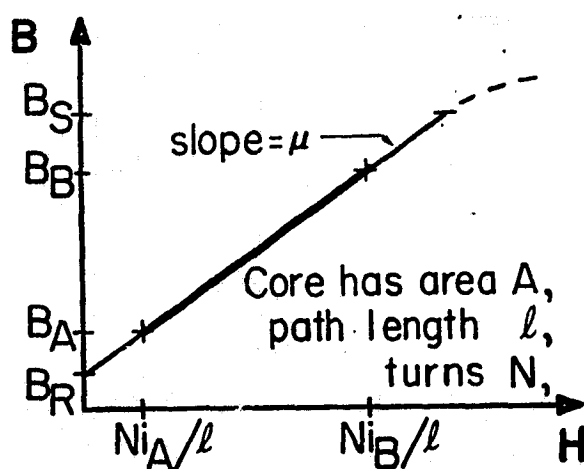
Figure 2.2 Magnetic core characteristic

2.3 Design Information

Using the assumptions made in the last section, circuit equations will be written and certain general relationships developed. Attention will then be focused on Mode 1 operation, and waveforms of current, voltage, and flux density will be presented for each converter configuration, which are applicable for any one of the three types of controllers considered. Design equations for Mode 1 operation will then developed for each of the nine combinations of converter and controller. Following a similar procedure, Mode 2 operation will then be considered and nine sets of design relationships applicable to this operation mode will be developed.

Instead of discussing and deriving relationships for each of the eighteen cases individually, information will be presented in the form of tables with equation numbers coded so that parallel relationships can be identified, as well as specific ones. For example, referring to Table 2.1 (6) refers to all three of the equations for t_{on}/t'_{off} in the row containing the symbol (6), whereas (6,CU) refers to the specific equation $t_{on}/t'_{off} = (V_0+V_D)/(V_I-V_0-V_Q)$ applicable only to a current step-up converter.

Table 2.1 presents general relationships for the three configurations. These relationships are independent of the mode of operation and the controller used. Equations for inductor current i_X and capacitor current i_C are presented for the time interval t_{on} that Q is saturated and the flux density in the core is increasing from B_A to B_B in Equation (1) and (2), and the interval t'_{off} that Q is cut off and the flux density is decreasing from B_B to B_A in (3) and (4). An additional time interval t''_{off} occurs in Mode 2 operation when the flux density remains constant at $B=B_A=B_R$ for a finite portion of each cycle. The total period T is defined in (5). Equating the increase and decrease of reactor current from (1) and (3) leads to the time relationship

Table 2.1 General Characteristics of the Three
Single-Winding Converters

		VOLTAGE STEP-UP CONVERTER (VU)	CURRENT STEP-UP CONVERTER (CU)	VOLTAGE STEP-UP/CURRENT STEP-UP CONVERTER (UD)
CIRCUIT EQUATIONS	DURING t_{on}	$L\frac{di_x}{dt} = V_I - V_Q$ (1,VU) $i_c = -I_0$ (2)	$L\frac{di_x}{dt} = V_I - V_0 - V_Q$ (1,CU) $i_c = i_x - I_0$	$L\frac{di_x}{dt} = V_I - V_Q$ (1,UD) $i_c = -I_0$
	DURING t'_{off}	$L\frac{di_x}{dt} = V_I - V_0 - V_D$ (3) $i_c = i_x - I_0$ (4)	$L\frac{di_x}{dt} = -V_0 - V_D$ $i_c = i_x - I_0$	$L\frac{di_x}{dt} = -V_0 - V_D$ $i_c = i_x - I_0$
TIME RELATIONSHIPS		$T = t_{on} + t'_{off} + t''_{off}$ $= t_{on} + t_{off}$ (5)	$T = t_{on} + t'_{off} + t''_{off}$ $= t_{on} + t_{off}$	$T = t_{on} + t'_{off} + t''_{off}$ $= t_{on} + t_{off}$
		$\frac{t_{on}}{t'_{off}} = \frac{V_0 + V_D - V_I}{V_I - V_Q}$ (6)	$\frac{t_{on}}{t'_{off}} = \frac{V_0 + V_D}{V_I - V_0 - V_Q}$	$\frac{t_{on}}{t'_{off}} = \frac{V_0 + V_D}{V_I - V_Q}$
AVERAGE REACTOR CURRENT		$I_X = \frac{P_0}{V_0}\frac{V_0 + V_D - V_Q}{V_I - V_Q}$ (7)	$I_X = \frac{P_0}{V_0}$	$I_X = \frac{P_0}{V_0}\frac{V_I + V_0 + V_D - V_Q}{V_I - V_Q}$

(6). Using (5) and (6), the fact that the average value of capacitor current must be zero, and that $P_0 = V_0 I_0$, the average value of reactor current I_X for Mode 1 or Mode 2 operation is given by (7).

(A) Mode 1

Considering now only mode 1 operation, three expressions-(8), (9), and (10)-are given at the top of Table2.2, relating the time intervals t_{on}, t''_{off}, and T. Also given in the table are sketches of waveshapes of inductor current i_X, input current i_I, capacitor current i_C, diode current i_D, flux density B, and voltage across the inductor V_X for all three basic converter configurations.

Table 2.3, because of the length of some of the expressions, is arranged in three parts, A, B, and C. However, the pattern of presentation and numbering of equations follow the same format as in the other tables. Table 2.3 gives the design relationships for each of the three basic converter configurations when driven by a constant frequency controller, a constant on-time controller, and a constant off-time controller. The first expression for each of the nine converter-controller combinations gives values for the peak flux-density excursion B_B and the minimum flux-density excursion B_A for any particular set of operating conditions V_I, V_0, and P_0, semiconductor parameters V_D and V_Q, inductor parameters N, μ, B_R, ℓ, and A, and conversion-frequency period T. The plus sign is to be used for B_B and the minus sign for B_A. This expression is obtained by recognizing that B_B, $B_A = B_{av} \pm (\Delta B/2)$ where $B_{av} = B_R + (\mu N I_X/\ell)$; for the VU and UD converters, $\Delta B = t_{on}(V_I - V_Q)/NA$, and for the CU converter, $\Delta B = t_{on}(V_I - V_0 - V_D)/NA$. Using the value of I_X from (7), and the value t_{on} in terms of T obtained from (5) and (6), leads to relationship (11).

Table 2.2 Mode 1 Time Relationships and Waveforms
for the Three Single-Winding Converter Circuits
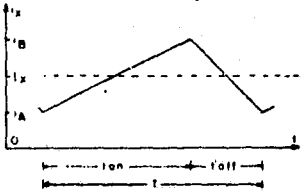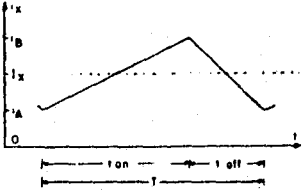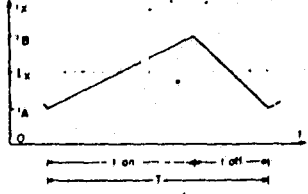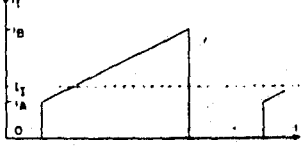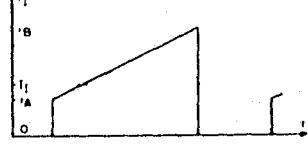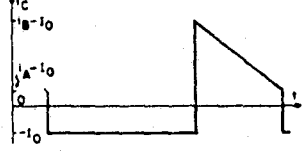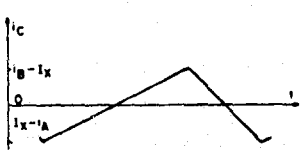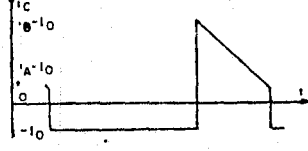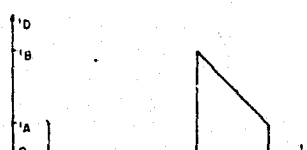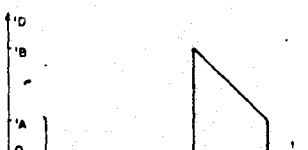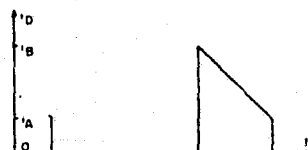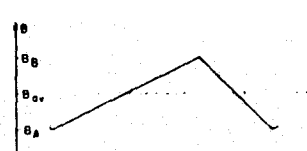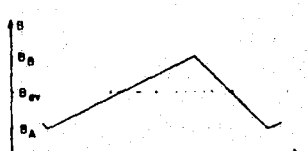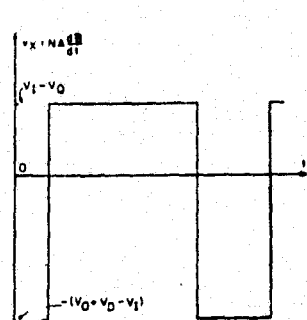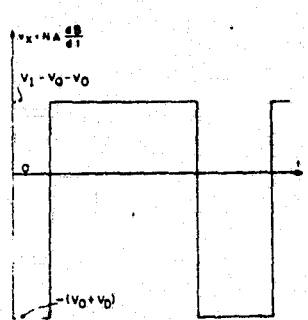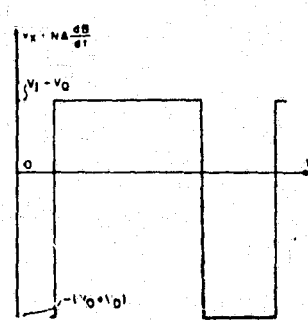
		VOLTAGE STEP-UP CONVERTER (VU)	CURRENT STEP-UP CONVERTER (CU)	VOLTAGE STEP-UP/CURRENT STEP-UP CONVERTER (UD)
TIME RELATIONSHIPS		$t_{on} = \dfrac{V_0 + V_D - V_I}{V_0 + V_D - V_Q} T$ (8,VU)	$t_{on} = \dfrac{V_0 + V_D}{V_I + V_D - V_Q} T$ (8,CU)	$t_{on} = \dfrac{V_0 + V_D}{V_I + V_0 + V_D - V_Q} T$ (8,UD)
		$t'_{off} = \dfrac{V_I - V_Q}{V_0 + V_D - V_Q} T$ (9)	$t'_{off} = \dfrac{V_I - V_0 - V_Q}{V_I + V_D - V_Q} T$	$t'_{off} = \dfrac{V_I - V_Q}{V_I + V_0 + V_D - V_Q} T$
		$t''_{off} = 0$ (10)	$t''_{off} = 0$	$t''_{off} = 0$
MODE 1	**WAVEFORMS**			

Table 2.3(A) Mode 1 Reactor Flux-Density and Turns Relationships for the Single-Winding Voltage Step-Up Converter

MODE 1

CONSTANT FREQUENCY CONTROLLER

$$B_B, B_A = B_R + \frac{\mu N P_0(V_0+V_D-V_Q)}{2V_0(V_I-V_Q)} \pm \frac{T(V_I-V_Q)(V_0+V_D-V_I)}{2NA(V_0+V_D-V_Q)} \qquad (11, VU)$$

B_B max occurs at $P_0 = P_{0\ max}$ and $V_I = V_{I\ min}$ $\qquad$ (12)

B_A min occurs at $P_0 = P_{0\ min}$ and at $V_I = V_R$ if $V_{I\ min} \le V_R \le V_{I\ max}$, or
at $V_I = V_{I\ min}$ if $V_R < V_{I\ min}$, or at $V_I = V_{I\ max}$ if $V_R > V_{I\ max}$ where $\qquad$ (13)
V_R is the positive real root of the cubic

$$V_I^3 - \frac{(V_0+V_D+5V_Q)V_I^2}{2} + V_Q(V_0+V_D+2V_Q)V_I - \frac{V_Q^2(V_0+V_D+V_Q)}{2} - \frac{\mu N^2 A P_{0\ min}(V_0+V_D-V_Q)^2}{2V_0 T} = 0$$

$$N = \frac{2V_0(V_{I\ min}-V_Q)}{2\mu P_{0\ max}(V_0+V_D-V_Q)}\left[(B_{max}-B_R)+\sqrt{(B_{max}-B_R)^2 - \frac{2\mu T P_{0\ max}}{2 A V_0}(V_0+V_D-V_{I\ min})}\right] \qquad (14)$$

CONSTANT ON-TIME CONTROLLER

$$B_B, B_A = B_R + \frac{\mu N P_0(V_0+V_D-V_Q)}{2V_0(V_I-V_Q)} \pm \frac{t_{on}(V_I-V_Q)}{2NA} \qquad (15)$$

B_B max occurs at $P_0 = P_{0\ max}$ and $V_I = V_{I\ min}$ $\qquad$ (16)

B_A min occurs at $P_0 = P_{0\ min}$ and $V_I = V_{I\ max}$ $\qquad$ (17)

$$N = \frac{2V_0(V_{I\ min}-V_Q)}{2\mu P_{0\ max}(V_0+V_D-V_Q)}\left[(B_{max}-B_R)+\sqrt{(B_{max}-B_R)^2 - \frac{2\mu t_{on} P_{0\ max}(V_0+V_D-V_Q)}{2 A V_0}}\right] \qquad (18)$$

CONSTANT OFF-TIME CONTROLLER

$$B_B, B_A = B_R + \frac{\mu N P_0(V_0+V_D-V_Q)}{2V_0(V_I-V_Q)} \pm \frac{t_{off}(V_0+V_D-V_I)}{2 N A} \qquad (19)$$

B_B max occurs at $P_0 = P_{0\ max}$ and $V_I = V_{I\ min}$ $\qquad$ (20)

B_A min occurs at $P_0 = P_{0\ min}$ and at $V_I = V_R$ if $V_{I\ min} \le V_R \le V_{I\ max}$, or
at $V_I = V_{I\ min}$ if $V_R < V_{I\ min}$, or at $V_I = V_{I\ max}$ if $V_R > V_{I\ max}$ $\qquad$ (21)

where $\quad V_R = N\sqrt{\dfrac{2\mu P_{0\ min}(V_0+V_D-V_Q)A}{t_{off}\, 2 V_0}} + V_Q$

$$N = \frac{2V_0(V_{I\ min}-V_Q)}{2\mu P_{0\ max}(V_0+V_D-V_Q)}\left[(B_{max}-B_R)+\sqrt{(B_{max}-B_R)^2 - \frac{2\mu t_{off}P_{0\ max}(V_0+V_D-V_{I\ min})(V_0+V_D-V_Q)}{2 A V_0(V_{I\ min}-V_Q)}}\right] \qquad (22)$$

Table 2.3(B) Mode 1 Reactor Flux-Density and Turns Relationships for the Single-Winding Current Step-Up Converter

MODE 1

CONSTANT FREQUENCY CONTROLLER

$$B_B, B_A = B_R + \frac{\mu N P_0}{\ell V_0} \pm \frac{T(V_I - V_0 - V_Q)(V_0 + V_D)}{2NA(V_I + V_D - V_Q)} \qquad (11, CU)$$

$B_{B\ max}$ occurs at $P_0 = P_{0\ max}$ and $V_I = V_{I\ max}$ $\qquad (12)$

$B_{A\ min}$ occurs at $P_0 = P_{0\ min}$ and $V_I = V_{I\ max}$ $\qquad (13)$

$$N = \frac{\ell V_0}{2\mu P_{0\ max}} \left[(B_{max} - B_R) + \sqrt{(B_{max} - B_R)^2 - \frac{2\mu T P_{0\ max}(V_{I\ max} - V_0 - V_Q)(V_0 + V_D)}{\ell A V_0(V_{I\ max} + V_D - V_Q)}} \right] \qquad (14)$$

CONSTANT OFF-TIME CONTROLLER

$$B_B, B_A = B_R + \frac{\mu N P_0}{\ell V_0} \pm \frac{t_{on}(V_I - V_0 - V_Q)}{2NA} \qquad (15)$$

$B_{B\ max}$ occurs at $P_0 = P_{0\ max}$ and $V_I = V_{I\ max}$ $\qquad (16)$

$B_{A\ min}$ occurs at $P_0 = P_{0\ min}$ and $V_I = V_{I\ max}$ $\qquad (17)$

$$N = \frac{\ell V_0}{2\mu P_{0\ max}} \left[(B_{max} - B_R) + \sqrt{(B_{max} - B_R)^2 - \frac{2\mu t_{on} P_{0\ max}(V_{I\ max} - V_0 - V_Q)}{\ell A V_0}} \right] \qquad (18)$$

CONSTANT OFF-TIME CONTROLLER

$$B_B, B_A = B_R + \frac{\mu N P_0}{\ell V_0} \pm \frac{t_{off}(V_0 + V_D)}{2NA} \qquad (19)$$

$B_{B\ max}$ occurs at $P_0 = P_{0\ max}$ and is independent of V_I $\qquad (20)$

$B_{A\ min}$ occurs at $P_0 = P_{0\ min}$ and is independent of V_I $\qquad (21)$

$$N = \frac{\ell V_0}{2\mu P_{0\ max}} \left[(B_{max} - B_R) + \sqrt{(B_{max} - B_R)^2 - \frac{2\mu t_{off} P_{0\ max}(V_0 + V_D)}{\ell A V_0}} \right] \qquad (22)$$

Table 2.3(C) **Mode 1 Reactor Flux-Density and Turns Relationships for the Single-Winding Voltage Step-Up/ Current Step-Up Converter**

$B_B, B_A = B_R + \dfrac{\mu N P_0 (V_I + V_0 + V_D - V_Q)}{\ell V_0 (V_I - V_Q)} \pm \dfrac{T(V_I - V_Q)(V_0 + V_D)}{2NA(V_I + V_0 + V_D - V_Q)}$	(11,UD)
$B_{B\,max}$ occurs at $P_0 = P_{0\,max}$ and $V_I = V_{I\,min}$	(12)
$B_{A\,min}$ occurs at $P_0 = P_{0\,min}$ and $V_I = V_{I\,max}$	(13)
$N = \dfrac{\ell V_0 (V_{I\,min} - V_Q)}{2\mu P_{0\,max}(V_{I\,min} + V_0 + V_D - V_Q)} \left[(B_{max} - B_R) + \sqrt{(B_{max} - B_R)^2 - \dfrac{2\mu T P_{0\,max}(V_0 + V_D)}{\ell A V_0}} \right]$	(14)
$B_B, B_A = B_R + \dfrac{\mu N P_0 (V_I + V_0 + V_D - V_Q)}{\ell V_0 (V_I - V_Q)} \pm \dfrac{t_{on}(V_I - V_Q)}{2NA}$	(15)
$B_{B\,max}$ occurs at $P_0 = P_{0\,max}$ and $V_I = V_{IO}$, where $V_{IO} = V_{I\,min}$ or $V_{I\,max}$ depending on the particular design.	(16)
$B_{A\,min}$ occurs at $P_0 = P_{0\,min}$ and $V_I = V_{I\,max}$	(17)
$N = \dfrac{\ell V_0 (V_{IO} - V_Q)}{2\mu P_{0\,max}(V_{IO} + V_0 + V_D - V_Q)} \left[(B_{max} - B_R) + \sqrt{(B_{max} - B_R)^2 - \dfrac{2\mu t_{on} P_{0\,max}(V_{IO} + V_0 + V_D - V_Q)}{\ell A V_0}} \right]$	(18)
$B_B, B_A = B_R + \dfrac{\mu N P_0 (V_I + V_0 + V_D - V_Q)}{\ell V_0 (V_I - V_Q)} \pm \dfrac{t_{off}(V_0 + V_D)}{2NA}$	(19)
$B_B\,max$ occurs at $P_0 = P_{0\,max}$ and $V_I = V_{I\,min}$	(20)
$B_{A\,min}$ occurs at $P_0 = P_{0\,min}$ and $V_I = V_{I\,max}$	(21)
$N = \dfrac{\ell V_0 (V_{I\,min} - V_Q)}{2\mu P_{0\,max}(V_{I\,min} + V_0 + V_D - V_Q)} \left[(B_{max} - B_R) + \sqrt{(B_{max} - B_R)^2 - \dfrac{2\mu t_{off} P_{0\,max}(V_{I\,min} + V_0 + V_D - V_Q)(V_0 + V_D)}{\ell A V_0 (V_{I\,min} - V_Q)}} \right]$	(22)

Row groups (left margin labels): CONSTANT FREQUENCY CONTROLLER — MODE 1 CONSTANT ON-TIME CONTROLLER — CONSTANT OFF-TIME CONTROLLER

To use (11) in a procedure to produce a converter design with a specified output voltage V_0 requires information on the particular values of V_I and P_0, within their respective specified operating ranges, that produce both the highest possible value of B_B, called $B_{B,max}$ and the lowest possible value of B_A called $B_{A,min}$. The two needed pairs of values for V_I and P_0 can be determined by evaluating expressions for the partial derivatives of B_B and B_A with respect to V_I and P_0. Appendix A outlines the steps which lead to the two pairs of desired values given in (12) and (13). These extremum values must be equal to or less than a maximum permissible value of flux density called B_{max}, specified by the designer, and equal to or greater than a minimum value B_{min}, also specified by the designer. Equation (14), obtained by solving (11) for N under the conditions of (12), gives a value for the number of turns on inductor. The detailed derivation of (14) is given in Appendix B.

(B) Mode 2

Next consider Mode 2 operation. Table 2.4 presents general relationships for the three converters operating in Mode 2. In Mode 2, the core flux density resides at the residual point (24) for a time period t''_{off} which is related to the other time intervals by (25). Of primary concern in the design of converters operating in this mode is the peak flux density excursion B_B which occurs at a peak reactor current i_B given by (23). Sketches of current, voltage, and flux density waveshapes are given in the table to assist visualization of similarities and differences among the three converters.

Table 2.5 presents design information, flux-density relationships, and time-interval expressions for the nine combinations of converter and controller when the circuit operates in Mode 2. The steps for deriving

Table 2.4 Mode 2 General Relationships and Waveforms
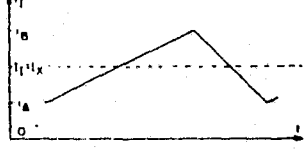for the Three Single-Winding Converter Circuits

		VOLTAGE STEP-UP CONVERTER (VU)	CURRENT STEP-UP CONVERTER (CU)	VOLTAGE STEP-UP/CURRENT STEP-UP CONVERTER (UD)
MODE 2	GENERAL RELATIONSHIPS	$i_B = \dfrac{2P_0}{V_0}\dfrac{T}{T-(t_{on}+t''_{off})}$ (23,VU)	$i_B = \dfrac{2P_0}{V_0}\dfrac{T}{T-t''_{off}}$ (23,CU)	$i_B = \dfrac{2P_0}{V_0}\dfrac{T}{T-(t_{on}+t''_{off})}$ (23,UD)
		$B_A = B_R$ (24)	$B_A = B_R$	$B_A = B_R$
		$t''_{off} = T - t_{on} - t'_{off}$ (25)	$t''_{off} = T - t_{on} - t'_{off}$	$t''_{off} = T - t_{on} - t'_{off}$
	WAVEFORMS			

Table 2.5 Mode 2 Time Flux-Density, and for the Three Single-Winding Converter Circuits

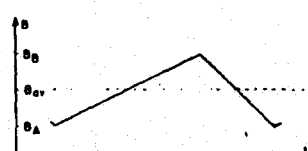|		VOLTAGE STEP-UP CONVERTER (VU)	CURRENT STEP-UP CONVERTER (CU)	VOLTAGE STEP-UP/CURRENT STEP-UP CONVERTER (UD)
MODE 2	**CONSTANT FREQUENCY CONTROLLER**	$B_B=B_R+\sqrt{\dfrac{2\mu T P_0(V_0+V_D-V_I)}{\ell A V_0}}$ (26,VU)	$B_B=B_R+\sqrt{\dfrac{2\mu T P_0(V_I-V_0-V_Q)(V_0+V_D)}{\ell A V_0\,(V_I+V_D-V_Q)}}$ (26,CU)	$B_B=B_R+\sqrt{\dfrac{2\mu T P_0(V_0+V_D)}{\ell A V_0}}$ (26,UD)
		$B_{B,max}$ occurs at $P_0=P_{0,max}$, $V_I=V_{I,min}$ (27)	$B_{B,max}$ occurs at $P_0=P_{0,max}$, $V_I=V_{I,max}$	$B_{B,max}$ occurs at $P_0=P_{0,min}$ and is independent of V_I.
		$t_{on}=\dfrac{N(V_0+V_D-V_I)}{(V_I-V_Q)}\sqrt{\dfrac{2\mu T P_0 A}{\ell V_0(V_0+V_D-V_I)}}$ (28)	$t_{on}=N\sqrt{\dfrac{2\mu T P_0 A(V_0+V_D)}{\ell V_0(V_I-V_Q+V_D)(V_I-V_0-V_Q)}}$	$t_{on}=\dfrac{N(V_0+V_D)}{(V_I-V_Q)}\sqrt{\dfrac{2\mu T P_0 A}{\ell V_0(V_0+V_D)}}$
		$t'_{off}=N\sqrt{\dfrac{2\mu T P_0 A}{\ell V_0(V_0+V_D-V_I)}}$ (29)	$t'_{off}=N\sqrt{\dfrac{2\mu T P_0 A(V_I-V_0-V_0)}{\ell V_0(V_I-V_Q+V_D)(V_0+V_D)}}$	$t'_{off}=N\sqrt{\dfrac{2\mu T P_0 A}{\ell V_0(V_0+V_D)}}$
	CONSTANT ON-TIME CONTROLLER	$B_B=B_R+\dfrac{t_{on}(V_I-V_Q)}{AN}$ (30)	$B_B=B_R+\dfrac{t_{on}(V_I-V_0-V_Q)}{AN}$	$B_B=B_R+\dfrac{t_{on}(V_I-V_Q)}{AN}$
		$B_{B,max}$ occurs at $V_I=V_{I\,max}$ and is independent of P_0 (31)	$B_{B,max}$ occurs at $V_I=V_{I\,max}$ and is independent of P_0	$B_{B,max}$ occurs at $V_I=V_{I\,max}$ and is independent of P_0
		$T=\dfrac{(V_I-V_Q)^2\,V_0\ell\,t_{on}^2}{2(V_0+V_D-V_I)P_0\mu N^2 A}$ (32)	$T=\dfrac{(V_I-V_Q+V_D)(V_I-V_0-V_Q)V_0\ell\,t_{on}^2}{2(V_0+V_D)P_0\mu N^2 A}$	$T=\dfrac{(V_I-V_Q)^2 V_0\ell\,t_{on}^2}{2(V_0+V_D)P_0\mu\,N^2 A}$
		$t'_{off}=\dfrac{(V_I-V_Q)t_{on}}{(V_0+V_D-V_I)}$ (33)	$t'_{off}=\dfrac{(V_I-V_0-V_Q)t_{on}}{(V_0+V_D)}$	$t'_{off}=\dfrac{(V_I-V_Q)t_{on}}{(V_0+V_D)}$
	CONSTANT OFF-TIME CONTROLLER	$B_B=B_R+\sqrt{\dfrac{2\mu T_R P_0(V_0+V_D-V_I)}{\ell A V_0}}$ (34)	$B_B=B_R+\sqrt{\dfrac{2\mu T_R P_0(V_I-V_0-V_Q)(V_0+V_D)}{\ell A V_0(V_I+V_D-V_Q)}}$	$B_B=B_R+\sqrt{\dfrac{2\mu T_R P_0(V_0+V_D)}{\ell A V_0}}$
		where T_R is the larger root of the quadratic $$T_R^2-2[t_{off}+\dfrac{\mu A N^2 P_0(V_0+V_D-V_I)}{\ell V_0(V_I-V_Q)^2}]T_R+t_{off}^2=0$$	where T_R is the larger root of the quadratic $$T_R^2-2[t_{off}+\dfrac{\mu A N^2 P_0(V_0+V_D)}{\ell V_0(V_I-V_0-V_Q)(V_I+V_D-V_Q)}]T_R+t_{off}^2=0$$	where T_R is the larger root of the quadratic $$T_R^2-2[t_{off}+\dfrac{\mu A N^2 P_0(V_0+V_D)}{\ell V_0(V_I-V_Q)^2}]T_R+t_{off}^2=0$$
		$B_{B,max}$ occurs at $P_0=P_{0,max}$ and $V_I=V_{I,min}$ (35)	$B_{B,max}$ occurs at $P_0=P_{0,max}$	$B_{B,max}$ occurs at $P_0=P_{0,max}$ and is independent of V_I.
		$T=T_R$ (36)	$T=T_R$	$T=T_R$
		$t_{on}=\dfrac{N(V_0+V_D-V_I)}{(V_I-V_Q)}\sqrt{\dfrac{2\mu T_R P_0 A}{\ell V_0(V_0+V_D-V_I)}}$ (37)	$t_{on}=N\sqrt{\dfrac{2\mu T_R P_0 A(V_0+V_D)}{\ell V_0(V_I-V_Q+V_D)(V_I-V_0-V_Q)}}$	$t_{on}=\dfrac{N(V_0+V_D)}{(V_I-V_Q)}\sqrt{\dfrac{2\mu T_R P_0 A}{\ell V_0(V_0+V_D)}}$
		$t'_{off}=\dfrac{(V_I-V_Q)t_{on}}{(V_0+V_D-V_I)}$ (38)	$t'_{off}=\dfrac{(V_I-V_0-V_Q)t_{on}}{(V_0+V_D)}$	$t'_{off}=\dfrac{(V_I-V_Q)t_{on}}{(V_0+V_D)}$

these equations are outlined in Appendix C. Although Table 2.5 for Mode 2 operation is analogous to Table 2.3 for Mode 1 operation, and the derivation procedure are similar, differences are apparent. The value of B_A, by definition, is B_R for all cases, and is not given in the table. The expressions for the number of turns N are also not given for the reasons to be explained later in the next section.

2.4 Mode Restriction

There are three possible ways in which a converter may work as far as the converter mode of operation is concerned: (i) Mode 1 over the entire operating range (ii) Mode 2 over the entire operating range, and (iii) Mode 1 and Mode 2 over different portions of the range. However, all of the designs considered in this dissertation operate in Mode 1 at least at the conditions given in (12), (16) or (20), i.e. the point at which $B_B = B_{B,max}$. In other words, case (ii) described above is not considered in this dissertation. The reasons for this are two-fold. First, given the same operating conditions, the peak reactor current for converters operating entirely in Mode 2 is larger than that for converters not operating entirely in Mode 2. Consequently, the stress on the power transistor is greater for an entirely Mode 2 design. Secondly, the peak flux density B_B for converters operating entirely in Mode 2 with constant frequency controllers is independent of the number of turns as can be seen from (26). This makes it impossible to determine N for a specified B_{max}.

Because of this mode restriction, $B_{B,max}$ occurs at the condition at which the converter must operate in Mode 1. Therefore, Mode 1 equations (14), (18) or (22) can always be used in the design procedure to determine the number of turns N, and the expressions for N are not given for Mode 2

operation. Once N is found for a given core geometry, $B_{A,min}$ can be determined from the expressions for B_A, (11), (15) or (19), and the conditions at which $B_{A,min}$ occurs, (13), (17) or (21). If $B_{A,min} > B_R$, then the converter operates in Mode 1 over the entire operating range, as in case (i) described above. Otherwise, the converter operates in Mode 1 and Mode 2 over different portions of the operating range as in case (iii).

2.5 Reactor Current, Wire Size, and Windability of the Core

In the following design procedure, after N is computed for a particular core, the rms value of the reactor current can be calculated from which wire size can be determined. In Table 2.5, the expressions for the rms value of the reactor current for both modes of operation for the nine combinations are presented. Mode 1 expressions are given by (39), (45) and (51), and Mode 2 expressions by (41), (47), and (53). The location of the maximum rms current $I_{Xe,max}$ are given by (40), (46) and (52) when the converters operate in Mode 1 for the entire operating range, and are given by (42), (48) and (54) when the converters operate in Mode 2 for the entire operating range. The derivations for these current expressions and the location at which $I_{Xe,max}$ occurs are outlined in Appendix D. Since the converter may operate in Mode 1 or Mode 2 over only a portion of the operating range, the location for $I_{Xe,max}$ for both Mode 1 or Mode 2 should be taken into consideration together to determine the location at which $I_{Xe,max}$ occurs. The results given in (43), (49) and (55) are obtained, respectively, from the pairs (40) and (42), (46) and (48), and (52) and (54), and are true no matter whether the converters operate only in Mode 1 or only in Mode 2 over the entire operating range or in Mode 1 or Mode 2 over the

Table 2.6(A) RMS Reactor Currents and Their Maximum Value for the Single-Winding Voltage Step-Up Converter

		Voltage Step-Up Converter (VU)	
CONSTANT FREQUENCY CONTROLLER	MODE 1	$I_{Xe}= \dfrac{P_0(V_0+V_D-V_Q)}{V_0(V_I-V_Q)}\sqrt{1+\dfrac{1}{12}\left[\dfrac{\ell TV_0(V_I-V_Q)^2(V_0+V_D-V_I)}{\mu N^2 AP_0(V_0+V_D-V_Q)^2}\right]^2}$	(39,VU)
		$I_{Xe,max}$ occurs at $P_{0,max}$ and $V_{I,min}$.	(40)
	MODE 2	$I_{Xe}=\sqrt{\dfrac{2P_0(V_0+V_D-V_Q)}{3V_0(V_I-V_Q)}}\sqrt{\dfrac{2\ell P_0 T(V_0+V_D-V_I)}{\mu N^2 AV_0}}$	(41)
		$I_{Xe,max}$ occurs at $P_{0,max}$ and $V_{I,min}$.	(42)
	$I_{Xe,max}$	$I_{Xe,max}$ occurs at $P_{0,max}$ and $V_{I,min}$.	(43)
		$I_{Xe,max}=\dfrac{P_{0,max}(V_0+V_D-V_Q)}{V_0(V_{I,min}-V_Q)}\sqrt{1+\dfrac{1}{12}\left[\dfrac{\ell TV_0(V_{I,min}-V_Q)^2(V_0+V_D-V_{I,min})}{\mu N^2 AP_{0,max}(V_0+V_D-V_Q)^2}\right]^2}$	(44)
CONSTANT ON-TIME CONTROLLER	MODE 1	$I_{Xe}=\dfrac{P_0(V_0+V_D-V_Q)}{V_0(V_I-V_Q)}\sqrt{1+\dfrac{1}{12}\left[\dfrac{\ell t_{on}V_0(V_I-V_Q)^2}{\mu N^2 AP_0(V_0+V_D-V_Q)}\right]^2}$	(45)
		$I_{Xe,max}$ occurs at $P_{0,max}$ and $V_{I,min}$.	(46)
	MODE 2	$I_{Xe}=\dfrac{(V_I-V_Q)t_{on}}{N}\sqrt{\dfrac{\ell}{3\mu A}}$	(47)
		$I_{Xe,max}$ occurs at $V_{I,max}$ and is independent of P_0.	(48)
	$I_{Xe,max}$	$I_{Xe,max}$ occurs at $P_{0,max}$ and $V_{I,min}$.	(49)
		$I_{Xe,max}=\dfrac{P_{0,max}(V_0+V_D-V_Q)}{V_0(V_{I,min}-V_Q)}\sqrt{1+\dfrac{1}{12}\left[\dfrac{\ell t_{on}V_0(V_{I,min}-V_Q)^2}{\mu N^2 AP_{0,max}(V_0+V_D-V_Q)}\right]^2}$	(50)
CONSTANT OFF-TIME CONTROLLER	MODE 1	$I_{Xe}=\dfrac{P_0(V_0+V_D-V_Q)}{V_0(V_I-V_Q)}\sqrt{1+\dfrac{1}{12}\left[\dfrac{\ell t_{off}V_0(V_I-V_Q)(V_0+V_D-V_I)}{\mu N^2 AP_0(V_0+V_D-V_Q)}\right]^2}$	(51)
		$I_{Xe,max}$ occurs at $P_{0,max}$ and $V_{I,min}$.	(52)
	MODE 2	$I_{Xe}=\sqrt{\dfrac{2P_0(V_0+V_D-V_Q)}{3V_0(V_I-V_Q)}}\sqrt{\dfrac{2\ell T_R(V_0+V_D-V_I)}{\mu N^2 AV_0}}$	(53)
		$I_{Xe,max}$ occurs at $P_{0,max}$ and $V_{I,min}$.	(54)
	$I_{Xe,max}$	$I_{Xe,max}$ occurs at $P_{0,max}$ and $V_{I,min}$.	(55)
		$I_{Xe,max}=\dfrac{P_{0,max}(V_0+V_D-V_Q)}{V_0(V_{I,min}-V_Q)}\sqrt{1+\dfrac{1}{12}\left[\dfrac{\ell t_{off}V_0(V_{I,min}-V_Q)(V_0+V_D-V_{I,min})}{\mu N^2 AP_{0,max}(V_0+V_D-V_Q)}\right]^2}$	(56)

Current Step-Up Converter (CU)		

<table>
<tr><td rowspan="8">CONSTANT FREQUENCY CONTROLLER</td><td rowspan="2">MODE 1</td><td>$I_{Xe} = \dfrac{P_0}{V_0}\sqrt{1+\dfrac{1}{12}\left[\dfrac{\ell T V_0 (V_I - V_0 - V_Q)(V_0 + V_D)}{\mu N^2 A P_0 (V_I + V_D - V_Q)}\right]^2}$</td><td>(39,CU)</td></tr>
<tr><td>$I_{Xe,max}$ occurs at $P_{0,max}$ and $V_{I,max}$.</td><td>(40)</td></tr>
<tr><td rowspan="2">MODE 2</td><td>$I_{Xe} = \sqrt{\dfrac{2P_0}{3V_0}}\sqrt{\dfrac{2\ell P_0 T (V_0 + V_D)(V_I - V_0 - V_Q)}{\mu N^2 A V_0 (V_I - V_Q + V_D)}}$</td><td>(41)</td></tr>
<tr><td>$I_{Xe,max}$ occurs at $P_{0,max}$ and $V_{I,max}$.</td><td>(42)</td></tr>
<tr><td rowspan="2">$I_{Xe,max}$</td><td>$I_{Xe,max}$ occurs at $P_{0,max}$ and $V_{I,max}$.</td><td>(43)</td></tr>
<tr><td>$I_{Xe,max} = \dfrac{P_{0,max}}{V_0}\sqrt{1+\dfrac{1}{12}\left[\dfrac{\ell T V_0 (V_{I,max} - V_0 - V_Q)(V_0 + V_D)}{\mu N^2 A P_{0,max}(V_{I,max} + V_D - V_Q)}\right]^2}$</td><td>(44)</td></tr>
<tr><td rowspan="6">CONSTANT ON-TIME CONTROLLER</td><td rowspan="2">MODE 1</td><td>$I_{Xe} = \dfrac{P_0}{V_0}\sqrt{1+\dfrac{1}{12}\left[\dfrac{\ell t_{on} V_0 (V_I - V_0 - V_Q)}{\mu N^2 A P_0}\right]^2}$</td><td>(45)</td></tr>
<tr><td>$I_{Xe,max}$ occurs at $P_{0,max}$ and $V_{I,max}$.</td><td>(46)</td></tr>
<tr><td rowspan="2">MODE 2</td><td>$I_{Xe} = \dfrac{(V_I - V_0 - V_Q)t_{on}}{N}\sqrt{\dfrac{\ell}{3\mu A}}$</td><td>(47)</td></tr>
<tr><td>$I_{Xe,max}$ occurs at $V_{I,max}$ and is independent of P_0.</td><td>(48)</td></tr>
<tr><td rowspan="2">$I_{Xe,max}$</td><td>$I_{Xe,max}$ occurs at $P_{0,max}$ and $V_{I,max}$.</td><td>(49)</td></tr>
<tr><td>$I_{Xe,max} = \dfrac{P_{0,max}}{V_0}\sqrt{1+\dfrac{1}{12}\left[\dfrac{\ell t_{on} V_0 (V_{I,max} - V_0 - V_Q)}{\mu N^2 A P_{0,max}}\right]^2}$</td><td>(50)</td></tr>
<tr><td rowspan="6">CONSTANT OFF-TIME CONTROLLER</td><td rowspan="2">MODE 1</td><td>$I_{Xe} = \dfrac{P_0}{V_0}\sqrt{1+\dfrac{1}{12}\left[\dfrac{\ell t_{off} V_0 (V_0 + V_D)}{\mu N^2 A P_0}\right]^2}$</td><td>(51)</td></tr>
<tr><td>$I_{Xe,max}$ occurs at $P_{0,max}$ and is independent of V_I.</td><td>(52)</td></tr>
<tr><td rowspan="2">MODE 2</td><td>$I_{Xe} = \sqrt{\dfrac{2P_0}{3V_0}}\sqrt{\dfrac{2\ell P_0 T_R (V_0 + V_D)(V_I - V_0 - V_Q)}{\mu N^2 A V_0 (V_I - V_Q + V_D)}}$</td><td>(53)</td></tr>
<tr><td>$I_{Xe,max}$ occurs at $P_{0,max}$ and $V_{I,max}$.</td><td>(54)</td></tr>
<tr><td rowspan="2">$I_{Xe,max}$</td><td>$I_{Xe,max}$ occurs at $P_{0,max}$ and $V_{I,max}$.</td><td>(55)</td></tr>
<tr><td>$I_{Xe,max} = \dfrac{P_{0,max}}{V_0}\sqrt{1+\dfrac{1}{12}\dfrac{\ell t_{off} V_0 (V_0 + V_D)}{\mu N^2 A P_{0,max}}}$</td><td>(56)</td></tr>
</table>

RMS Reactor Currents and Their Maximum
Table 2.6(C) Value for the Single-Winding Voltage
Step-Up/Current Step-Up Converter

25

		Voltage Step-Up/Current Step-Up Converter (UD)	
CONSTANT FREQUENCY CONTROLLER	MODE 1	$I_{Xe} = \dfrac{P_0(V_I+V_0+V_D-V_Q)}{V_0(V_I-V_Q)}\sqrt{1+\dfrac{1}{12}\left[\dfrac{\ell T V_0(V_I-V_Q)^2(V_0+V_D)}{\mu N^2 A P_0(V_I+V_0+V_D-V_Q)}\right]^2}$	(39,UD)
		$I_{Xe,max}$ occurs at $P_{0,max}$ and $V_{I,min}$	(40)
	MODE 2	$I_{Xe} = \sqrt{\dfrac{2P_0(V_0+V_D+V_I-V_Q)}{3V_0(V_I-V_Q)}\sqrt{\dfrac{2\ell P_0 T(V_0+V_D)}{\mu N^2 A V_0}}}$	(41)
		$I_{Xe,max}$ occurs at $P_{0,max}$ and $V_{I,min}$.	(42)
	$I_{Xe,max}$	$I_{Xe,max}$ occurs at $P_{0,max}$ and $V_{I,min}$.	(43)
		$I_{Xe} = \dfrac{P_{0,max}(V_{I,max}+V_0+V_D-V_Q)}{V_0(V_{I,min}-V_Q)}\sqrt{1+\dfrac{1}{12}\left[\dfrac{\ell T V_0(V_{I,min}-V_Q)^2(V_0+V_D)}{\mu N^2 A P_{0,max}(V_{I,min}+V_0+V_D-V_Q)^2}\right]^2}$	(44)
CONSTANT ON-TIME CONTROLLER	MODE 1	$I_{Xe} = \dfrac{P_0(V_I+V_0+V_D-V_Q)}{V_0(V_I-V_Q)}\sqrt{1+\dfrac{1}{12}\left[\dfrac{\ell t_{on} V_0(V_I-V_Q)^2}{\mu N^2 A P_0(V_I+V_0+V_D-V_Q)}\right]^2}$	(45)
		$I_{Xe,max}$ occurs at $P_{0,max}$ and $V_{I,max}$ or $V_{I,min}$.	(46)
	MODE 2	$I_{Xe} = \dfrac{(V_I-V_Q)t_{on}}{N}\sqrt{\dfrac{\ell}{3\mu A}}$	(47)
		$I_{Xe,max}$ occurs at $V_{I,max}$ and is independent of P_0.	(48)
	$I_{Xe,max}$	$I_{Xe,max}$ occurs at $P_{0,max}$ and $V_{I,max}$. or $V_{I,min}$	(49)
		Using (45,UD), compute $I_X(P_0=P_{0,max}, V_I=V_{I,max}$ and $I_X(P_0=P_{0,max}, V_I=V_{I,min})$ and $I_{X,max}$ is equal to the larger of the two.	(50)
CONSTANT OFF-TIME CONTROLLER	MODE 1	$I_{Xe} = \dfrac{P_0(V_I+V_0+V_D-V_Q)}{V_0(V_I-V_Q)}\sqrt{1+\dfrac{1}{12}\left[\dfrac{\ell t_{off} V_0(V_I-V_Q)(V_0+V_D)}{\mu N^2 A P_{0,max}(V_I+V_0+V_D-V_Q)}\right]^2}$	(51)
		$I_{Xe,max}$ occurs at $P_{0,max}$ and $V_{I,min}$.	(52)
	MODE 2	$I_{Xe} = \sqrt{\dfrac{2P_0(V_0+V_D+V_I-V_Q)}{3V_0(V_I-V_Q)}\sqrt{\dfrac{2\ell P_0 T_R(V_0+V_D)}{\mu N^2 A V_0}}}$	(53)
		$I_{Xe,max}$ occurs at $P_{0,max}$ and $V_{I,min}$.	(54)
	$I_{Xe,max}$	$I_{Xe,max}$ occurs at $P_{0,max}$ and $V_{I,min}$.	(55)
		$I_{Xe,max} = \dfrac{P_{0,max}(V_{I,min}+V_0+V_D-V_Q)}{V_0(V_{I,min}-V_Q)}\sqrt{1+\dfrac{1}{12}\left[\dfrac{\ell t_{off} V_0(V_{I,min}-V_Q)(V_0+V_D)}{\mu N^2 A P_{0,max}(V_{I,max}+V_0+V_D-V_Q)}\right]^2}$	(56)

different portions of the range. The locations given in (43), (49) and (55) coincide with those in (12),(16), and (20), at which the core flux density B_B reaches a maximum. Because of the mode restriction imposed in Sec. 2.4, the converters must operate in Mode 1 at the locations given in (43), (49) and (55). Thus, Mode 1 expressions are used to determine $I_{Xe,max}$, as are given in (44), (50) and (56). Using the value of the maximum rms current, the winding wire size can then be determined from commercially available wire tables.

It should be noted that the turns equations given in (14),(18), and (22) are obtained without considering the size of the wire. Once the wire size has been determined, the windability of the core must be checked by considering the winding factor F_W,

$$F_W = \frac{NA_{wr}}{A_{wn}}$$

where A_{wr} is the total cross-sectional area of the wire and its insulation and A_{wn} is the window area of the core. In the next section, examples are given to illustrate the design procedure.

2.6 Design Examples

Three numerical examples are given in this section. In Example 1 is a constant-frequency current step-up converter design which illustrates the design procedure which applies to all of the nine controller-converter combinations with the exceptions of the constant on-time voltage step-up converter and the constant on-time voltage step-up/current step-up converter. For the latter two cases, the design procedures are somewhat different and are described in Examples 2 and 3. The cores chosen for these

examples are toroidal powder permalloy cores obtained from commercial catalog MPP-303 S by Magnetics Inc.

Example 1

Design the inductor for a current step-up converter with a constant-frequency controller with T = 50 microseconds. The remaining specifications are: V_0 = 15V; $V_{I,min}$ = 22V, $V_{I,max}$ = 28V; $P_{0,max}$ = 30W; V_Q = 0.5V, V_D = 0.7V; B_{max} = 0.35T, B_R = 0.01T; $F_{w,max}$ = 0.4.

Design Procedures

[A] Choose a core and determine number of turns N:

Arbitrarily select a core (Magnetics Catalog Number 55585) with $A = 0.454 \times 10^{-4} m^2$, $\ell = 8.95 \times 10^{-2} m$, $A_{wn} = 4.00 \times 10^{-4} m^2$, (788·500 cir. mils) and $\mu = 125 \mu_0$ ($\mu_0 = 4\pi \times 10^{-7} H/m$).

From (14,CU), N = 84

[B] Determine wire size:

Using (44,CU),

$I_{xe,max}$ = 2A

For a current density of $5.0671 \times 10^{-7} m^2/A$ (1000 circular mils/A), use wire table to find wire sizes. Wire AWG #17 ($A_{wr} = 1.177 \times 10^{-6} m^2$).

[C] Check winding factor:

$$F_w = NA_{wr}/A_{wn} = 84 \times 1.177 \times 10^{-6}/4.00 \times 10^{-4} = 0.24 < F_{w,max}$$

In this case, the first core size-permeability selection yields a design which satisfies the specifications. It is not possible to arbitrarily pick a core which will yield a design which will meet the specifications, however. For example, another selection of core (catalog No. 55059) with $A = 0.331 \times 10^{-4} m^2$, $\ell = 5.67 \times 10^{-2} m$, $A_{wn} = 1.41 \times 10^{-4} m^2$ and $\mu = 60 \mu_0$ yields

[A]: N = 110 [B] $I_{Xe,max}$= 2A (AWG #17) [C] F_w = 0.91 > $F_{w,max}$. This design does not meet the maximum winding factor specification. In another example, a core (M55308) with the same dimensions as just described above but with μ = 160μ_0 is not workable for this particular set of specifications, because with these parameters, the term inside the square root sign in (14,CU) is negative, which results in a complex number and therefore a nonphysical solution for N.

If the designer is not satisfied with the first workable design, another core is selected and the same procedure is followed to determine N and windability.

Example 2

Design an inductor for a voltage step-up converter with a constant on-time controller with t_{on} = 50 microseconds. Converter specifications are: V_0 = 28V; $V_{I,min}$ = 12V, $V_{I,max}$ = 22V, $P_{0,max}$ = 40W, V_Q = 0.7V, V_D = 1V, B_{max} = 0.35T, B_R = 0.01 and $F_{w,max}$ = 0.4.

Design Procedure

The design procedure for this controller-converter combination is somewhat more complicated. Because of (30,VU), the core flux density of the reactor with the number of turns determined from (18,VU) may exceed the specified value of B_{max} at P_0 = $P_{0,max}$ and V_I = $V_{I,max}$ if the converter operates in Mode 2 at that condition. Consequently, in the design procedure, an extra step must be included to ensure that the value of B_{max} is not exceeded by B_B at that condition.

[A] Choose a core and determine the number of turns N:

Arbitrarily select a core (M-55324) with A = $0.678 \times 10^{-4} m^2$, ℓ = $8.98 \times 10^{-2} m$, A_{wn}=$3.64 \times 10^{-4} m^2$ and μ = 125μ_0.

From (18,VU), N = 37. With this number of turns, the core flux density will reach the specified value B_{max} at $(P_0 = P_{0,max}, V_I = V_{I,min})$ but may exceed B_{max} at $(P_0 = P_{0,max}, V_I = V_{I,max})$ due to (30,VU) if the converter operates in Mode 2 at this condition because of (30,VU). If the converter does operate in Mode 2 at this condition, and if the flux density at this condition exceeds B_{max}, this core is discarded and a new core is selected for return to (18,VU) to find N. Otherwise, proceed to step [B].

For this particular example, the converter operates in Mode 2 at $(P_{0,max}, V_{I,max})$ because from (15,VU), $B_A(P_0 = P_{0,max} = 40W, V_I = V_{I,max} = 22V) = -0.012T < B_R$, which is 0.01T by specification. Thus, (29,VU) should be used to compute $B_B(P_{0,max}, V_{I,max})$.

$$B_B(P_0 = P_{0,max} = 40W, V_I = V_{I,max} = 22V)$$

$$= 0.01 + \frac{(50 \times 10^{-6}) \times (22 - 0.7)}{(0.678 \times 10^{-4}) \times 37}$$

$$= 0.43T > B_{max}, \text{ which is } 0.35T$$

Thus, the first selection of core does not work for this design specification. Select a new core (M-55254) with $A = 1.072 \times 10^{-4} m^2$, $\ell = 9.84 \times 10^{-2} m$, $A_{wn} = 4.27 \times 10^{-4} m^2$, $\mu = 125 \mu_0$. From (18,VU), N = 50. From (15,VU), $B_A(P_0 = P_{0,max} = 40W, V_I = V_{I,max} = 22V) = 0.059T > B_R$. Thus, with N = 50 on the newly selected core, the converter operates in Mode 1 at $(P_{0,max}, V_{I,max})$, and there is no need to check the value of B_B at this condition because of (16,VU).

[B] Determine wire size

From (50,VU), $I_{Xe,max} = 3.52A$. For current density of 5.067×10^{-7} m^2/A(1000 cir.mils/A), wire AWG #14 ($A_{wr} = 2.294 \times 10^{-6} m^2$) is chosen.

[C] Check winding factor

$F_w = NA_{wr}/A_{wn} = 0.27 < F_{w,max}$, and this design meets the specifications.

The results of this design procedure are core (M-555254), N = 50, wire size AWG #14. The comment concerning core-size-permeability selection which followed Example 1 applies here as well.

Example 3

Design an inductor for a voltage step-up/current step-up converter with a constant on-time controller of t_{on} = 50 microseconds. Converter specifications are V_0 = 15V, $V_{I,min}$ = 12V, $V_{I,max}$ = 20V, $P_{0,max}$ = 30W. V_Q = 0.5V, V_D = 0.8V, B_{max} = 0.35T, B_R = 0.01T and $F_{w,max}$ = 0.4.

Design Procedure

The design procedure for this controller-converter combination is similar to but is even more complicated than that in Example 2. Because of the uncertainty of the location of $B_{B,max}$ expressed in (16,UD), V_{I0} in the turn equation (18,UD) is equal to either $V_{I,min}$ or $V_{I,max}$. The value of V_{I0} depends on which extreme value corresponds to the number of turns which does not cause the core flux density to exceed B_{max} within the converter operating range.

[A] Choose a core an determine the number of turns N:

Arbitrarily select a core (M-55586) with A = $0.454 \times 10^{-4} m^2$, $\ell = 8.95 \times 10^{-2} m$, $A_{wn} = 4.0 \times 10^{-4} m^2$, $\mu = 60\mu_0$ Setting $V_{I0} = V_{I,min}$ = 12V and substituting the other specification into (18,UD), N = 58. Using this calculated number of turns, the converter will operate in Mode 2 at $(P_{0,max}, V_{I,max})$ because from (15,UD), $B_A(P_0 = P_{0,max}, V_I = V_{I,max})$ = 0.001T < B_R, which, by specification, is 0.01T. Thus, the Mode 2 expression for B_B,

(30,UD), should be used to compute B_B at $(P_{0,max}, V_{I,max})$. $B_B(P_0 = P_{0,max}, V_I = V_{I,max}) = 0.395T > B_{max}$, which is 0.35T by specification. Thus, this core should be discarded, because the maximum flux density value is exceeded.

Select another core (M-55086) with parameter $A = 1.34 \times 10^{-4} m^2$, $\ell = 11.63 \times 10^{-2}m$, $\mu = 200\mu_0$. $A_{wn} = 6.11 \times 10^{-4} m^2$. Set $V_{I0} = V_{I,min} = 12V$, and use (18,UD), $N = 25$. With this turn on the particular core, the converter will operate in Mode 1 at $(P_{0,max}, V_{I,max})$ because from (15,UD), $B_A(P_0 = P_{0,max}, V_I = V_{I,max}) = 0.06T > B_R$, which is 0.01T. Thus, Mode 1 equation (15,UD) should be used to check B_B at $(P_{0,max}, V_{I,max})$. $B_B(P_0 = P_{0,max}, V_I = V_{I,max}) = 0.354 > B_{max}$. Thus, this design should also be discarded. Set $V_{I0} = V_{I,max} = 20V$ in (18,UD) for the same core, $N = 24$. Using the calculated number of turns for this particular core, the flux density at $(P_{0,max}, V_{I,min})$ should be checked to see if B_B at $(P_{0,max}, V_{I,min})$ exceeds B_{max}. Using (15,UD), $B_A(P_{0,max}, V_{I,min}) = 0.335 < B_{max}$. Thus, for this particular core with $N = 24$, the core flux density will reach B_{max} at $(P_{0,max}, V_{I,max})$ but will never exceed B_{max} within the specified operating range.

[B] Determine Wire Size

From (50,UD),

$$I_{Xe}(P_{0,max}, V_{I,max}) = 3.99A$$
$$I_{Xe}(P_{0,max}, V_{I,min}) = 4.85A$$

Thus, $I_{Xe,max} = 4.85A$; on the basis of $5.0671 \times 10^{-7} m^2/A$, the wire size is AWG #13 with wire area $A_{wr} = 2.87 \times 10^{-6} m^2$.

[C] Check winding factor

$$F_W = (24 \times 2.87 \times 10^{-6})/6.11 \times 10^{-4} = 0.11 < F_{w,max}.$$

Therefore, core (M55086), $\mu = 200\mu_0$, with $N = 24$, AWG #13 meets the design requirements.

2.7 Computer-Aided Design

As can be seen from the three examples given in the last section, the design procedure starts with the arbitrary selection of a core, and then uses equations presented in the tables to determine the number of winding turns, wire size and the winding factor. If the first selected core fails to produce a design which meets the design requirements, then additional cores are tried until a workable core is found. This is a time-consuming process if the design is done by hand calculations. By automating the design procedure on a digital computer, each available core can be tested rapidly, and only those cores which produce designs which meet the design requirements are selected. Such programs have been written and run on a minicomputer with 8K words of memory. Fig. 2.3 gives an example of the computer printout for a constant frequency voltage step-up converter. The operating conditions which must be specified include the desired regulated output voltage, the ranges of input voltage and output power, transistor and diode forward voltage drops, the converter operating frequency, the magnetic residual flux density, the range of permitted core flux density, and the maximum permitted winding factor. A list of designs matching the design specifications are printed including the core size and permeability identification numbers, the relative permeability, the core volume, the number of turns, the wire gauge, the value of inductance value, the actual winding factor, mode of operation 1 indicates that the converter operates in Mode 1 for the entire operating range, and 2 indicates that converter operates in Mode 2 over a portion of the operating range), and the maximum value of peak reactor current which is the same as the maximum value of peak transistor collector current.

TTY I/O IN VOLTS,AMPERES,WATTS,TESLA,KHZ

V OUT:28

V IN(MIN):12

V IN(MAX):20

P OUT(MIN):10

P OUT(MAX):40

V SAT:.5 AT I COLL.:1

V.DIODE:.8

CONV. FREQ:20

B RES:0.01

B MIN:0.01

B MAX:0.35

MAX. WDG. FACTOR:0.4

CORES MATCHING CONSTRAINTS   DATE: 8/ 4/ 75

CORE NO.	MU NO.	MU	VOL. CU.CM.	NO. TURNS	AWG	INDUCT. MH.	WDG. FAC.	MODE NO.	IB(MAX) AMP.
8	2	125	4.032	28	15	0.123	0.321	2	4.9014
9	2	125	5.306	40	15	0.203	0.249	2	4.3553
9	3	160	5.306	28	15	0.128	0.174	2	4.8545
9	4	200	5.306	18	14	0.066	0.140	2	6.1074
10	2	125	4.001	39	15	0.120	0.177	2	4.9331
11	2	125	6.023	46	15	0.248	0.231	2	4.2045
11	3	160	6.023	34	15	0.173	0.171	2	4.5008
11	4	200	6.023	24	14	0.108	0.150	2	5.0974
12	2	125	10.42	56	15	0.527	0.239	1	3.8394
12	3	160	10.42	42	15	0.380	0.179	1	3.9653
12	4	200	10.42	32	15	0.275	0.137	2	4.1354
13	2	125	22.48	66	15	1.248	0.282	1	3.6523
13	3	160	22.48	51	15	0.954	0.218	1	3.6944
13	4	200	22.48	40	15	0.734	0.171	1	3.7482
14	2	125	16.18	69	15	0.855	0.206	1	3.7152
14	3	160	16.18	53	15	0.646	0.158	1	3.7800
14	4	200	16.18	42	15	0.507	0.125	1	3.8524
15	2	125	16.49	76	15	0.885	0.189	1	3.7084
15	3	160	16.49	58	15	0.660	0.144	1	3.7742
15	4	200	16.49	46	15	0.519	0.114	1	3.8446
16	1	60	21.81	184	15	2.612	0.361	1	3.5809
16	2	125	21.81	86	15	1.189	0.169	1	3.6591
16	3	160	21.81	67	15	0.924	0.132	1	3.7003
16	4	200	21.81	53	15	0.723	0.104	1	3.7518

Figure 2.3 Computer Printout for an Example of a Constant Frequency Voltage Step-Up Converter Design

2.8 Conclusions

Three widely used single-winding converter types-- voltage step-up, current step-up, and voltage step-up/current step-up-- are analyzed after the circuits are modeled on a piecewise linear basis. Design equations are presented and procedures for designing the energy-storage reactors are developed to accommodate any combination of the three converter types and the three controller types. Each controller-converter combinations has the potential for operating in Mode 1 or Mode 2 so that a total of eighteen different possibilities are examined.

A number of converters of various types operating with various controllers have been designed using the relationships and the procedure presented in this chapter. When tested in the laboratory, the measured currents, flux density levels, on-times, and converter frequencies have agreed with values predicted from the analytic expressions within three to five percent.

The design procedures presented have been automated in a set of digital computer programs to demonstrate the feasibility of computer-aided design procedures for single-winding energy storage reactors for dc-to-dc converters.

Chapter III

DESIGN OF ENERGY-STORAGE REACTORS FOR TWO-WINDING

VOLTAGE STEP-UP/CURRENT STEP-UP DC-TO-DC CONVERTERS

3.1 Introduction

In this chapter, the basic concept used for designing the energy-storage reactors for the three single-winding converters is extended to include a two-winding converter configuration as shown in Fig. 3.1. This configuration, operating like the single-winding voltage step-up/current step-up converter described in Chapter I, is capable of stepping up the source voltage or stepping up the source current to a higher level of voltage or current. However, the presence of two windings in this converter enables a much greater range of performance characteristics than is possible in the single-winding configurations. For example, the ability to obtain a voltage step-up or a current step-up by appropriate choice of turns ratio removes many of the problems associated with the very narrow range and tight control of the duty cycle required of single-winding circuits when large step-up ratios in voltage or current are required. In addition, the second winding makes it possible to isolate input and output circuits from each other. By utilizing the extra freedom provided by the additional winding, ten design options are presented in this chapter to permit a customized design of the converter with respect to a particular performance characteristic.

(35)
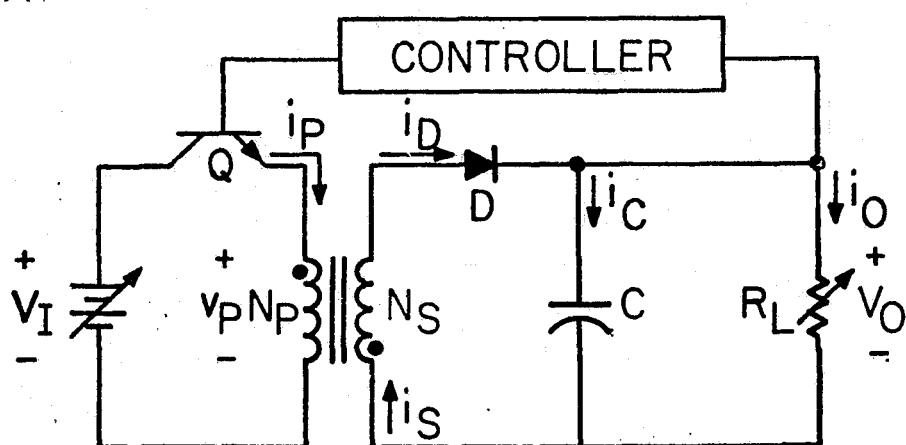
Figure 3.1 Two-winding voltage step-up/
current step-up converter (2UD)

As in the previous chapter on single-winding converters, three types of controllers are considered-- constant-frequency, constant transistor on-time, and constant transistor off-time, and two modes of operation are considered-- Mode 1 and Mode 2. For single-winding converters, these two modes of operation are often referred to as the continuous and the discontinuous inductor current mode respectively. For the two-winding configuration, these modes of operation might more properly be called the continuous and the discontinuous mmf modes.

The material in this chapter builds heavily on the work presented in References [4,5]. The format of the presentation follows closely that of the preceding chapter. All of the useful expressions are presented in a tabular format so that they may be readily used for designing energy-storage reactors for two-winding converters. Two numerical examples are given at the end of the chapter to illustrate the step-by-step design procedure developed.

3.2 Circuit Analysis and Design Relationships

The operation of this converter configuration is similar to the operation of the single-winding voltage step-up/current ste-up converter. A difference, however, is the fact that the winding currents for this configuration are interrupted each time the transistor is turned on or off. When the transistor is turned on the diode is reverse biased and no secondary current flows. When the transistor is turned off, the primary current is suddenly interrupted, and the energy stored in the reactor core is released through the secondary winding.

The conventions used and the assumptions made in the analysis of this configuration build upon the analytical approach followed in the last

chapter. By using these assumptions and referring to the sketches of flux density, current, and voltage waveforms shown in Fig. 3.2, circuit equations are written as Eq. (1) to (6) of Table 3.1. Equating the increase to the decrease of core flux density leads to the time relationship (8).

Table 3.2 presents relationships for time, duty cycle, and flux density for both modes of operation. Because of the length of some of the expressions, the table is arranged in three parts, A,B, and C, corresponding to the three controller types. To simplify the presentation, each controller is identified by two letters: FQ for the constant frequency controller, TN for the constant on-time controller, and TF for the constant off-time controller. The equation numbers in the tables are coded so that parallel relationships can be identified as well as specific ones. For example, referring to Table 3.2, (18) refers to the equations for α for the cases of all the three controllers, whereas (18, FQ) refers to the specific equation for α for the case of constant-frequency controller.

Considering first only Mode 1 operation, Eq. (9) follows by definition. From (7), (8), and (9), the duty cycle α, of the power transistor is given by (10).

By evaluating the partial derivatives of α with respect to the input voltage V_I and output power P_0, α can be shown to decrease as V_I increases and to be independent of P_0 (11). Of primary concern in the design of converters are the extrema of the flux-density-excursion values, B_B and B_A. Equations (12) and (13) give the values of B_B and B_A for any set of operating conditions (V_I, V_0, and P_0), semiconductor parameters (V_D and V_Q), transformer parameters (N_P, N_S, μ, ℓ, A, and B_R), and controller time parameters (T, t_{on}, t_{off}). The plus sign is used for B_B and the minus sign for B_A. These expressions are obtained by recognizing that $(B_B,B_A) = B_{av} +$
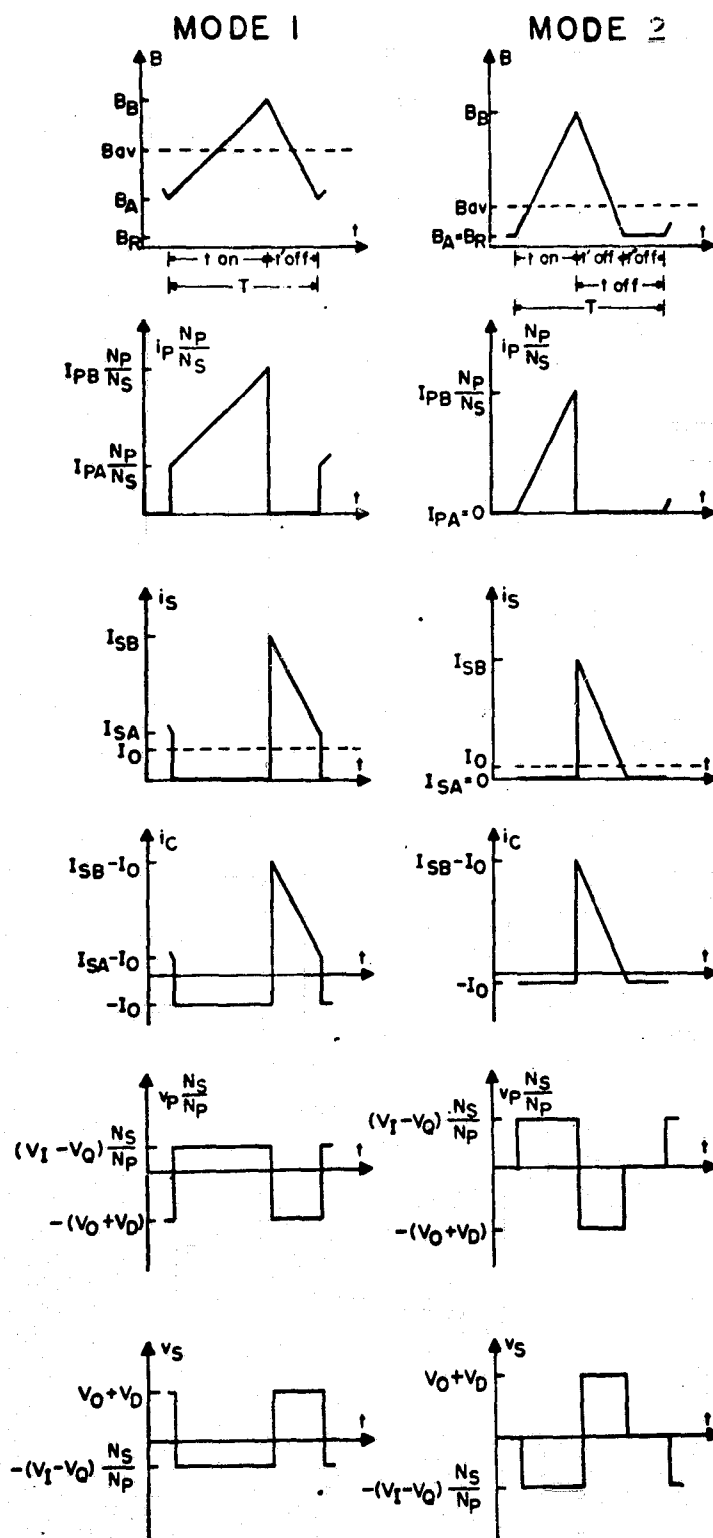
Figure 3.2 Flux-density, current, and voltage waveform for the two-winding voltage step-up/current step-up converter

Table 3.1 General Characteristics for the Two-Winding
Voltage Step-Up/Current Step-Up Converter

GENERAL RELATIONSHIPS			
CIRCUIT EQUATIONS	DURING t_{on}	$\dfrac{\mu N_P^2 A}{\ell} \dfrac{di_P}{dt} = V_I - V_Q$	(1)
		$i_C = -I_0$	(2)
		$i_S = 0$	(3)
	DURING t'_{off}	$\dfrac{\mu N_S^2 A}{\ell} \dfrac{di_S}{dt} = V_0 + V_D$	(4)
		$i_C = i_S - I_0$	(5)
		$i_P = 0$	(6)
TIME RELATION-SHIPS		$T = t_{on} + t'_{off} + t''_{off} = t_{on} + t_{off}$	(7)
		$\dfrac{t_{on}}{t'_{off}} = \dfrac{N_P(V_0 + V_D)}{N_S(V_I - V_Q)}$	(8)

Table 3.2(A)   Time and Flux-Density Relationships for Constant Frequency Two-Winding Voltage Step-Up/Current Step-Up Converter

CONSTANT FREQUENCY CONTROLLER	
MODE 1	
$t''_{off} = 0$	(9,FQ)
$\alpha = \dfrac{N_P(V_0+V_D)}{N_P(V_0+V_D)+N_S(V_I-V_Q)}$	(10)
α decreases with V_I and is independent of P_0.	(11)
$B_B, B_A = B_R + \dfrac{\mu P_0}{\ell V_0}\left[\dfrac{N_P(V_0+V_D)+N_S(V_I-V_Q)}{V_I-V_Q}\right]$ $\pm \dfrac{(V_0+V_D)(V_I-V_Q)T}{2A[N_P(V_0+V_D)+N_S(V_I-V_Q)]}$	(12),(13)
$B_{B\ max}$ occurs at $P_0 = P_{0\ max}$ and $V_I = V_{I\ min}$.	(14)
$B_{A\ min}$ occurs at $P_0 = P_{0\ min}$ and $V_I = V_{I\ max}$.	(15)
MODE 2	
$t''_{off} = T - \dfrac{N_P}{V_I-V_Q}\sqrt{\dfrac{2\mu TP_0 A(V_0+V_D)}{\ell V_0}} - N_S\sqrt{\dfrac{2\mu TP_0 A}{\ell V_0(V_0+V_D)}}$	(16)
$t_{on} = \dfrac{N_P}{V_I-V_Q}\sqrt{\dfrac{2\mu TP_0 A(V_0+V_D)}{\ell V_0}}$	(17)
$\alpha = \dfrac{N_P}{V_I-V_Q}\sqrt{\dfrac{2\mu P_0 A(V_0+V_D)}{\ell V_0 T}}$	(18)
α decreases with V_I and increases with P_0.	(19)
$B_B = B_R + \sqrt{\dfrac{2\mu TP_0(V_0+V_D)}{\ell AV_0}}$	(20)
$B_{B\ max}$ occurs at $P_0 = P_{0\ max}$ and is independent of V_I.	(21)
$B_A = B_R$	(22)

Table 3.2(B) Time and Flux-Density Relationships for Constant On-Time Voltage Step-Up/ Current Step-Up Converter

CONSTANT ON-TIME CONTROLLER	
MODE 1	
$t''_{off} = 0$	(9,TN)
$\alpha \triangleq \dfrac{t_{on}}{T} = \dfrac{N_P(V_0+V_D)}{N_P(V_0+V_D)+N_S(V_I-V_Q)}$	(10)
α decreases with V_I and is independent of P_0.	(11)
$B_B,\ B_A = B_R + \dfrac{\mu P_0}{\ell V_0}\left(N_S + \dfrac{(V_0+V_D)N_P}{V_I-V_Q}\right) \pm \dfrac{(V_I-V_Q)t_{on}}{2AN_P}$	(12),(13)
$B_{B,max}$ occurs at $P_0 = P_{0,max}$ and $V_I = V_{IO}$, where $V_{IO} = V_{I,min}$ or $V_{I,max}$, depending on the particular design.	(14)
$B_{A,min}$ occurs at $P_0 = P_{0,min}$ and $V_I = V_{I,max}$.	(15)
MODE 2	
$t'_{off} = \dfrac{N_S(V_I-V_Q)t_{on}}{N_P(V_0+V_D)}$	(16)
$T = \dfrac{\ell(V_I-V_Q)^2 V_0 t_{on}^2}{2N_P^2 \mu A(V_0+V_D)}$	(17)
$\alpha \triangleq \dfrac{t_{on}}{T} = \dfrac{2N_P^2 \mu A P_0(V_0+V_D)}{\ell(V_I-V_Q)^2 V_0 t_{on}}$	(18)
α decreases with V_I and increases with P_0.	(19)
$B_B = B_R + \dfrac{(V_I-V_Q)t_{on}}{AN_P}$	(20)
$B_{B,max}$ occurs at $V_{I,max}$ and is independent of P_0.	(21)
$B_A = B_R$	(22)

Table 3.2(C) Time. and Flux-Density Relationships for Constant Off-Time Voltage Step-Up/ Current Step-Up Converter

CONSTANT OFF-TIME CONTROLLER	
MODE 1	
$t''_{off} = 0$	(9,TF)
$\alpha \triangleq \dfrac{t_{on}}{T} = \dfrac{N_P(V_0+V_D)}{N_P(V_0+V_D)+N_S(V_I-V_Q)}$	(10)
α decreases with V_I and is independent of P_0.	(11)
$B_B,\ B_A = B_R + \dfrac{\mu P_0}{\ell V_0}\left(N_S + \dfrac{(V_0+V_D)N_P}{V_I-V_Q}\right) \pm \dfrac{(V_0+V_D)t_{off}}{2AN_S}$	(12),(13)
$B_{B,max}$ occurs at $P_0 = P_{0,max}$ and $V_I = V_{I,min}$.	(14)
$B_{A,min}$ occurs at $P_0 = P_{0,min}$ and $V_I = V_{I,max}$.	(15)
MODE 2	
$T = T_R$ where T_R is the larger root of the quadratic $$T_R^2 - 2\left(t_{off} + \dfrac{N_P^2\mu AP_0(V_0+V_D)}{\ell V_0(V_I-V_Q)^2}\right)T_R + t_{off}^2 = 0$$	(16)
$t''_{off} = t_{off} - \sqrt{\dfrac{2N_S^2\mu AP_0 T_R}{\ell V_0(V_0+V_D)}}$	(17)
$\alpha \triangleq \dfrac{t_{on}}{T} = \dfrac{1}{(V_I-V_Q)}\sqrt{\dfrac{2N_P^2\mu AP_0(V_0+V_D)}{\ell T_R V_0}}$	(18)
α decreases with V_I and increases with P_0	(19)
$B_B = B_R + \sqrt{\dfrac{2\mu P_0(V_0+V_D)T_R}{\ell AV_0}}$	(20)
$B_{B,max}$ occurs at $P_0 = P_{0,max}$ and $V_{I,min}$.	(21)
$B_A = B_R$	(22)

$(\Delta B/2)$, where $B_{av} = B_R + [\mu N_S(I_{SB} + I_{SA})/2\ell]$ and $\Delta B = \mu N_S(I_{SB} - I_{SA})/\ell$.

The use of (4), (10) and the fact that the average output current $P_0/V_0 = (t'_{off}/T)[(I_{SB} + I_{SA})/2]$ leads to (12) and (13). Evaluation of the partial derivatives of these expressions with respect to P_0 and V_I shows that the two extremum values, $B_{B,max}$ and $B_{A,min}$, occur for the conditions given in (14) and (15). Appendix A outlines the steps leading to these two pairs of conditions.

The time relationships for Mode 2 operation are given by (16), and (17). Manipulation of (7), (8), and (16) leads to the expression for duty cycle in (18). By examining the partial derivatives of α with respect to V_I and P_0, the duty cycle α can be shown to decrease as V_I increases and to increase as P_0 increases (19). The peak value of the flux excursion B_B is obtained by using $B_B = B_R + (\mu N_S I_{SB}/\ell)$ and the fact that the average output current $P_0/V_0 = (t'_{off}/T)(I_{SB}/2)$. Elimination of I_{SB} from these two relationships and the use of (8) and (18) leads to (20). Appendix C gives a more detailed derivation of the Mode 2 time relationships and the flux-density expressions just described. The circuit operating conditions for which B_B has its extremum value is given by (21), obtained by examining the partial derivatives of B_B with respect to P_0 and V_I.

Table 3.3(A),(B) and (C) present expressions for the transformer rms primary current I_{Pe} amd rms secondary current I_{Se} for both modes of operation. The method for locating the maximum currents, and the reasons for selecting mode 1 expressions to compute the maximum rms currents are similar to those discussed in Sec.2.4. The derivation for the expressions for currents, and the conditions at which the currents reache their maximum values are given in Appendix D.

RMS Primary and Secondary Currents for
TABLE 3.3(A) Constant Frequency Two-Winding Voltage
Step-up/Current Step-up Converter

MODE 1	$$I_{Pe} = \sqrt{\left[\left[\frac{P_0}{V_0}\left(\frac{N_S}{N_P}\right) + \frac{V_0+V_D}{V_I-V_Q}\right]^2 + \frac{1}{12}\left[\frac{\ell(V_0+V_D)(V_I-V_Q)T}{\mu A[N_P^2(V_0+V_D)+N_P N_S(V_I-V_Q)]}\right]^2\right] \cdot \frac{N_P(V_0+V_D)}{N_P(V_0+V_D)+N_S(V_I-V_Q)}}$$	(23,FQ)
	$I_{Pe,max}$ occurs at $P_0 = P_{0,max}$ and $V_I = V_{I,min}$.	(24)
MODE 2	$$I_{Pe} = \sqrt{\frac{2P_0(V_0+V_D)}{3(V_I-V_Q)V_0}}\sqrt{\frac{2\ell P_0(V_0+V_D)T}{N_P^2\,\mu\,AV_0}}$$	(25)
	$I_{Pe,max}$ occurs at $P_0 = P_{0,max}$ and $V_I = V_{I,min}$.	(26)
$I_{Pe,max}$	$I_{Pe,max}$ occurs at $P_0 = P_{0,max}$ and $V_I = V_{I,min}$.	(27)
	$I_{Pe,max} = I_{Pe}(P_0 = P_{0,max},\ V_I = V_{I,min})$ using Eq. (23) for I_{Pe}	(28)
MODE 1	$I_{Se} = I_{Pe}\sqrt{\dfrac{N_P(V_I-V_Q)}{N_S(V_0+V_D)}}$ using (23) for I_{Pe}	(29)
	$I_{Se,max}$ occurs at $P_0 = P_{0,max}$ and $V_I = V_{I,min}$.	(30)
MODE 2	$I_{Se} = I_{Pe}\sqrt{\dfrac{N_P(V_I-V_Q)}{N_S(V_0+V_D)}}$ using (25) for I_{Pe}	(31)
	$I_{Se,max}$ occurs at $P_0 = P_{0,max}$ and $V_I = V_{I,min}$.	(32)
$I_{Se,max}$	$I_{Se,max}$ occurs at $P_0 = P_{0,max}$ and $V_I = V_{I,min}$.	(33)
	$I_{Se,max} = I_{Pe,max}\sqrt{\dfrac{N_P(V_{I,min}-V_Q)}{N_S(V_0+V_D)}}$ using (28) for I_{Pe}.	(34)

TABLE 3.3(B) RMS Primary and Secondary Currents for Constant On-Time Two-Winding Voltage Step-up/Current Step-up Converter

MODE 1	$I_{Pe} = \sqrt{\left[\left[\dfrac{P_0}{V_0}\left(\dfrac{N_S}{N_P} + \dfrac{V_0+V_D}{V_I-V_Q}\right)\right]^2 + \dfrac{1}{12}\left[\dfrac{\ell(V_I-V_Q)t_{off}}{N_P^2 \mu A}\right]^2\right]} \cdot \dfrac{N_P(V_0+V_D)}{N_P(V_0+V_D)+N_S(V_I-V_Q)}$ (23,TN)
	I_{Pe} occurs at $P_0 = P_{0,max}$ and $V_I = V_{I,min}$ or $V_{I,max}$. (24)
MODE 2	$I_{Pe} = \sqrt{\dfrac{2\mu P_0(V_0+V_D)t_{on}}{N_P^2 \mu A V_0}}$ (25)
	$I_{Pe,max}$ occurs at $P_0 = P_{0,max}$ and is independent of V_I. (26)
$I_{Pe,max}$	$I_{Pe,max}$ occurs at $P_0 = P_{0,max}$ and $V_I = V_{I,min}$ or $V_{I,max}$ (27)
	$I_{Pe,max} = I_{Pe}(P_0 = P_{0,max}, V_I = V_{I,min})$ or $I_P(P_0 = P_{0,max}, V_I = V_{I,max})$ whichever is the larger, using (23) for I_{Pe}. (28)
MODE 1	$I_{Se} = I_{Pe}\sqrt{\dfrac{N_P(V_I-V_Q)}{N_S(V_0+V_D)}}$ using (23) for I_{Pe} (29)
	$I_{Se,max}$ occurs at $P_0 = P_{0,max}$ and $V_I = V_{I,min}$ or $V_{I,max}$. (30)
MODE 2	$I_{Se} = I_{Pe}\sqrt{\dfrac{N_P(V_I-V_Q)}{N_S(V_0+V_D)}}$ using (25) for I_{Pe} (31)
	$I_{Se,max}$ occurs at $P_0 = P_{0,max}$ and $V_I = V_{I,max}$. (32)
$I_{Se,max}$	$I_{Se,max} = I_{Se}(P_0 = P_{0,max}, V_I = V_{I,min})$ or $I_{Se}(P_0 = P_{0,max}, V_I = V_{I,max})$ whichever is the larger, using (29) for I_{Se}. (33)

TABLE 3.3(C)

RMS Primary and Secondary Currents for
Constant Off-Time Two-Winding Voltage
Step-up/Current Step-up Converter

MODE 1	$$I_{Pe} = \sqrt{\left[\left[\frac{P_0}{V_0}\left(\frac{N_S}{N_P} + \frac{V_0+V_D}{V_I-V_Q}\right)\right]^2 + \frac{1}{12}\left[\frac{\ell(V_0+V_D)t_{off}}{N_P N_S \mu A}\right]^2\right] \cdot \frac{N_P(V_0+V_D)}{N_P(V_0+V_D)+N_S(V_I-V_Q)}} \qquad (23,TF)$$
	$I_{Pe,max}$ occurs at $P_0 = P_{0,max}$ and $V_I = V_{I,min}$. $\qquad (24)$
MODE 2	$$I_{Pe} = \sqrt{\frac{2P_0(V_0+V_D)}{3(V_I-V_Q)V_0}} \qquad \sqrt{\frac{2\ell P_0(V_0+V_D)T_R}{N_P^2 \mu A V_0}} \qquad (25)$$
	$I_{Pe,max}$ occurs at $P_0 = P_{0,max}$ and $V_I = V_{I,min}$. $\qquad (26)$
$I_{Pe,max}$	$I_{Pe,max}$ occurs at $P_0 = P_{0,max}$ and $V_I = V_{I,min}$. $\qquad (27)$
	$I_{Pe,max} = I_{Pe}(P_0 = P_{0,max}, \ V_V = V_{I,min})$ using (23) for I_{Pe}. $\qquad (28)$
MODE 1	$I_{Se} = I_{Pe} \cdot \sqrt{\frac{N_P(V_I-V_Q)}{N_S(V_0+V_D)}} \qquad$ using (23) for I_{Pe}. $\qquad (29)$
	$I_{Se,max}$ occurs at $P_{0,max}$ and $V_{I,min}$. $\qquad (30)$
MODE 2	$I_{Se} = I_{Pe} \sqrt{\frac{N_P(V_I-V_Q)}{N_S(V_0+V_D)}} \qquad$ using (25) for I_{Pe} $\qquad (31)$
	$I_{Se,max}$ occurs at $P_0 = P_{0,max}$ and $V_I = V_{I,min}$. $\qquad (32)$
$I_{Se,max}$	$I_{Se,max}$ occurs at $P_0 = P_{0,max}$ and $V_I = V_{I,min}$ $\qquad (33)$
	$I_{Se,max} = I_{Pe,max} \sqrt{\frac{N_P(V_{I,min}-V_Q)}{N_S(V_0+V_D)}} \qquad$ using (28) for I_{Pe}. $\qquad (34)$

3.3 Mode Restriction

In Chapter II, a discussion of a mode restriction in the design pro-
cedures for single-winding converters is presented. For similar reasons,
all of the designs considered in this chapter must operate in Mode 1 at
least at the operating point given by (14), the point at which $B_B = B_{B,max}$.
Thus, Mode 1 equation for B_B (12) should be used to determine N from a spec-
ified value of B_{max}. Setting $B_B = B_{B,max}$ in (12) for the condition of (14)
and manipulating the resultant equations leads to (35) for each of the three
controllers

$$N_S + \frac{(V_0+V_D)}{(V_1-V_Q)} N_P = \frac{\ell V_0}{2\mu P_2} \left[(B_{max}-B_R) + \sqrt{(B_{max}-B_R)^2 - \frac{2\mu T P_2(V_0+V_D)}{\ell A V_0}} \right] \quad (35,FQ)$$

$$\frac{\mu P_2}{\ell V_0} \left[N_P N_S + \frac{(V_0+V_D)N_P^2}{(V_{10}-V_Q)} \right] - (B_2-B_R)N_P + \frac{(V_{10}-V_Q)t_{on}}{2A} = 0 \quad (35,TN)$$

$$\frac{\mu P_2}{\ell V_0} \left[\frac{(V_0+V_D)}{(V_1-V_Q)} N_P N_S + N_S^2 \right] - (B_2-B_R)N_S + \frac{(V_0+V_D)t_{off}}{2A} = 0 \quad (35,TF)$$

where $V_1 \triangleq V_{I,min}$, $B_2 \triangleq B_{max}$, $P_2 = P_{0,max}$ and $V_{10} = V_{I,min}$ or $V_{I,max}$, de-
pending on which condition yields $B_{B,max}$ as described in (14,TN). In other
words, any converter-transformer design which satisfies (35) will never ex-
ceed the specified B_{max} at any point of its operating range. As can be seen
from (35), even for a particular core with known core parameters and defined
operating range, N_P and N_S are not uniquely determined. Consequently, this
relationship provides an additional degree of freedom over that available
when a single-winding energy-storage converter is used to meet the same
specifications. It therefore opens the way for the designer to choose an
additional performance criterion to be met by his design. The next section

discusses and shows how this additional degree of freedom provides a variety of useful options to the designer.

3.4 Design Options

Ten design options are considered:

(A) Duty cycle centered at a particular value

(B) Minimum duty cycle

(C) Range of duty-cycle variation

(D) Maximum transistor collector-to-emitter voltage

(E) Maximum reverse diode voltage

(F) Maximum peak transistor current

(G) Maximum peak diode current

(H) Maximum duty cycle

(I) Total number of turns

(J) Turns ratio

Each of these ten options leads to an option constraint equation which involves N_p or N_S or both. The mathematical description of the design options and the option constraint equations for the ten options listed above are summarized in Table 3.4, where U_y represents the value of a special performance constraint. The subscript y corresponds to one of the ten design options identified by letters A through J. In the column labeled MODE NO.,

1 indicates that the converter-transformer design which uses this option will operate in Mode 1 over the entire operating range of output-power/input-voltage while 1 or 2 indicates that the design will operate either in Mode 1 entirely or in Mode 2 over a portion of the operating range. Mode 2 operation is not included in options A, B, and C, because the resultant constraint equations are not amenable to analytical solutions for N_p and N_S.

Table 3.4 Option Descriptions and Option
Constraint Equations

OPTION NO	OPTION DESCRIPTION	MODE NO	OPTION CONSTRAINT EQUATION
A	$\dfrac{\alpha_{min}+\alpha_{max}}{2}=U_A$	1	$\dfrac{N_S}{N_P}=\gamma_A=\dfrac{-(V_0+V_D)}{2(V_1-V_Q)(V_Q-V_Q)}\left[(V_1+V_2-2V_Q)(1-\dfrac{1}{2U_A})\right.$ $\left.+\sqrt{(V_1+V_2-2V_Q)^2(1-\dfrac{1}{2U_A})^2-4(V_1-V_Q)(V_2-V_Q)(1-\dfrac{1}{U_A})}\right.$
B	$\alpha_{min}=U_B$	1	$\dfrac{N_S}{N_P}=\gamma_B=\dfrac{V_0+V_D}{V_2-V_Q}(\dfrac{1}{U_B}-1)$
C	$\alpha_{max}-\alpha_{min}=U_C$	1	$\dfrac{N_S}{N_P}=\gamma_C=\dfrac{-(V_0+V_D)}{2(V_1-V_Q)(V_2-V_Q)}\left[(V_1+V_2-2V_Q-\dfrac{V_2-V_1}{U_C})\right.$ $\left.+\sqrt{(V_1+V_2-2V_Q-\dfrac{V_2-V_1}{U_C})^2-4(V_1-V_Q)(V_2-V_Q)}\right]$
D	$V_{CE_{max}}=U_D$	1 or 2	$\dfrac{N_S}{N_P}=\gamma_D=\dfrac{V_0+V_D}{U_D-V_2}$
E	$V_{DR_{max}}=U_E$	1 or 2	$\dfrac{N_S}{N_P}=\gamma_E=\dfrac{U_E-V_0}{V_2-V_Q}$
F	$i_{coll_{max}}=U_F$	1 or 2	$N_P=\dfrac{\ell(B_2-B_R)}{\mu\,U_F}$
G	$i_{D_{max}}=U_G$	1 or 2	$N_S=\dfrac{\ell(B_2-B_R)}{\mu\,U_G}$
H	$\alpha_{max}=U_H$	1 or 2	$\dfrac{N_S}{N_P}=\gamma_H=\dfrac{V_0+V_D}{V_1-V_Q}(\dfrac{1}{U_H}-1)$
I	$N_P+N_S=U_I$	1 or 2	$N_P+N_S=U_I$
J	$\dfrac{N_S}{N_P}=U_J$	1 or 2	$\dfrac{N_S}{N_P}=U_J$

Option Solutions for N_P and N_S for

Table 3.5(A) Constant Frequency Two-Winding Voltage Step-Up/Current Step-Up Converter

	CONSTANT FREQUENCY CONTROLLER	
	COMMON EQUATION	
	$$N_S + \frac{(V_0+V_D)}{(V_1-V_Q)}\,N_P = \frac{\ell\,V_0}{2\mu P_2}\left[(B_2-B_R) + \sqrt{(B_2-B_R)^2 - \frac{2\mu T P_2(V_0+V_D)}{\ell A\,V_0}}\right] \triangleq K \quad (35,FQ)$$	

OPTION NO	OPTION DESCRIPTION	MODE NO	SOLUTION FOR N_P	SOLUTION FOR N_S
A	$\dfrac{\alpha_{min}+\alpha_{max}}{2}=U_A$	1	$N_P = \dfrac{K(V_1-V_Q)}{\gamma_A(V_1-V_Q)+(V_0+V_D)}$	$N_S = \gamma_A N_P$
B	$\alpha_{min}=U_B$	1	$N_P = \dfrac{K(V_1-V_Q)}{\gamma_B(V_1-V_Q)+(V_0+V_D)}$	$N_S = \gamma_B N_P$
C	$\alpha_{max}-\alpha_{min}=U_C$	1	$N_P = \dfrac{K(V_1-V_Q)}{\gamma_C(V_1-V_Q)+(V_0+V_D)}$	$N_S = \gamma_C N_P$
D	$V_{CE_{max}}=U_D$	1 or 2	$N_P = \dfrac{K(V_1-V_Q)}{\gamma_D(V_1-V_Q)+(V_0+V_D)}$	$N_S = \gamma_D N_P$
E	$V_{DR_{max}}=U_E$	1 or 2	$N_P = \dfrac{K(V_1-V_Q)}{\gamma_E(V_1-V_Q)+(V_0+V_D)}$	$N_S = \gamma_E N_P$
F	$i_{coll._{max}}=U_F$	1 or 2	$N_P = \dfrac{\ell(B_2-B_R)}{\mu\,U_F}$	$N_S = K - \dfrac{(V_0+V_D)N_P}{(V_1-V_Q)}$
G	$i_{D_{max}}=U_G$	1 or 2	$N_P = \left(K - \dfrac{\ell(B_2-B_R)}{\mu U_G}\right)\dfrac{V_1-V_Q}{V_0+V_D}$	$N_S = \dfrac{\ell(B_2-B_R)}{\mu U_G}$
H	$\alpha_{max}=U_H$	1 or 2	$N_P = \dfrac{K(V_1-V_Q)}{\gamma_H(V_1-V_Q)+(V_0+V_D)}$	$N_S = \gamma_H N_P$
I	$N_P+N_S=U_I$	1 or 2	$N_P = (K-U_I)\dfrac{V_1-V_Q}{V_0+V_D-V_1+V_Q}$	$N_S = U_J N_P$
J	$\dfrac{N_S}{N_P}=U_J$	1 or 2	$N_P = \dfrac{K(V_1-V_Q)}{U_J(V_1-V_Q)+(V_0+V_D)}$	$N_S = U_J N_P$

Table 3.5(B) Option Solutions for N_p and N_s for Constant On-Time Two-Winding Voltage Step-Up/Current Step-Up Converter

			CONSTANT ON-TIME CONTROLLER	
			COMMON EQUATION $\frac{\mu P_2}{\ell V_0}\left\{N_p N_s + \frac{(V_0+V_D)N_p^2}{(V_{IO}-V_Q)}\right\} - (B_2-B_R)N_p + \frac{(V_{IO}-V_Q)t_{on}}{2A} = 0$ (35, 3H)	
OPTION NO	OPTION DESCRIPTION	MODE NO	SOLUTION FOR N_P	SOLUTION FOR N_S
A	$\frac{a_{min}+a_{max}}{2}=U_A$	1	$N_P=\frac{\ell V_0\,(V_{IO}-V_Q)}{2\mu P_2[V_0+V_D+\gamma_A(V_{IO}-V_Q)]}\left[(B_2-B_R)+\sqrt{(B_2-B_R)^2-\frac{2\mu P_2}{\ell A V_0}[\gamma_A(V_{IO}-V_Q)+V_0+V_D]t_{on}}\right]$	$N_S=-\gamma_A N_P$
B	$a_{min}=U_B$	1	$N_P=\frac{\ell V_0\,(V_{IO}-V_Q)}{2\mu P_2[V_0-V_D+\gamma_B(V_{IO}-V_Q)]}\left[(B_2-B_R)+\sqrt{(B_2-B_R)^2-\frac{2\mu P_2}{\ell A V_0}[\gamma_B(V_{IO}-V_Q)+V_0+V_D]t_{on}}\right]$	$N_S=\gamma_B N_P$
C	$a_{max}-a_{min}=U_C$	1	$N_P=\frac{\ell V_0\,(V_{IO}-V_Q)}{2\mu P_2[V_0+V_D+\gamma_C(V_{IO}-V_Q)]}\left[(B_2-B_R)+\sqrt{(B_2-B_R)^2-\frac{2\mu P_2}{\ell A V_0}[\gamma_C(V_{IO}-V_Q)+V_0+V_D]t_{or}}\right]$	$N_S=\gamma_C N_P$
D	$V_{CE_{max}}=U_D$	1 or 2	$N_P=\frac{\ell V_0\,(V_{IO}-V_Q)}{2\mu P_2[V_0-V_D+\gamma_D(V_{IO}-V_Q)]}\left[(B_2-B_R)+\sqrt{(B_2-B_R)^2-\frac{2\mu P_2}{\ell A V_0}[\gamma_D(V_{IO}-V_Q)+V_0+V_D]t_{on}}\right]$	$N_S=\gamma_D N_P$
E	$V_{DR_{max}}=U_E$	1 or 2	$N_P=\frac{\ell V_0\,(V_{IO}-V_Q)}{2\mu P_2[V_0+V_D+\gamma_E(V_{IO}-V_Q)]}\left[(B_2-B_R)+\sqrt{(B_2-B_R)^2-\frac{2\mu P_2}{\ell A V_0}[\gamma_E(V_{IO}-V_Q)+V_0+V_D]t_{on}}\right]$	$N_S=\gamma_E N_P$
F	$I_{coll._{max}}=U_F$	1 or 2	$N_P=\frac{\ell(B_2-B_R)}{\mu U_F}$	$N_S=\frac{\ell V_0}{\mu P_2}\left((B_2-B_R)-\frac{(V_{IO}-V_Q)t_{on}}{2AN_p}\right)-\frac{(V_0+V_D)\ell_P}{(V_{IO}-V_Q)}$
G	$I_{D_{max}}=U_G$	1 or 2	$N_P=\frac{\ell V_0(V_{IO}-V_Q)}{2\mu P_2(V_0+V_D)}\left[(B_2-B_R)-\frac{\mu P_2}{\ell V_0}N_S+\sqrt{(B_2-B_R-\frac{\mu P_2}{\ell V_0}N_S)^2-\frac{2\mu P_2(V_0+V_D)t_{on}}{\ell A V_0}}\right]$	$N_S=\frac{\ell(B_2-B_R)}{\mu U_G}$
H	$a_{max}=U_H$	1 or 2	$N_P=\frac{\ell V_0\,(V_{IO}-V_Q)}{2\mu P_2[V_0+V_D+\gamma_H(V_{IO}-V_Q)]}\left[(B_2-B_R)+\sqrt{(B_2-B_R)^2-\frac{2\mu P_2}{\ell A V_0}[\gamma_H(V_{IO}-V_Q)+V_0+V_D]t_{on}}\right]$	$N_S=\gamma_H N_P$
I	$N_p+N_s=U_I$	1 or 2	$N_P=\frac{\ell V_0\,(V_{IO}-V_Q)}{2\mu P_2(V_0+V_D-V_{IO}+V_Q)}\left[((B_2-B_R)-\frac{\mu P_2}{\ell V_0}U_I+\sqrt{(B_2-B_R-\frac{\mu P_2}{\ell V_0}U_I)^2-\frac{2\mu P_2(V_0+V_D-V_{IO}+V_Q)t_{on}}{\ell A V_0}}\right]$	$N_S=U_I-N_P$
J	$\frac{N_s}{N_p}=U_J$	1 or 2	$N_P=\frac{\ell V_0\,(V_{IO}-V_Q)}{2\mu P_2[V_0+V_D+\gamma_J(V_{IO}-V_Q)]}\left[(B_2-B_R)+\sqrt{(B_2-B_R)^2-\frac{2\mu P_2}{\ell A V_0}[\gamma_J(V_{IO}-V_Q)+V_0+V_D]t_{on}}\right]$	$N_S=\gamma_J N_P$

TABLE 3.5 (C)   Option Solutions for N_P and N_S for Constant Off-Time Two-Winding Voltage Step-up/Current Step-up Converter

			CONSTANT OFF-TIME CONTROLLER	
			COMMON EQUATION $\dfrac{\mu F_2}{\Lambda V_0}\left(\dfrac{(V_0+V_0)}{(V_1-V_0)}\right)N_P N_S \ast N_S{}^2 - (b_2-B_R)N_S + \dfrac{(V_0+V_0)t_{off}}{\Lambda} = 0 \quad (35, TF)$	
OPTION NO	OPTION DESCRIPTION	MODE NO	SOLUTION FOR N_P	SOLUTION FOR N_S
A	$\dfrac{P_{mir}+P_{max}}{2} = U_A$	1	$N_P = \dfrac{\lambda V_0\,(V_1-V_0)}{2\mu P_2[V_0+V_0+\gamma_A(V_1-V_0)]}\left[(B_2-B_R)\right.$ $\left.+\sqrt{(B_2-B_R)^2 - \dfrac{2\mu P_2(V_0+V_0)}{\lambda A V_0}[1+\dfrac{(V_0+V_0)}{\gamma_A(V_1-V_0)}]t_{off}}\right]$	$N_S = \gamma_A N_P$
B	$P_{min} = U_B$	1	$N_P = \dfrac{\lambda V_0\,(V_1-V_0)}{2\mu P_2[V_0+V_0+\gamma_B(V_1-V_0)]}\left[(B_2-B_R)\right.$ $\left.+\sqrt{(B_2-B_R)^2 - \dfrac{2\mu P_2(V_0+V_0)}{\lambda A V_0}[1+\dfrac{(V_0+V_0)}{\gamma_B(V_1-V_0)}]t_{off}}\right]$	$N_S = \gamma_B N_P$
C	$P_{max} = P_{min} = U_C$	1	$N_P = \dfrac{\lambda V_0\,(V_1-V_0)}{2\mu P_2[V_0+V_0+\gamma_C(V_1-V_0)]}\left[(B_2-B_R)\right.$ $\left.+\sqrt{(B_2-B_R)^2 - \dfrac{2\mu P_2(V_0+V_0)}{\lambda A V_0}[1+\dfrac{(V_0+V_0)}{\gamma_C(V_1-V_0)}]t_{off}}\right]$	$N_S = \gamma_C N_P$
D	$V_{CE_{max}} = U_D$	1 or 2	$N_P = \dfrac{\lambda V_0\,(V_1-V_0)}{2\mu P_2[V_0+V_0+\gamma_D(V_1-V_0)]}\left[(B_2-B_R)\right.$ $\left.+\sqrt{(B_2-B_R)^2 - \dfrac{2\mu P_2(V_0+V_0)}{\lambda A V_0}[1+\dfrac{(V_0+V_0)}{\gamma_D(V_1-V_0)}]t_{off}}\right]$	$N_S = \gamma_D N_P$
E	$V_{DR_{max}} = U_E$	1 or 2	$N_P = \dfrac{\lambda V_0\,(V_1-V_0)}{2\mu P[V_0+V_0+\gamma_E(V_1-V_0)]}\left[(B_2-B_R)\right.$ $\left.+\sqrt{(B_2-B_R)^2 - \dfrac{2\mu P_2(V_0+V_0)}{\lambda A V_0}[1+\dfrac{(V_0+V_0)}{\gamma_E(V_1-V_0)}]t_{off}}\right]$	$N_S = \gamma_E N_P$
F	$I_{coll._{max}} = U_F$	1 or 2	$N_P = \dfrac{\lambda(B_2-B_R)}{\mu U_F}$	$N_S = \dfrac{\lambda V_0}{2\mu P_2}\left[(B_2-B_R)-\dfrac{\mu P_2(V_0+V_0)}{\lambda V_0(V_1-V_0)}N_P\right.$ $\left.+\sqrt{[B_2-B_R-\dfrac{\mu P_2(V_0+V_0)}{\lambda V_0(V_1-V_0)}N_P]^2-\dfrac{2\mu P_2(V_0+V_0)t_{off}}{\lambda A V_0}}\right]$
G	$I_{D_{max}} = U_G$	1 or 2	$N_P = \dfrac{\lambda V_0(V_1-V_0)}{\mu P_2(V_0+V_0)}\left[(B_2-B_R)-\dfrac{(V_0+V_0)t_{off}}{2\lambda N_S}\right.$ $\left.-\dfrac{(V_1-V_0)N_S}{(V_3+V_0)}\right]$	$N_S = \dfrac{\lambda(B_2-B_R)}{\mu U_G}$
H	$I_{max} = U_H$	1 or 2	$N_P = \dfrac{\lambda V_0\,(V_1-V_0)}{2\mu P_2[V_0+V_0+\gamma_H(V_1-V_0)]}\left[(B_2-B_R)\right.$ $\left.+\sqrt{(B_2-B_R)^2 - \dfrac{2\mu P_2(V_0+V_0)}{\lambda A V_0}[1+\dfrac{(V_0+V_0)}{\gamma_H(V_1-V_0)}]t_{off}}\right]$	$N_S = \gamma_H N_P$
I	$N_P+N_S = U_I$	1 or 2	$N_P = U_I - \dfrac{\lambda V_0(V_1-V_0)}{2\mu P_2(V_1-V_0-V_0)}\left[\left((B_2-B_R)-\dfrac{\mu P_2(V_0+V_0)U_I}{\lambda V_0(V_1-V_0)}\right)\right.$ $+\sqrt{\left[B_2-B_R-\dfrac{\mu P_2(V_0+V_0)}{\lambda V_0(V_1-V_0)}U_I\right]^2}$ $\left.-\left(\dfrac{2\mu P_2(V_0+V_0)}{\lambda A V_0}\right)\left(1-\dfrac{V_0+V_0}{V_1-V_0}\right)t_{off}\right]$	$N_S = U_I - N_P$
J	$\dfrac{N_S}{N_P} = U_J$	1 or 2	$N_P = \dfrac{\lambda V_0\,(V_1-V_0)}{2\mu P_2[V_0+V_0+\gamma_J(V_1-V_0)]}\left[(B_2-B_R)\right.$ $\left.+\sqrt{(B_2-B_R)^2 - \dfrac{2\mu P_2(V_0+V_0)}{\lambda A V_0}[1+\dfrac{(V_0+V_0)}{\gamma_J(V_1-V_0)}]t_{off}}\right]$	$N_S = \gamma_J N_P$

The derivations of these constraint equations are given in Appendix E.

The option constraint equations presented in Table 3.4 are independent of controller types. Each of the constraint equations can be solved simultaneously with each of the three equations (35,FQ), (35,TN), and (35,TF) to yield solutions for N_p and N_S for each of the three controller types. These solution sets are in terms of core parameters and converter operating conditions, and are presented in Table 3.5-A,B, and C, with the appropriate (35) repeated at the top of each table. Appendix F outlines the steps followed in these solution sets. Each of these three solution sets provides the principal equations for each option to be used later in the design procedure. It should be noted that the solution sets obtained are based on the maximum specified flux density B_{max} at the critical input-output conditions given in (14) and on the value of a special performance constraint. The detailed use of these tables for designing energy-storage transformers for two-winding converters is illustrated with numerical examples in the next section.

3.5 Design Examples

In this section two examples are presented which demonstrate the procedures for designing the energy-storage transformers for two-winding converters employing a constant on-time controller and a constant off-time controller. For the case of a constant-frequency controller, the design procedure is quite similar to the case of a constant off-time controller and will not be presented here. The magnetic cores chosen for these examples are obtained from commerical catalog MPP-303S by Magnetics Inc.

Example 1

Design the transformer for a constant off-time controller-converter

with t_{off} = 20 microseconds. Design option (D) is selected to provide a maximum collector-to-emitter voltage = 80 volts. Other specifications are:

$V_{I,min}$ = 10V, $P_{0,max}$ = 10W, V_0 = 15V, V_D = 0.7V, V_Q = 0.2V, B_{max} = 0.35T, B_R = 0.01T, $F_{w,\,max}$ = 0.4

Design Procedures

[A] Choose a core and determine number of turns N_p and N_S:

Arbitrarily select a core (Magnetics Catalog Number 55324) with A = $0.678 \times 10^{-4} m^2$, ℓ = $8.98 \times 10^{-2} m$, A_{wn} = $3.64 \times 10^{-4} m^2$, (719,100 circular mils) and μ = $125 \mu_0$ (μ_0 = $4\pi \times 10^{-7} H/m$).

Use the equation for option D in Table 3.2 to find γ_D, and the equations for option D in Table 3.4-C to find N_p and N_S.

$$\gamma_D = \frac{15+0.7}{80-20} = 0.261$$
$$N_p = 129$$
$$N_S = 0.261 \times 129 = 34$$

[B] Determine wire sizes:

Compute $I_{pe,max}$ using (28,TF); $I_{se,max}$ using (34,TF) of Table 3.3-C

$$I_{pe,max} = \sqrt{\left[\frac{10}{15}\left(0.261 + \frac{15+0.7}{10-0.2}\right)\right]^2 + \frac{1}{12}\left[\frac{(8.98\times10^{-2})\times(15+0.7)\times20\times10^{-6}}{129\times34\times(125\times4\pi\times10^{-7})\times0.678\times10^{-2}}\right]^2}\,.$$

$$\sqrt{\frac{129\times(15+0.7)}{129\times(15+0.7)+34\times(10-0.2)}} = 1.15A$$

$$I_{se,max} = 1.15\sqrt{\frac{10-0.2}{0.261\times(15+0.7)}} = 1.78A$$

For current density of $5.0671 \times 10^{-7} m^2/A$, use wire table to find wire sizes. Wire AWG #19 (A_{wr} = $7.544 \times 10^{-7} m^2$) is chosen for primary winding, and AWG #17 (A_{wr} = $1.177 \times 10^{-6} m^2$) is chosen for secondary winding.

[C] Check winding factor:

$$F_w = [(NA_{wr})_P + (NA_{wr})_S]/A_{wn}$$

$$= [129 \times 7.544 \times 10^{-7} + 34 \times 1.177 \times 10^{-6}]/3.64 \times 10^{-4}$$

$$= 0.38 < F_{w,max}, \text{ which is 0.4 by converter specification.}$$

The pertinent information concerning this design is: $N_P = 129$, $N_S = 34$, primary wire AWG #19, secondary wire AWG #17, and $F_w = 0.38$.

In this example, the core size-permeability combinations selected yields a satisfactory design. However, arbitrarily selected combinations may fail to produce a workable design due to either an excessively large winding factor or a nonrealizable complex number for N_P or N_S. In this case, repetitive trials are necessary to find workable cores.

Example 2

Using the specifications from Example 1, design a transformer for a constant on-time controller with t_{on} = 50 microseconds. The turns ratio (Option J) to be 1.2.

Design Procedure

Similar to the case of the constant on-time single-winding voltage step-up/current step-up converter given in Example 3 of Chapter II, special steps must be included to ensure that the core flux density at any condition within the specified operating range does not exceed B_{max}.

[A] Choose a core and determine number of turns N_P and N_S:

Arbitrarily select a core (Magnetics Catalog Number 55585) with $\mu = 125\mu_0$, $A = 0.454 \times 10^{-4} m^2$, $\ell = 8.95 \times 10^{-2} m$, $A_{wn} = 4.00 \times 10^{-4} m^2$. From Option J in Table 3.4, $\gamma_J = 1.2$. Using the expressions for N_P and N_S in Table 3.5-B, calculate N_P and N_S for $V_{IO} = V_{I,min} = 10V$; $N_P = 83$, and $N_S = 100$. Compute B_B for $N_P = 83$, $N_S = 100$, $V_I = V_{I,max} = 20V$, and $P_0 = P_{0,max} = 10W$,

using (12,TN) or (20,TN) depending on which mode the converter operates in under these conditions. Using (13,TN), $B_A(P_0 = P_{0,max}, V_I = V_{I,max}) = 0.06$ tesla > B_R, which is 0.01 tesla; therefore the converter is in Mode 1 and the Mode 1 expression (12,TN) should be used to check B_B at $P_0 = P_{0,max}$ and $V_I = V_{I,max}$ and $B_B(P_{0,max}, V_{I,max}) = 0.33$ tesla < B_{max}. Thus, for this first trial design, the core flux density does not exceed B_{max} within the converter operating range.

[B] Determine wire sizes

From (28,TN),

$I_{Pe}(P_{0,max}, V_{I,min}) = 1.89A$

$I_{Pe}(P_{0,max}, V_{I,max}) = 0.92A$

Thus, $I_{Pe,max} = 1.89$ and wire size AWG #17 ($A_{wr,P} = 1.18 \times 10^{-6} m^2$) is chosen for the primary winding wire

From (33,TN),

$I_{Se}(P_0 = P_{0,max}, V_{I,min}) = 1.36A$

$I_{Se}(P_0 = P_{0,max}, V_{I,max}) = 0.94A$

Thus, $I_{Se,max} = 1.36A$, and wire size AWG #18 ($A_{wr,S} = 9.16 \times 10^{-7} m^2$) is chosen for the secondary winding wire.

[C] Check winding factor

$$F_W = (N_P A_{wr,P} + N_S A_{wr,S})/A_{wn} = 0.47 > F_{W,max}.$$

Thus, this trial design does not meet the winding factor requirement, and should be discarded.

Try another core, starting from step [A], repeating the same procedure.

[A] Select core (MAG. 55583) which has the same dimension as that of the first trial core, but with $\mu = 160\mu_0$.

$N_P = 67$, $N_S = 80$.

$B_A(P_{0,max}, V_{I,max}) = 0.02 > B_R$. Thus converter operates in Mode 1 at $P_0 = P_{0,max}$ and $V_I = V_{I,max}$. Using (12,TN), $B_B(P_{0,max}, V_{I,max}) = 0.345 < B_{max}$. Thus, the flux density requirement is met.

[B] Determine Wire Size

$$I_{Pe,max} = 1.88A \quad AWG \#17$$

$$I_{Se,max} = 1.35A \quad AWG \#18$$

[C] Check winding factor

$$F_w = 0.38 < F_{w, max}$$

Thus, the second trial design meets all the design requirements. A summary of the significant quantities resulting from this design is core Cat. No. 55583 with $\mu = 160\mu_0$, $N_P = 67$, $N_S = 80$ primary wire size is AWG 17; Secondary wire size is AWG 18, Winding factor is 0.38.

3.6 Conclusions

The analysis of the two-winding energy-storage converter presented in this chapter led to the recognition of an additional constraint relationship not available in single-winding converters. By expressing this relationship in suitable mathematical form, the additional constraint concept was incorporated into specific design equations to provide the designer new freedom to meet additional design objectives not heretofore available. The design relationships are presented in tabular form and can be readily automated in a digital computer to greatly reduce the time and effort required of the designer.

Measurements have been made of critical circuit variables for a number of energy-storage transformer designs obtained from the design procedures presented in this chapter. The measured values agree with those predicted from the analytical relationships within three to five percent.

Chapter IV

LOWER-BOUND ON WORKABLE REACTOR CORE VOLUME

4.1 Introduction

This chapter develops the theory for a basic constraint relation-
ship for the energy-storage reactors for the twelve controller-converter
combinations considered in the last two chapters. This constraint rela-
tionship is evolved through an analysis of the converters from an energy
point of view. Through this constraint relationship, a lower-bound condi-
tion on the volume of workable reactor cores is established. This lower-
bound condition not only provides a useful criterion for the comparison of
the various controller-converter combinations, but it also leads to an
easily used rule for quickly selecting candidate cores for given converter
specification, thus considerably simplifying the search process which is a
necessary part of the design procedures developed in the last two chapters.

This chapter follows closely the material presented in Ref. [6].
The scheme used in the last two chapters for identifying the various con-
troller-converter combinations are used in this chapter as well. The three
controllers are identified by the two-letter combinations: FQ for constant
frequency, TN for constant on-time, and TF for constant off-time controllers.
The converter configurations are identified by two letters: VU for the vol-
tage step-up, CU for the current step up, UD for the single-winding voltage
step-up/current step-up, and 2UD for the two-winding voltage step-up/current

(59)

step-up converters. Using these identification codes and referring to Table 4.1, (1,FQVU) refers to the specific equation $\Delta W_m = TP_0(V_0+V_D-V_I)/V_0$, for the voltage step-up converter with a constant-frequency controller. To simplify the presentation, when an equation applies to all controllers, the controller identifier is omitted. For example, (1,VU) refers to all three of the equations for ΔW_m for the voltage step-up converter with all three types of controllers. When both the controller and the converter identification codes are absent, the equation reference applies to all twelve controller-converter combinations.

4.2 Development of Constraint Relationship

Several fundamental papers [9,10,11] point out that in any efficient dc-to-dc conversion process taking place in an electric network, an internal cyclic or ac power flow is an inherent feature of the power processing system. The analytical approach followed in those papers is based on considerations of the energy balance in a general dc-to-dc conversion system and leads to a number of statements or laws which provide fundamental insight into the conversion process. In this chapter, a constraint relationship is developed from a similar energy-balance approach, but it is derived in the context of a set of piecewise-linear circuit models developed in Chapters II and III. In the converters under consideration, part or all of the energy supplied by the input source is stored as magnetic energy during the first portion of a switching cycle, and is then transferred to the filter capacitor and load during the last portion of the cycle. The energy received by the filter capacitor during the last portion of a switching cycle subsequently is released to supply the load during the first portion of the next cycle.

The parameter of most concern in this chapter is ΔW_m, and it repre-
sents the magnetic energy which must be transferred through the reactor dur-
ing each cycle of steady-state operation. ΔW_m is defined as the difference
between the maximum and the minimum of the energy stored during each steady-
state cycle. Analyses of the four converter types considered in this dis-
ertation yield expressions for ΔW_m in terms of converter operating condi-
tions and the switching-cycle time parameters which are dictated by the type
of controller employed in the feedback loop. These expressions form the
bases from which the lower-bound conditions on reactor core volumes are de-
rived.

4.2.1 Expressions for ΔW_m and $\Delta W_{m,max}$

Using the piecewise- linearized circuit models described in Chapters
II and III and some results from those two chapters, the expressions for
ΔW_m can be derived and are presented in Table 4.1. The expressions for ΔW_m
for the various controller-converter combinations are presented for Mode 1
operation as (1), and for Mode 2 operation as (3). The expressions are in
terms of converter operating conditions, input and output voltages V_I and V_0
and output power P_0; semiconductor voltage drops V_Q and V_D; controller time
parameters (conversion period T for the constant-frequency controller, trans-
istor on-time t_{on} for the constant on-time controller, and transistor off-
time t_{off} for the constant off-time controller) and for some cases, induct-
ance value and a winding parameter γ. These expressions are obtained by
integrating the input power to the energy-storage reactor over a period of
time during which energy is flowing into the magnetic core. Detailed deriva-
tions of these equations are given in Appendix G.

To use these expressions to obtain a lower bound for the required

Table 4.1 Expressions for ΔW_m and $\Delta W_{m,max}$ for
the Twelve Controller-Converter Combinations

		SINGLE-WINDING VOLTAGE STEP-UP CONVERTER (VU)	SINGLE-WINDING CURRENT STEP-UP CONVERTER (CU)	VOLTAGE STEP-UP/CURRENT STEP-UP CONVERTER	
				SINGLE-WINDING (UD) $\gamma = 1$; $L_X = L$	TWO-WINDING (2UD) $\gamma = N_s/N_p$; $L_X = L_p$
CONSTANT-FREQUENCY CONTROLLER (FQ) — MODE 1		$\Delta W_m=TP_0(V_0+V_D-V_I)/V_0$ (1)	$\Delta W_m=[TP_0(V_0+V_D)(V_I-V_0-V_Q)]/[V_0(V_I+V_D-V_Q)]$ (1)	$\Delta W_m=TP_0(V_0+V_D)/V_0$ (1)	
		$\partial\Delta W_m/\partial V_I < 0; \partial\Delta W_m/\partial P_0 > 0$ (2)	$\partial\Delta W_m/\partial V_I > 0; \partial\Delta W_m/\partial P_0 > 0;$ (2)	$\partial\Delta W_m/\partial V_I = 0; \partial\Delta W_m/\partial P_0 > 0$ (2)	
MODE 2		Same as (1) (3)	Same as (1) (3)	Same as (1) (3)	
		Same as (2) (4)	Same as (2) (4)	Same as (2) (4)	
$\Delta W_{m,max}$		$\Delta W_{m,max}$ occurs at $V_{I,min}$ and $P_{0,max}$ (5)	$\Delta W_{m,max}$ occurs at $V_{I,max}$ and $P_{0,max}$ (5)	$\Delta W_{m,max}$ occurs at $P_{0,max}$ and is independent of V_I (5)	
		$\Delta W_{m,max} = TP_{0,max}(V_0+V_D-V_{I,min})/V_0$ (6)	$\Delta W_{m,max}=[TP_{0,max}(V_0+V_D)(V_{I,max}-V_0-V_Q)]/[V_0(V_{I,max}+V_D-V_Q)]$ (6)	$\Delta W_{m,max}=TP_{0,max}(V_0+V_D)/V_0$ (6)	
CONSTANT ON-TIME CONTROLLER (TN) — MODE 1		$\Delta W_m=t_{on}P_0(V_0+V_D-V_0)/V_0$ (1)	$\Delta W_m=t_{on}P_0(V_I-V_0-V_Q)/V_0$ (1)	$\Delta W_m=t_{on}P_0[V_0+V_D+\gamma(V_I-V_0)]/V_0$ (1)	
		$\partial\Delta W_m/\partial V_I=0; \partial\Delta W_m/\partial P_0>0$ (2)	$\partial\Delta W_m/\partial V_I > 0, \partial\Delta W_m/\partial P_0 > 0$ (2)	$\partial\Delta W_m/\partial V_I > 0; \partial\Delta W_m/\partial P_0 > 0$ (2)	
MODE 2		$\Delta W_m=t_{on}^2(V_I-V_0)^2/2L$ (3)	$\Delta W_m=t_{on}^2(V_I-V_0-V_Q)^2/2L$ (3)	$\Delta W_m=t_{on}^2(V_I-V_0)^2/2L_X$ (3)	
		$\partial\Delta W_m/\partial V_I > 0; \partial\Delta W_m/\partial P_0 = 0$ (4)	$\partial\Delta W_m/\partial V_I > 0; \partial\Delta W_m/\partial P_0 = 0$ (4)	$\partial\Delta W_m/\partial V_I > 0; \partial\Delta W_m/\partial P_0 = 0$ (4)	
$\Delta W_{m,max}$		$\Delta W_{m,max}$ occurs at $V_{I,max}$ and $P_{0,max}$ (5)	ΔW_m occurs at $V_{I,max}$ and $P_{0,max}$ (5)	$\Delta W_{m,max}$ occurs at $V_{I,max}$ and $P_{0,max}$ (5)	
		$\Delta W_{m,max}=t_{on}P_{0,max}(V_0+V_D-V_Q)/V_0$ (6)	$\Delta W_{m,max}=t_{on}P_{0,max}(V_{I,max}-V_0-V_Q)/V_0$ (6)	$\Delta W_{m,max} = t_{on}P_{0,max}[V_0+V_D+\gamma(V_{I,max}-V_Q)]/V_0$ (6)	
CONSTANT OFF-TIME CONTROLLER (TF) — MODE 1		$\Delta W_m=[t_{off}P_0(V_0+V_D-V_I)(V_0+V_D-V_Q)]/[V_0(V_I-V_Q)]$ (1)	$\Delta W_m=t_{off}P_0(V_0+V_D)/V_0$ (1)	$\Delta W_m=t_{off}P_0(V_0+V_D)[1+(V_0+V_D)/\gamma(V_I-V_Q)]/V_0$ (1)	
		$\partial\Delta W_m/\partial V_I < 0; \partial\Delta W_m/\partial P_0 > 0$ (2)	$\partial\Delta W_m/\partial V_I = 0; \partial\Delta W_m/\partial P_0 > 0$ (2)	$\partial\Delta W_m/\partial V_I < 0; \partial\Delta W_m/\partial P_0 > 0$ (2)	
MODE 2		$\Delta W_m=T_RP_0(V_0+V_D-V_I)/V_0$, where (3) T_R is the larger root of the quadratic: $T_R^2-2\left(t_{off}+\dfrac{LP_0(V_0+V_D-V_I)}{V_0(V_I-V_Q)^2}\right)T_R+t_{off}^2=0$	$\Delta W_m=[T_RP_0(V_0+V_D)(V_I-V_0-V_Q)]/[V_0(V_I+V_D-V_Q)]$, where (3) T_R is the larger root of the quadratic: $T_R^2-2\left(t_{off}+\dfrac{LP_0(V_0+V_D)}{V_0(V_I-V_0-V_Q)(V_I+V_D-V_Q)}\right)+t_{off}^2=0$	$\Delta W_m=T_RP_0(V_0+V_D)/V_0$, where (3) T_R is the larger root of the quadratic: $T_R^2-2\left(t_{off}+\dfrac{L_XP_0(V_0+V_D)}{V_0(V_I-V_Q)^2}\right)T_R+t_{off}^2=0$	
		$\partial\Delta W_m/\partial V_I < 0; \partial\Delta W_m/\partial P_0 > 0$ (4)	$\partial\Delta W_m/\partial V_I$ undetermined; $\partial\Delta W_m/\partial P_0 > 0$ (4)	$\partial\Delta W_m/\partial V_I < 0; \partial\Delta W_m/\partial P_0 > 0$ (4)	
$\Delta W_{m,max}$		$\Delta W_{m,max}$ occurs at $V_{I,min}$ and $P_{0,max}$ (5)	$\Delta W_{m,max}$ occurs at $P_{0,max}$ (5)	$\Delta W_{m,max}$ occurs at $V_{I,min}$ and $P_{0,max}$ (5)	
		$\Delta W_m=[t_{off}P_{0,max}(V_0+V_D-V_{I,min})(V_0+V_D-V_Q)]/[V_0(V_{I,min}-V_Q)]$ (6)	$\Delta W_{m,max}=t_{off}P_{0,max}(V_0+V_D)/V_0$ (6)	$\Delta W_{m,max}=t_{off}P_{0,max}(V_0+V_D)[1+(V_0+V_D)/\gamma(V_{I,min}-V_Q)]/V_0$ (6)	

62

magnetic-core volume requires knowledge of the particular input-voltage and output-power condition, lying within the operating range, for which ΔW_m has a maximum value $\Delta W_{m,max}$. This information is obtained by evaluating the partial derivatives of ΔW_m with respect to V_I and P_0. This evaluation yields the results given by (2) and (4). Since a converter may operate in Mode 1 or Mode 2 over only a portion of the P_0-V_I operating range, results of both (2) and (4) should be taken into consideration together to determine the location at which $\Delta W_{m,max}$ occurs. It can be seen from (2) and (4), that for each con-troller-converter combination, $\partial\Delta W_m/\partial P_0$ is nonnegative, and $\partial\Delta W_m/\partial V_I$ is either nonnegative or nonpositive but never changes sign within the operating range. In other words, ΔW_m is a monotonically increasing function of P_0 and is either a monotonically increasing or monotonically decreasing function of V_I. Thus, $\Delta W_{m,max}$ occurs at one of the extremities of the converter opera-ting range as given in (5), no matter whether the converters operate only in Mode 1 or only in Mode 2 over the entire operating range or in Mode 1 and Mode 2 over different portions of the operating range. An exception is the Mode 2 case of TFCU, where the sign of $\partial\Delta W_m/\partial V_I$ is undetermined; it only can be concluded that $\Delta W_{m,max}$ occurs at $P_{0,max}$ as given in (5,TFCU). Once the location where $\Delta W_{m,max}$ occurs is known, its value can be found by substi-tuting condition (5) into expressions for ΔW_m in (1) or (3), depending on which mode the converter operates in at that particular condition. However, converters considered in this chapter, as those considered in earlier chapters are designed to operate in Mode 1 at least at the location where core flux density B_B reaches its maximum prescribed value B_{max}. This pre-cludes for some controller-converter combinations such as TNCU, and for all constant frequency FQ and constant off-time TF controller-converter combi-nations, the possibility of operating in Mode 2 at the condition given in

in (5) and, thus, Mode 1 expressions for ΔW_m should be used to compute $\Delta W_{m,max}$ for such cases. For the cases of TNVU, TNUD, and TN2UD, $\Delta W_{m,max}$ may occur in Mode 1 or Mode 2, but Mode 1 expressions are used to compute $\Delta W_{m,max}$ as given in (5) for these three cases, for reasons to be explained in the section on lower-bound conditions on core volume. In summary, for the various reasons stated above, Mode 1 expressions for ΔW_m are always used to compute $\Delta W_{m,max}$ in (6) for all controller-converter combinations.

4.2.2 Lower-Bound on Workable Core Volumes

In this section, a lower-bound condition on the volume of workable reactor cores for given converter specifications is established by considering the amount of energy $\Delta W_{m,max}$ required to be transferred under worst-case conditions by the controller-converter and the energy-transferring capability of a magnetic core. The capability of a core to store and release energy is a function of its volume, the B-H characteristic of the magnetic material used, and the maximum allowed flux density B_{max}. The latter is the maximum which the flux density is designed to reach at least at one operating condition but which must not be exceeded. Referring to Fig. 4.1, the maximum energy which a converter core could possibly store and release over a complete switching cycle is equal to the volume of the core times the integral of the magnetic field strength H with respect to the flux density B over the limits B_R and B_{max}.

$$\Delta W_m = \ell A \int_{B_R}^{B_{max}} H dB = V \int_{B_R}^{B_{max}} H dB$$

From the condition that the energy transfer capability of cores which meet
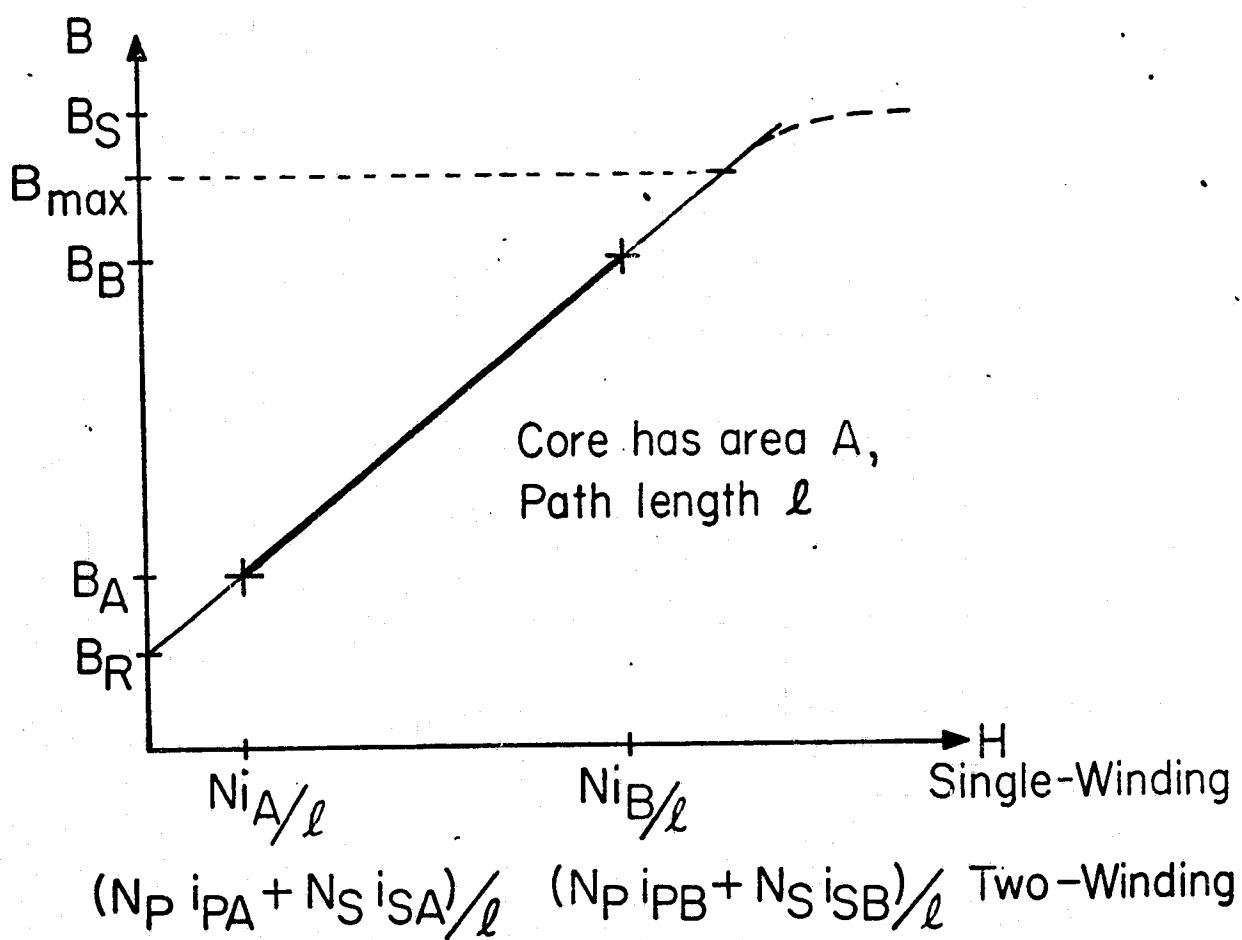
Figure 4.1 Magnetic core characteristic

the design specifications must be equal to or greater than $\Delta W_{m,max}$, a lower-bound condition on the core volume V_{LB} is established, expressed in the form of an inequality:

$$V \geq \Delta W_{m,max}/[\int_{B_R}^{B_{max}} H dB] \triangleq V_{LB} \qquad (4.8)$$

where $\Delta W_{m,max}$ can be computed using (6) in Table 4.1 for given specifications. As discussed in the last section, for the combinations of TNVU, TNUD, and TN2UD, $\Delta W_{m,max}$ may occur in Mode 1 or in Mode 2, but Mode 1 expressions are always used to determine $\Delta W_{m,max}$. The reason for doing so is that for such cases, a prior knowledge of the value of the reactor inductance (transformer primary inductance for TN2UD) is required in using Mode 2 expressions to determine $\Delta W_{m,max}$, and from this parameter, the lower-bound core volume V_{LB}. The Mode 2 expressions thus imply that an additional constraint is imposed on the converter core, so that the lower-bound value obtained in this manner will not be the absolute lower-bound value.

Returning to the lower-bound value of workable core volume, if the core is operated over the linear range of the B-H characteristic with constant permeability μ, then the integral of H with respect to B becomes $(B_{max} - B_R)^2/2\mu$ and (4.8) may be rewritten as:

$$V \geq 2\mu \Delta W_{m,max}/(B_{max} - B_R)^2 \triangleq V_{LB} \qquad (4.9)$$

Details on the use of this expression with Table 4.1 to determine the lower bound of workable converter cores will be illustrated in the next section.

4.3 An Example

A numerical example is given in this section to illustrate the use

of Table 4.1 to determine the lower-bound core volume for a particular con-
verter.

Example

Find the lower-bound volume of workable cores for a constant-
frequency voltage step-up converter with specifications:

$$V_{I,min} = 12V; \quad V_0 = 28V; \quad V_D = 0.7V$$

$$P_{0,max} = 30W; \quad B_{max} = 0.35T; \quad B_R = 0.01T$$

Conversion period $T = 100\mu s$

From (6, FQVU) in Table 4.1 and (4.9),

$$\Delta W_{m,max} = TP_{0,max}(V_0+V_D-V_{I,min})/V_0 = 1.789 \times 10^{-3} J$$

$$\text{for } \mu = 125\mu_0, \text{ where } \mu_0 = 4\pi \times 10^{-7} H/m$$

$$V_{LB} = 2\mu\Delta W_{m,max}/(B_{max} - B_R)^2 = 4.86 \times 10^{-6} m^3$$

4.4 Comparative Evaluation of Controller-Converter Combinations

Using the derived lower-bound conditions on workable reactor core
volumes, comparative evaluations of the various controller-converter combi-
nations now may be made. In this section comparisons are made for conver-
ters in the following two categories: all four converter configurations
with the same type of controller; and all three types of controllers with a
single converter configuration. In the first category, comparisons are made
between configurations VU and UD; CU and UD; and UD and 2UD, according to
the converter function. Both VU and UD configurations are capable of step-
ping up the output voltage above the input voltage level, while both CU and
UD are capable of stepping up the output current above the input current
level. Configurations UD and 2UD are capable of stepping up either the out-
put voltage or the output current over the corresponding input voltage or
current. The identification scheme used in Tables 4.1 to code the

controller-converter combinations is used in this section as the subscript accompanying the lower-bound (LB) values of core volume V_{LB}. For example, $V_{LB,VU}$ stands for the lower-bound volume of workable cores in a voltage step-up converter.

It can be seen from (4.9) that the lower bound of core volume V_{LB} is proportional to $\Delta W_{m,max}$ for a given magnetic material and specified B_{max}. Thus, comparison of V_{LB} can be made by comparing $\Delta W_{m,max}$ values for the various combinations. All comparisons are based on identical magnetic material and converter specifications of input voltage and output power. The results of the comparison are summarized below.

4.4.1 Comparisons of Different Converter Configurations for the Same Controller Type.

Comparison Between Configurations VU and UD:

$$V_{LB,VU} < V_{LB,UD}$$

This comparison shows that for a voltage step-up application, the lower-bound volume of workable cores for single-winding voltage step-up converters is always less than the lower-bound volume of workable cores for single-winding voltage step-up/current step-up converters.

Comparison Between Configurations CU and UD:

$$V_{LB,CU} < V_{LB,UD}$$

This comparison shows that for a current step-up application, the lower-bound volume of workable cores for single-winding current step-up converters is always less than the lower-bound volume of workable cores for single-winding voltage step-up/current step-up converters.

Comparison Between Configurations UD and 2UD:

For a voltage step-up/current step-up application, a comparison of the lower-bound volume on workable cores for the two possible configurations UD and 2UD must include a consideration of the type of controller employed. If a constant frequency controller is employed in both converter configurations, $V_{LB,FQUD} = V_{LB,FQ2UD}$. For configurations TN2UD and TF2UD, V_{LB} is influenced by the winding parameter γ. $V_{LB,TN2UD}$ increases with an increase of γ, but $V_{LB,TF2UD}$ is decreased with an increase of γ, and the results of the comparisons are as follows:

$$V_{LB,FQUD} = V_{LB,FQ2UD}$$

$$V_{LB,TNUD} > V_{LB,TN2UD}; \quad V_{LB,TFUD} < V_{LB,TF2UD}; \quad \text{for } \gamma < 1$$

$$V_{LB,TNUD} = V_{LB,TN2UD}; \quad V_{LB,TFUD} = V_{LB,TF2UD}; \quad \text{for } \gamma = 1$$

$$V_{Lb,TNVD} > V_{LB,TN2UD}; \quad V_{LB,TFUD} > V_{LB,TF2UD}; \quad \text{for } \gamma > 1$$

4.4.2 Comparisons of Different Controller Types for the Same Converter Configuration.

Configuration VU:

$$\frac{(V_{LB,FQVU}/T)}{(V_{I,min}-V_Q)(V_0+V_D-V_{I,min})} = \frac{(V_{LB,TNVU}/t_{on})}{(V_{I,min}-V_Q)(V_0+V_D-V_Q)} = \frac{(V_{LB,TFVU}/t_{off})}{(V_0+V_D-V_{I,min})(V_0+V_D-V_Q)}$$

$$(4.10)$$

Configuration CU:

$$\frac{(V_{LB,FQCU}/T)}{(V_0+V_D)(V_{I,max}-V_0-V_Q)} = \frac{(V_{LB,TNCU}/t_{on})}{(V_{I,max}+V_D-V_Q)(V_{I,max}-V_0-V_Q)} = \frac{(V_{LB,TFCU}/t_{off})}{(V_0+V_D)(V_{I,max}+V_D-V_Q)}$$

$$(4.11)$$

Configurations UD ($\gamma=1$) and 2UD ($\gamma = N_S/N_P$):

$$\frac{(\mathcal{V}_{LB,FQUD,2UD}/T)}{(V_{I,min}-V_Q)(V_0+V_D)} = \frac{(\mathcal{V}_{LB,TNUD,2UD}/t_{on})}{(V_{I,min}-V_Q)[V_0+V_D+\gamma(V_{I,max}-V_Q)]}$$

$$= \frac{\gamma(\mathcal{V}_{LB,TFUD,2UD}/t_{off})}{(V_0+V_D)[V_0+V_D+\gamma(V_{I,min}-V_Q)]} \tag{4.12}$$

A numerical example is given below to illustrate how to make use of these comparisons.

Example

For a voltage step-up converter with specifications $V_0 = 28V$, $V_{I,min} = 18V$, $V_D = 0.8V$, and $V_Q = 0.2$,

(A) determine the ratio of the lower-bound volume of workable cores for this converter with a constant-frequency controller of period $T = 100\mu s$ to the lower-bound volume of workable cores for the same converter with a constant on-time controller with $t_{on} = 50\mu s$.

(B) determine the ratio of T to t_{on} if the ratio of the lower-bound volume of workable cores for this converter with a constant-frequency controller to the lower-bound volume of workable cores for the same converter with a constant on-time controller is unity.

(A) From the first equality in Eq. (4.10),

$$\frac{\mathcal{V}_{LB,FQVU}}{\mathcal{V}_{LB,TNVU}} = \frac{T(V_0+V_D-V_{I,min})}{t_{on}(V_0+V_D-V_Q)} = \frac{(100\times10^{-6})(28+0.8-18)}{(50\times10^{-6})(28+0.8-0.2)} = 0.76$$

(B) From the first equality in Eq. (4.10),

$$\frac{T}{t_{on}} = \frac{(V_0+V_D-V_Q)}{(V_0+V_D-V_{I,min})}\frac{\mathcal{V}_{LB,FQVU}}{\mathcal{V}_{LB,TNVU}} = \frac{28+0.8-0.2}{28+0.8-18} = 2.63$$

4.5 Conclusions

A study of energy-storage dc-to-dc converters from an energy point of view leads to a better understanding of the process by which energy is transferred through the reactors and leads to a fundamental and useful constraint relationship on the magnetic reactor. From this constraint relationship, a lower-bound condition on the volume of workable reactor cores for each controller-converter combination is established. This lower-bound value provides a numerical cutoff which may be used by a designer to easily screen the population of available magnetic cores thereby locating those cores which are candidates for a particular converter design. It should be noted, however, that while this lower-bound condition provides a useful criterion for eliminating unworkable cores from the core population, it does not guarantee that any core with a volume greater than the lower-bound volume is practically usable because the core may not be windable.

Using derived lower-bound conditions, a comparative evaluation among the various controller-converter combinations considered is presented. The results of this comparative evaluation of the various combinations should be useful to designers of dc-to-dc converters by providing some guidance not previously available for making choices among the many possible combinations of controllers and converters.

Chapter V

TABLE-AIDED DESIGN PROCEDURES FOR ENERGY-STORAGE REACTORS

5.1 Introduction

The procedures described in Chapters II and II for designing the magnetic reactors required in energy-storage dc-to-dc converters include a search through a data file of magnetic core specifications and yield as an output a list of windable cores which meet particular converter specifications. This search process usually begins with the smallest available core size and proceeds sequentially toward the largest size. The search algorithm is readily implemented with a digital computer program, but it is a time consuming approach when the procedure must be followed with hand computations or with a small computer which does not have sufficient memory to accommodate the necessary magnetic core data.

This chapter, based on work presented in Reference [7], presents a new set of procedures for desiging energy-storage reactors for the twelve controller-converter combinations which were described in earlier chapters. These new procedures eliminate the need for an automated computer search algorithm. The heart of the new design procedures depends on the development of a special table of parameters calculated from catalog data provided by manufacturers of magnetic cores. With the assistance of the special table and the lower-bound condition on workable converter core volumes as developed in Chapter IV, the search process can be reduced to a

(72)

methodical table search. With several relatively simple calculations and a few trials, a core can be selected to match the controller-converter specifications and the number of turns can be determined.

The design equations are given in tabular format and are placed together at the end of this chapter for convenient reference. Equation numbers in the tables run from (1) through (17) and continue sequentially in the text, starting with (5.18). Within the tables, where appropriate, equations are identified with converter types as in earlier chapters. For example, (7,CU) refers to the particular expression for N given by (7) in Table 5.1(B) for the current step-up converter. Following the presentation of the design procedure, a number of examples are given to illustrate the step-by-step design process.

5.2 Design Relationships for Single- and Two-Winding Converters

Table 5.1 presented in four parts, A,B,C, and D, gives expressions for computing maximum rms current and the number of turns for the winding of the nine single-winding and the three two-winding controller-converter units. These expressions are obtained directly from Tables 2.6 and 3.3 except for (4,TNUD). This expression is obtained from (50,UD) of Table 2.6 and an additional constraint imposed on TNUD to be described in the last paragraph of this section. For each combination, the number of turns N, given by (7), is seen to depend on a specification parameter ζ, a grouping of terms common to all three controllers for a given type of converter, and two magnetic core parameters, $\{V/\mu\}$ and $\{\ell/\mu\}$. The parameter ζ is a function of the converter specifications and is specific to the chosen controller-controller combination. The quantities $\{V/\mu\}$ and $\{\ell/\mu\}$ are obtained from a special table of core parameters to be discussed in a later section. Parameter values from

this table are identified by enclosing braces. The expressions for N in (7) are obtained from Tables 2.3 and 3.5 and are rearranged to allow the use of the specification parameters and the core parameters $\{V/\mu\}$ and $\{\ell/\mu\}$. As described in Chapters II and III, a condition required of these expressions is that the core flux density, at one point in the operating range called the design operating point, reaches but never exceeds a specified upper-bound value B_{max}; and that at this point, to which the equations for N correspond, the converter operates in Mode 1, the continuous mmf mode.

In the two-winding configuration, the presence of the additional winding not only provides input-output conductive isolation, but, as pointed out in Chapter III, also provides an additional degree of freedom in the design procedure beyond those for single-winding converters. By utilizing the extra degree of freedom, it is possible to incorporate particular performance or design constraints into the design procedure. Seven of the ten options considered in Chapter III are presented in this chapter using the same option letter symbols previously employed. These are: (A) duty cycle centered at a specified value; (B) minimum duty cycle; (C) specified range of duty-cycle variation; (D) maximum transistor collector-to-emitter voltage; (E) maximum diode reverse voltage; (H) maximum duty cycle; and (J) turns ratio. Each of these options leads to an option constraint equation from which the turns ratio γ is determined. Options (F), (G), and (I) presented in Chapter III are not considered in this chapter since the turns ratio for these three options can not be determined directly from a given set of converter specifications, and the design procedure presented in this chapter is not applicable to the two-winding configurations without knowing the turns ratio. Table 5.2 presents the option constraint equations from which the particular value of turns ratio $\gamma = \gamma_y$, where $y = A,B,C,D,E,H$ or J, to be used in

Table 5.1(D) is determined for each of the seven options described.

As can be seen by referring to the expressions for B_B in Tables 2.3 and 3.2, for each of the controller-converter configurations considered except TNUD and TN2UD, there is a well-defined extremum point in the output-power/input-voltage operating range at which the peak value of the flux-density excursion has a maximum $B_{B,max}$. Since the designer's choice for the maximum permissible value of core flux density B_{max} assumes the role of a basic constraint in the design procedure, the expressions for turns N given by (7) are written in terms of the output power and input voltage at these well-defined extremum points where $B_{B,max} = B_{max}$. For each of the two exceptional cases of TNUD and TN2UD, the maximum flux density occurs at either the point $(P_{0,max}, V_{I,min})$ or at the point $(P_{0,max}, V_{I,max})$ as can be seen from (16,UD) of Chapter II and (14,TN) of Chapter III. To determine at which of the input-voltage extremes the maximum flux density occurs requires a somewhat involved set of computations and comparisons of results. These are not well suited to the manipulation capability of a pocket calculator, whereas the computations and mathematical operations required in the design of the other ten controller-converter combinations are. For this reason, for the TNUD and TN2UD cases, the design operating point where the turns N are calculated using Mode 1 conditions is assigned to be located at the point $(P_{0,max}, V_{I,min})$ although this assignment may decrease the number of designs available . A related complexity still remains with these two configurations in comparison with the other ten in that there is no assurance that the peak value of the flux-density excursion B_B at the point $(P_{0,max}, V_{I,max})$ may not exceed the value at the design point $(P_{0,max}, V_{I,min})$ where the design procedure forces the peak value of the flux-density excursion to be the designer's choice for B_{max}. A method for eliminating the possibility of

such a design is obtained from a study of the equations for the peak value of the flux-density excursion B_B as functions of N given in Equations (15,UD) of Chapter II, and (12,TN) of Chapter III, from which it can be shown that $(\partial B_B/\partial N) > 0$. This means that at any point throughout the converter output-power/input-voltage operating range increasing the number of turns on a particular core increases the peak value of the core flux density excursion. Consideration of this fact permits determining whether this undesirable set of circumstances exists. The procedure is to compute the turns N in the normal fashion using values of P_O, V_I and B_B corresponding to $P_{O,max}$, $V_{I,min}$ and B_{max} and compare it to an artificial value of turns N' using values corresponding to $P_{O,max}$, $V_{I,max}$ and B_{max}. The two values N and N' correspond to values obtained by setting $V_{IO} = V_{I,min}$ and $V_{I,max}$ in (18,UD) of Chapter II (or the solution expressions for N_p in Table 3.3-B). If the value calculated for N' is greater than the value of N then it can be concluded that with N turns on the winding the peak of the core flux-density excursion at the point $(P_{O,max}, V_{I,max})$ will be less than the specified design maximum of B_{max} and the design is satisfactory. Such a test is included in the design procedure for these two exceptional cases and is described in detail in a later section.

5.3 Energy Transfer Requirement and Screening Rule

The fundamental process in an energy-storage dc-to-dc converter consists of storing in the form of magnetic energy part of all of the energy to be transferred from the supply to the load. Energy is stored in a magnetic core during the first portion of a switching cycle and then released to the output capacitor and the load during the last portion of the cycle. From consideration of the amount of energy required to be transferred during

each switching cycle, and the energy-transferring capability of a magnetic core when employed in a particular controller-converter configuration, a lower-bound condition on the volume of workable cores has been established in Chapter IV. The inequality in (5.18) expresses this lower-bound condition.

$$V_{total} \geq \frac{2\mu \Delta W_{m,max}}{(B_{max}-B_R)^2} \tag{5.18}$$

V_{total} is the total volume of the core or stack of cores, μ is the permeability of the magnetic material and B_{max} and B_R are, respectively, the specified maximum allowable flux-density and the residual flux density in the core. $\Delta W_{m,max}$ is the amount of energy transferred by the core over a switching cycle at the particular operating point of input voltage and output power where the energy transfer is a maximum. This point may occur in either Mode 1 (continuous mmf mode) or Mode 2.

Table 5.3 presents the explicit expressions for $\Delta W_{m,max}$ to be used in conjunction with the lower-bound core-volume condition of (5.18) for the twelve controller-converter combinations considered. These expressions are developed from Table 4.1, and, for the purpose of this chapter, are somewhat different from those given in Table 4.1. For all except the three combinations TNVU, TNUD, and TN2UD, $\Delta W_{m,max}$ occurs at the design point where the design procedure requires that the converter operate in Mode 1. Consequently, Mode 1 expressions are used to determine $\Delta W_{m,max}$ for these nine cases. For the three exceptions listed, TNVU, TNUD, and TN2UD, $\Delta W_{m,max}$ occurs at an operating point where the converter may operate in either Mode 1 or in Mode 2. However, Mode 2 expressions, instead of Mode 1 expressions as used in Table 4.1, are used to compute $\Delta W_{m,max}$ for these cases, since the maximum energy transfer for Mode 2 operation is greater than that required in Mode 1,

and (5.18) must be true independent of mode. Appendix H contains a detailed derivation justifying the need for using the Mode 2 energy relationship for calculating $\Delta W_{m,max}$ for these three exceptions. There it is shown that for TNVU, this is a natural consequence of the system dynamics. For TNUD and TN2UD, the occurrence of $\Delta W_{m,max}$ while in Mode 2 is a consequence of the imposed design constraint that $B_{B,max}$ occur at $P_{0,max}$ and $V_{I,min}$, as discussed in the previous section.

When several identical cores are stacked before winding, as sometimes is done to achieve a particular component package shape, the required minimum volume of an individual core is defined by $V = (V_{total})/J$, where J is the number of cores in the stack. A more useful form of the relationship given by (5.18), expressed in terms of volume of a single core, is given by:

$$\frac{V}{\mu} \geq \delta \triangleq \frac{2\Delta W_{m,max}}{J(B_{max}-B_R)^2} \qquad (5.19)$$

In this expression, the left side of the inequality depends only on the parameters V and μ of the magnetic core. The right side, defined as the quantity δ will be shown to be a useful parameter in pursuing an orderly search for cores which satisfy the energy transfer requirement. This parameter depends through the relationships for $\Delta W_{m,max}$ given Table 5.3 on the converter specifications and on the designer's choice of B_{max} and the value of the residual flux density B_R. The value of B_R usually is small compared to the value of B_{max} specified by the designer and therefore does not affect the right side of (5.19) appreciably. How numerical values for the parameter δ, calculated from the expressions in Table 5.1 are used to choose the candidate cores capable of transferring the required energy is discussed in the following sections.

5.4 Special Table of Core Parameters

The data for generating the special table of core parameters,
Table 5.4A and 5.4B, are obtained from catalogs of commercially available
permalloy powder cores. The table is arranged so that core volume increases
with downward position in the tables and permeability increases with
position to the right. Table 5.4A contains data for cores with relative
permeabilities from 14 through 160, while data for relative permeabilities
from 173 through 550 are found in Table 5.4B. To distinguish between an
equation variable such as V/μ and the numerical value of V/μ associated
with a particular core, core-parameter values obtained from Table 5.4 are
identified by enclosing braces as $\{V/\mu\}$. Each distinct core size is assign-
ed a size number S which appears in the first column of the table. In the
second column, opposite the core size number S, are listed the core volume
$\{V\}$ (upper number) and the window area $\{A_{wn}\}$ (lower number). Four para-
meters are associated with each core size-permeability combination; a blank
section is inserted into the table if a particular combination is not of-
fered by core manufacturers. Beginning with the lower left entry in each
box of four parameters, these numbers represent, moving clockwise: volume
divided by permeability $\{V/\mu\}$; mean magnetic path length divided by perme-
ability $\{\ell/\mu\}$; inductance divided by the square of the number of turns
$\{L/N^2\}$; and the mean magnetic path length divided by the product of the
permeability and the window area of the core $\{\ell/\mu A_{wn}\}$.

From the relationship in (5.19) which must be satisfied, it can be
seen that one may locate a boundary separating those cores capable of trans-
ferring the energy required by the converter specifications from those
which cannot do so. Because of the arrangement of the parameters in the
table, the boundary which separates the two regions will be diagonal-like,

running from the upper-left part downward toward the lower-right part. The dividing line, above which cores immediately may be eliminated from further consideration, is found by using the value of δ calculated from the appropriate expression (1), (3) or (5) and comparing it to the values of core parameter $\{V/\mu\}$ listed in the table which satisfy inequality (5.19). The remaining three parameters in each box in Table 5.4 are provided for computing other design quantities such as number of turns, winding wire size, and winding factor. In a subsequent section, the use of Tables 5.1, 5.2 and 5.4 to design practical energy-storage reactors and transformers will be described.

5.5 Procedure for Identifying Windable Cores

The prediction of windability through computation of the winding factor F_w is as important in obtaining a workable design as is the determination of turns and wire size. Although it is defined in many different ways for different applications, for the purpose of this dissertation, F_w is defined as $NA_{wr}/\{A_{wn}\}$ for single-winding converters and as $(N_P A_{wr,P} + N_S A_{wr,S})/\{A_{wn}\}$ for two-winding converters, where A_{wr} is the cross-sectional area of the wire with its insultation and $\{A_{wn}\}$ is the window area of the core. Obviously, the winding factor cannot be computed until both turns and wire area are found for a given core. In this section, a method for identifying windable cores, based on an initial trial design, is developed. For single-winding converters, by using (7,VU), (7,CU), or (7,UD) and the definition of winding factor, an expression is obtained for the ratio of the winding factors for two trial designs using different cores but for the same converter specifications and for the same choice of B_{max}.

$$\frac{F_{w,1}}{F_{w,2}} = \frac{\{\ell/\mu A_{wn}\}_1 \left[1+\sqrt{1-\frac{\zeta}{\{V/\mu\}_1}}\right] A_{wr,1}}{\{\ell/\mu A_{wn}\}_2 \left[1+\sqrt{1-\frac{\zeta}{\{V/\mu\}_2}}\right] A_{wr,2}} \tag{5.20}$$

where subscript 1 is used to indicate the parameters associated with the initial trial design and subscript 2 with the second trial design. Assuming, as is often the case, that the winding wire size does not change with a change in core, then for the same specifications, (5.20) can be arranged as

$$F_{w,2} = F_{w,1} \cdot \frac{\{\ell/\mu A_{wn}\}_2 \left[1+\sqrt{1-\frac{\zeta}{\{V/\mu\}_2}}\right]}{\{\ell/\mu A_{wn}\}_1 \left[1+\sqrt{1-\frac{\zeta}{\{V/\mu\}_1}}\right]} \tag{5.21}$$

It can be seen from (5.21) that the winding factor of the second trial core can be determined from knowledge of the winding factor and core parameters of the initial design and the parameters of the second trial core. Whether core 2 is windable or not depends on the relative magnitude of $F_{w,2}$ with respect to the maximum allowable winding factor $F_{w,max}$. If $F_{w,2} \leq F_{w,max}$, then core 2 is windable; otherwise it is not. These two cases--windable versus non-windable--will be discussed later separately.

Identification of windable or non-windable cores from an initial trial design is not quite as easily accomplished in the case of two-winding converters (2UD), especially with a constant on-time controller (TN2UD). The ratio of the winding factors for two trial designs to meet the same specifications and for the same choice of B_{max} is given by the expression:

$$\frac{F_{w,1}}{F_{w,2}} = \frac{\{\ell/\mu A_{wn}\}_1 \cdot \left[1 + \sqrt{1 - \frac{\zeta}{\{V/\mu\}_1}}\right] A_{wr,P,1} \left[1 + \gamma \frac{A_{wr,S,1}}{A_{wr,P,1}}\right]}{\{\ell/\mu A_{wn}\}_2 \cdot \left[1 + \sqrt{1 - \frac{\zeta}{\{V/\mu\}_2}}\right] A_{wr,P,2} \cdot \left[1 + \gamma \frac{A_{wr,S,2}}{A_{wr,P,2}}\right]} \qquad (5.22)$$

If the assumption is made that neither the primary nor the secondary wire size changes between the first and second trial designs, then equation (5.22) reduces to expression (5.21) obtained for the three single-winding converters. A slight additional complication exists in applying (5.21) to the constant on-time two-winding (TN2UD) converter because of the uncertainty expressed in (4P,2UD) and (4S,2UD) on whether the maximum values of I_{Pe} and I_{Se} occur at $V_{I,min}$ or $V_{I,max}$. In the case of the other two controllers FQ and TF, this uncertainty does not exist so there is no possibility that the maximum current values may change from occurring at $V_{I,min}$ for the initial trial design to $V_{I,max}$ for the second trail design, or vice versa. Although not precisely correct, experience indicates (5.21) still can serve as a useful guide for identifying windable cores in the case of the TN2UD converter and will be employed for this purpose in the procedure to be described subsequently.

It is thus seen from (5.21) that the winding factor of the second trial core can be computed from knowledge of the winding factor and core parameters of the initial design and the parameters of the second trial core. Whether core 2 is windable or not depends on the relative magnitude of $F_{w,2}$ with respect to a specified maximum allowable winding factor $F_{w,max}$. If $F_{w,2} \leq F_{w,max}$, then core 2 is windable; otherwise it is not. These two cases now will be discussed separately.

5.5.1 Windable Cores

For core 2 to be windable, $F_{w,2} \leq F_{w,max}$. Using this inequality and (5.21) leads to (5.23)

$$\{\ell/\mu A_{wn}\}_2 \leq \{\ell/\mu A_{wn}\}_1 \cdot \frac{F_{w,max}}{F_{w,1}} \cdot \frac{1+\sqrt{1- \frac{\zeta}{\{V/\mu\}_1}}}{1+\sqrt{1- \frac{\zeta}{\{V/\mu\}_2}}} \qquad (5.23)$$

Incorporating the fact that $[1+\sqrt{1- \zeta/\{V/\mu\}_2}] \leq 2$, yields (5.24),

$$\{\ell/\mu A_{wn}\}_2 \leq \eta \triangleq \frac{1}{2} \{\ell/\mu A_{wn}\}_1 \cdot \frac{F_{w,max}}{F_{w,1}} \cdot \left[1+\sqrt{1- \frac{\zeta}{\{V/\mu\}_1}}\right] \qquad (5.24)$$

which is a useful, but often overly conservative requirement on $\{\ell/\mu A_{wn}\}$ for the second trial core to be windable. The parameter η, defined as the right side of (5.24), will be used in the design procedure in the identification of windable cores.

5.5.2 Non-windable Cores

If $F_{w,2} > F_{w,max}$, core 2 will not be windable. Using (21) under this condition leads to (25).

$$\{\ell/\mu A_{wn}\}_2 > \{\ell/\mu A_{wn}\}_1 \cdot \frac{F_{w,max}}{F_{w,1}} \cdot \frac{1+\sqrt{1- \frac{\zeta}{\{V/\mu\}_1}}}{1+\sqrt{1- \frac{\zeta}{\{V/\mu\}_2}}} \qquad (5.25)$$

Incorporating the fact that $[1+\sqrt{1-\zeta/\{V/\mu\}_2}] \geq 1$ leads to (5.26), where the right side is seen to be equal to 2η.

$$\{\ell/\mu A_{wn}\}_2 > \{\ell/\mu A_{wn}\}_1 \cdot \frac{F_{w,max}}{F_{w,1}} \cdot \left[1+\sqrt{1- \frac{\zeta}{\{V/\mu\}_1}}\right] = 2\eta \qquad (5.26)$$

Following an initial trial design, windable cores can be readily identified from the large number of candidate cores that meet the energy-

transfer requirement by use of the above relationships. In the following
section, the step-by-step procedure for identifying windable cores is pre-
sented.

5.6 Design Procedures for Single-Winding and Two-Winding Converters

Using Tables 5.1, 5.2 and 5.4, a general procedure for designing
energy-storage reactors and transformers is now presented. The specifica-
tions for single-winding converter configurations which are considered in
this procedure are V_0, $V_{I,min}$, $V_{I,max}$, $P_{0,max}$, V_D, V_Q, B_{max}, B_R, $F_{w,max}$,
and the controller-converter type with the appropriate controller time para-
meter T, t_{on}, or t_{off}. For two-winding converters, the specifications in-
clude all those above for the single-winding configurations plus an addi-
tional performance or design constraint.

Having decided, from consideration of the overall system and envir-
onmental requirements, on a particular combination of controller and con-
verter to be implemented, the first step in the design procedure is to
identify which one of the four parts of Table 5.1 is applicable. In what
follows, if the converter to be designed is a two-winding voltage step-up/
current step-up configuration, then, for example, when the procedure calls
for the computation of the number of turns N using equation (7), it is
understood that equations (7P) and (7S) are both to be used to calculate,
respectively, the number of turns on the primary winding N_P and the number
of secondary turns N_S.

A. <u>Identify Converter Configuration and Associated Table 5.1 Equations</u>

For the three single-winding converters, choose Table 5.1-A, 5.1-B, or
5.1-C, then go to step B. For the two-winding converter, identify the
desired option A,B,C,D,E,H, or J and calculate the turns ratio γ from

C-2

the associated option constraint equation in Table 5.2 and use Table 5.1-D.

B. __Identify Candidate Cores Capable of Transferring Required Energy per Cycle__

1. Choose number of cores J to be stacked and calculate ζ and δ from (1), (3) or (5), according to the controller type.

2. Identify the cores in Table 5.4 satisfying (5.19); these cores become candidates for further consideration. To highlight the dividing line between possibly usable and unusable cores, one may wish for each relative-permeability column in Table 5.4 to draw a line above the parameter box corresponding to the smallest core size which just satisfies the condition $\{V/\mu\} \geq \delta$. Cores below this staircase-like line are candidates for further consideration.

C. __Determine the Number of Turns and Inductance__

1. Select a particular core size and relative permeability, according to the designer's preference from the array of candidate cores obtained in step B.

2. Compute inductance $L = \{L/N^2\}JN^2$ using parameter $\{L/N^2\}$ from Table 5.4 for the chosen core, J for the number of cores in the stack, and the value of N obtained in step C-2.

D. __Determine Wire Size__

Compute maximum rms winding current using (2), (4) or (6). Using the maximum allowable current density specified by the designer, determine the required wire size and cross-sectional area from a wire table.

E. __Check winding Factor F_W to Determine Windability__

Compute winding factor F_W using $\{A_{wn}\}$ from Table 5.4. If

$F_W \leq F_{W,max}$, trial core meets the specifications and the design is completed for all configurations but TNUD and TN2UD. For TNUD and TN2UD, go to step G. For all configurations, if $F_W > F_{W,max}$ of if designer wishes to try another core, go to step F.

F. **Identification of Windable Core**

1. As the first step in identifying a new trial core, compute η from (5.27) using the value of ζ from step B-1 and the initial trial values $F_{w,1}$, $\{\ell/\mu A_{wn}\}_1$ and $\{V/\mu\}_1$ where the subscript 1 stands for the values used for the first trial core.

    $$\eta = \frac{1}{2} \{\ell/\mu A_{wn}\}_1 \cdot \frac{F_{w,max}}{F_{w,1}} \cdot \left[1 + \sqrt{1 - \frac{\zeta}{\{V/\mu\}_1}} \right] \tag{5.27}$$

2. Cores which satisfy (5.28) are windable.

    $$\{\ell/\mu A_{wn}\} \leq \eta \tag{5.28}$$

    Those which do not satisfy (5.28) may be eliminated from further consideration if they fail to satisfy (5.29)

    $$\{\ell/\mu A_{wn}\} \leq 2\eta \tag{5.29}$$

    Cores which satisfy (5.29) are windable if they satisfy the more exacting inequality (5.30)

    $$\{\ell/\mu A_{wn}\} \left[1 + \sqrt{1 - \frac{\zeta}{\{V/\mu\}}} \right] \leq 2\eta \tag{5.30}$$

3. If a windable core is not found in step E-2, increase the number of cores in the stack by one and go to step B-1. If a windable core is obtained, compute turns and inductance using steps C-2 and C-3. For TNUD and TN2UD, go to step G; for all other configurations, go to step F-4.

4. Using step D, obtain wire size, which will nearly always be the initially computed size; if it is no larger than the initial size, the design is completed. If it is larger and the new winding factor exceeds $F_{w,max}$, or if the designer wishes to try another core, go to step F-2.

G. Check for $\underline{B_{B,max} < B_{max}}$ for TNUD and TN2UD

1. Using the windable core obtained from step 3 or from step F, compute the number of turns N' using (5.31) for TNUD, or (5.32) for TN2UD.

$$N' = \frac{V_0(V_{I,max}-V_Q)(B_{max}-B_R)}{2P_{0,max}(V_{I,max}+V_0+V_D-V_Q)} \cdot \{\ell/\mu\} \cdot$$

$$\cdot \left[1+\sqrt{1-\frac{\varsigma(V_{I,max}+V_0+V_D-V_Q)}{\{V/\mu\}(V_{I,min}+V_0+V_D-V_Q)}}\right] \tag{5.31}$$

$$N_P' = \frac{V_0(V_{I,max}-V_Q)(B_{max}-B_R)}{2P_{0,max}[\gamma(V_{I,max}-V_Q)+V_0+V_D)]} \cdot \{\ell/\mu\} \cdot$$

$$\cdot \left[1+\sqrt{1-\frac{\varsigma[\gamma(V_{I,max}-V_Q)+V_0+V_D)]}{\{V/\mu\}[\gamma(V_{I,min}-V_Q)+V_0+V_D)]}}\right] \tag{5.32}$$

2. If the value of N' (or N_P') exceeds the value of N for TNUD (or N_P for TN2UD) from step C-2, then N (or N_P) is to be used and the design is completed. The flux density in cores which fail this test will exceed the specified value B_{max} at the operating point $P_0 = P_{0,max}$ and $V_I = V_{I,max}$. If this test is failed or if the designer wishes to try another core, and this step was reached by going directly from step E to step G, then go to step F-1 and continue. If the core under consideration was obtained from the procedure of step F, go to step F-2 and select a new windable core using the original value of n.

5.7 Design Examples

Four examples are given in this section which illustrate the procedure for designing energy-storage reactors and transformers for various controller-converter combinations. Example 1 considers a current step-up converter with a constant-frequency controller. In Example 2, the reactor for a constant on-time voltage step-up configuration is designed. Example 3 illustrates a two-winding converter core design for use with a constant-frequency controller. Example 4 considers a voltage step-up/current step-up converter with constant on-time controller.

Example 1

Design the inductor for a current step-up converter with a constant-frequency controller (FQCU) with $T = 100$ microseconds. The remaining specifications are: $V_0 = 15$ V; $V_{I,min} = 20$ V; $V_{I,max} = 28$ V; $P_{0,max} = 40$ W; $V_0 = 0.5$ V; $V_D = 0.7$ V; $B_{max} = 0.35$ T; $B_R = 0.01$ T; $F_{w,max} = 0.4$.

A. Use Table 5.1-B

B. 1. Choose $J = 1$. Using (1,CU), $\zeta = \delta = 3.21 \times 10^{-2}$

C. 1. Select core size $S = 18$ with $\mu_r = 60$, with parameters $\{V/\mu\} = 5.39 \times 10^{-2}$, $\{\ell/\mu\} = 1.19 \times 10^3$, $\{L/N^2\} = 3.82 \times 10^{-8}$, $\{\ell/\mu A_{wn}\} = 2.97 \times 10^6$, and $\{A_{wn}\} = 4.0 \times 10^{-4} m^2$.

   2. Using (7,CU), $N = 124$

   3. Using parameter $\{L/N^2\}$ and N found in step C-2, $L = 0.59$ mH.

D. Using (2,CU), $I_{Xe,max} = 2.67$ A; on the basis of $5.0671 \times 10^{-7} m^2/A$ (1000 circular mils/A), the wire size is AWG 15 with wire area $A_{wr} = 1.836 \times 10^{-6} m^2$ (3624 circular mils).

E. Using N and A_{wr} from steps C-2 and D and parameter $\{A_{wn}\} = 4.0 \times 10^{-4} m^2$ (2.78×10^5 circular mils), $F_w = 0.57 > F_{w,max}$ and the core is not windable.

F. 1. Using (5.27) $\eta = 1.71 \times 10^6$; $2\eta = 3.42 \times 10^6$.

2. Select trial core size S = 21 with μ_r = 125, with parameters $\{V/\mu\}$ = 3.49×10^{-2}, $\{\ell/\mu\} = 5.19 \times 10^2$, $\{L/N^2\} = 1.30 \times 10^{-7}$, $\{\ell/\mu A_{wn}\} = 1.77 \times 10^6$, and $\{A_{wn}\} = 2.93 \times 10^{-4} m^2$. The value of parameter $\{\ell/\mu A_{wn}\}$ does not satisfy (28) but does satisfy (29) and yields for the left side of (30) 2.27×10^6 which is less than 2η and so is windable.

C. 2. Using (7,CU), N = 42.

3. Using $\{L/N^2\} = 1.30 \times 10^{-7}$, L = 0.23 mH.

D. Using (2,CU), $I_{Xe,max} = 2.8$ A. The wire size is unchanged (AWG 15).

E. Using N = 42, $A_{wr} = 1.836 \times 10^{-6} m^2$ and for the new trial core $\{A_{wn}\}$ = $2.93 \times 10^{-4} m^2$, $F_w = 0.26 < F_{w,max}$ and the core is windable, as predicted in step F.

The pertinent information concerning the core chosen as the second candidate includes the following: core size S = 21; μ_r = 125; N = 42; L = 0.23 mH; maximum rms inductor current $I_{Xe,max}$ = 2.8 A; wire size AWG 15; winding factor F_w = 0.26, which is less than the allowable maximum and the core is windable.

Example 2

Design the energy-storage inductor for a constant on-time voltage step-up controller-converter combination with transistor on-time t_{on} = 20 microseconds. The remaining specifications are: V_0 = 30 V; $V_{I,min}$ = 8 V; $V_{I,max}$ = 22 V; $P_{0,max}$ = 30 W; V_Q = 0.5 V; V_D = 0.7 V; B_{max} = 0.35 T; B_R = 0.01 T; and $F_{w,max}$ = 0.4.

A. Use Table 5.1-A

B. 1. Choose J=1. Using (3,VU), $\zeta = 1.04 \times 10^{-2}$, h = 2.87, $\delta = 1.80 \times 10^{-2}$.

C. 1. Select core size S = 16 with μ_r = 60, with parameters $\{V/\mu\}$ = 2.49x 10^{-2}; $\{\ell/\mu\} = 7.52 \times 10^2$; $\{L/N^2\} = 4.40 \times 10^{-8}$; $\{\ell/\mu A_{wn}\} = 5.34 \times 10^6$;

and $\{A_{wn}\} = 1.41 \times 10^{-4} m^2$.

2. Using (7,VU), N = 56.

3. L = 0.138 mH.

D. Using (4,VU), $I_{Xe,max}$ = 4.04 A; on the basis of $5.0671 \times 10^{-7} m^2/A$ (1000 circular mils/A), the wire size is AWG 14 with wire area A_{wr} = 2.29 $\times 10^{-6} m^2$ (4529 circular mils).

E. F_w = 0.91 > $F_{w,max}$ and the core is not windable.

F. 1. Using (5.27), η = 2.07 x 10^6.

2. Select trial core size S = 18 with μ_r = 125, with parameters $\{V/\mu\}$ = 2.59×10^{-2}; $\{\ell/\mu\}$ = 5.70×10^2; $\{L/N^2\}$ = 7.97×10^{-8}; $\{\ell/\mu A_{wn}\}$ = 1.43 $\times 10^6$; and $\{A_{wn}\}$ = $4.00 \times 10^{-4} m^2$. The parameter $\{\ell/\mu A_{wn}\}$ satisfies (28) and so is windable.

C. 2. Using (7,VU), N = 43.

3. L = 0.147 mH.

D. Using (4,VU), $I_{Xe,max}$ = 4.04 A and the wire size is unchanged.

E. F_w = 0.246 < $F_{w,max}$ and the core is windable as predicted in step F.

The significant quantities resulting from the design procedure are: core size S = 18; μ_r = 125; N = 43; L = 0.147 mH; maximum winding rms current $I_{Xe,max}$ = 4.04 A; wire size is AWG 14; and winding factor F_w = 0.246 and core is windable.

Example 3

Design the transformer for a two-winding voltage step-up/current step-up converter with a constant-frequency controller (FQ2UD) with T=100 microseconds. The remaining specifications are: V_0 = 12 V; $V_{I,min}$ = 10 V; $V_{I,max}$ = 15 V; $P_{0,max}$ = 30 W; V_Q = 0.5 V; V_D = 0.7 V; B_{max} = 0.35 T; B_R = 0.01 T; $F_{W,max}$ = 0.4; and the option constraint of a minimum value

for duty cycle α of 0.3.

A. Using Table 5.2, U_B = 0.3 for option B. From (9), N_S/N_P = γ_B = 2.04. Use Table 5.1-D for remaining relationships.

B. 1. Choose J = 1. Using (1,2UD), ζ = δ = 5.49×10^{-2}.

C. 1. Select core size S = 21 with μ_r = 60, with parameters $\{^V/\mu\}$ = 7.26×10^{-2}; $\{\ell/\mu\}$ = 1.08×10^3; $\{L/N^2\}$ = 6.22×10^{-8}; $\{\ell/\mu A_{wn}\}$ = 3.69×10^6; and $\{A_{wn}\}$ = $2.93 \times 10^{-4} m^2$.

2. Using (7P,2UD), N_P = 32.

Using (7S,2UD), N_S = 65.

3. L_P = 0.048 mH.

D. Using (2P,2UD) and (2S,2UD), $I_{Pe,max}$ = 5.47 A and $I_{Se,max}$ = 3.35 A; on the basis of $5.0671 \times 10^{-7} m^2/A$ (1000 circular mils/A), the primary wire size is AWG 12 with wire area $A_{wr,P}$ = $3.592 \times 10^{-6} m^2$ (7088 circular mils) and the secondary wire size is AWG 14 with wire area $A_{wr,S}$ = $2.295 \times 10^{-6} m^2$ (4529 circular mils).

E. F_W = 0.9 > $F_{W,max}$ and the core is not windable

F. 1. Using (5.27), η = 1.22×10^6.

2. Select core size S = 26 with μ_r = 125, with parameter $\{\ell/\mu A_{wn}\}$ = 1.08×10^6 which is less than η and should be windable. The other parameters are $\{^V/\mu\}$ = 1.01×10^{-1}; $\{\ell/\mu\}$ = 8.10×10^2; $\{L/N^2\}$ = 1.54×10^{-7}; and $\{A_{wn}\}$ = $7.52 \times 10^{-4} m^2$.

C. 2. Using (7P,2UD), N_P = 27.

Using (7S,2UD), N_S = 55.

3. L_P = 0.11 mH.

D. Using (2P,2UD) and (2S,2UD), $I_{Pe,max}$ = 5.37 A and $I_{Se,max}$ = 3.29 A, and the wire sizes are unchanged from the previous trial design.

E. F_W = 0.3 < $F_{W,max}$ and the core is windable.

A review of the quantities associated with the core meeting the converter specifications follows: core size $S = 26$; $\mu_r = 125$; $N_p = 27$; $N_S = 55$; $L_p = 0.11$ mH; $I_{Pe,max} = 5.37$ A; $I_{Se,max} = 3.29$ A; wire sizes are primary AWG 12, secondary AWG 14; winding factor = 0.3.

Example 4

De.ign the inductor for a voltage step-up/current step-up converter with a constant on-time controller (TNUD) for the same converter specifications as given in Example 3 of Chapter II: $V_0 = 15$ V; $V_{I,min} = 12$ V; $V_{I,max} = 20$ V; $P_{0,max} = 30$ W; $V_Q = 0.5$ V; $V_D = 0.8$ V; $B_{max} = 0.35$ T; $B_R = 0.01$ T, $F_{w,max} = 0.4$ and $t_{on} = 50$ microseconds.

A. Use Table 5.1-C

B. 1. Choose J=1. Using (3,UD), $\zeta = 4.72 \times 10^{-2}$, $h = 1.70$, $\delta = 5.67 \times 10^{-2}$.

C. 1. Select core size $S = 21$ with $\mu_r = 60$, with parameter $\{V/\mu\} = 7.26 \times 10^{-2}$, $\{\ell/\mu\} = 1.08 \times 10^3$, $\{L/N^2\} = 6.22 \times 10^{-8}$, $\{\ell/\mu A_{wn}\} = 3.69 \times 10^6$, and $\{A_{wn}\} = 2.93 \times 10^{-4} m^2$.

   2. Using (7,UD), $N = 60$

   3. $L = 0.22$

D. Using (4,UD), $I_{Xe,max} = 4.8$ A; on the basis of $5.0671 \times 10^{-7} m^2/A$, the wire size is AWG 13 with wire area $\{A_{wr}\} = 2.87 \times 10^{-6} m^2$.

E. $F_w = 0.59 > F_{w,max}$ and the core is not windable

F. 1. $\eta = 1.99 \times 10^6$

   2. Select core size $S = 25$ with $\mu_r = 200$, with parameter $\{V/\mu\} = 6.20 \times 10^{-2}$, $\{\ell/\mu\} = 4.63 \times 10^2$, $\{L/N^2\} = 2.90 \times 10^{-7}$, $\{\ell/\mu A_{wn}\} = 7.57 \times 10^5$ and $\{A_{wn}\} = 6.11 \times 10^{-4}$.

G. 1. Using (5.31) $N' = 24$

   2. Using (7,UD), $N = 25 > N'$. Thus, the flux density will exceed the specified value B_{max} at the operating point $P_0 = P_{0,max}$ and

$V_I = V_{I,max}$, and this core is not workable.

F. 2. Select another core with $S = 25$, $\mu_r = 125$ with $\{V/\mu\} = 9.92 \times 10^{-2}$, $\{\ell/\mu\} = 7.40 \times 10^2$, $\{L/N^2\} = 1.81 \times 10^{-7}$, $\{\ell/\mu A_{wn}\} = 1.21 \times 10^6$, and $\{A_{wn}\} = 6.11 \times 10^{-4} m^2$

G. 1. $N' = 56$

G. 2. $N = 46 < N'$. Thus, the flux density will never exceed B_{max}, and the design is completed.

E. $F_w = 0.22$

A summary of this workable design follows:

$S = 25$, $\mu_r = 125$, $N = 46$, AWG 13, and $F_w = 0.22$.

5.8 Conclusions

The new set of design procedures presented in this chapter illustrates a straight-forward method for designing energy-storage reactors for a group of widely-used dc-to-dc converters. The design procedure is developed from analyses of piecewise-linearized circuit models of the various controller-converter combinations as described in Chapters II and III. As indicated in those chapters, the design relationships developed for calculating winding turns and maximum rms reactor currents are valid only when each converter operates in Mode 1 at least at the point in its output-power/input-voltage operating range where the peak instantaneous value of core flux density is encountered. Only in the two cases of the single-winding and the two-winding voltages step-up/current step-up converters with constant on-time controllers does this condition require the additional constraint, not imposed in Chapters II and III, that the maximum of the peak flux density occur at $P_{0,max}$ and $V_{I,min}$. This might result in a design

which uses a slightly larger core than might be necessary.

The most important features of the new procedure are the facility provided the designer to eliminate from the population of available cores those which cannot meet the energy transfer requirement and a method for identifying windable cores. These new features, along with a specially constructed table of magnetic core parameters, enable the designer to select from among the wide selection of powder permalloy cores those which meet the design specifications, eliminating the need for repetitive trial designs.

Table 5.1(A)   Design Expressions for Single-Winding
Voltage Step-Up Converter (VU)

CONTROLLER TYPE	SINGLE-WINDING VOLTAGE-STEP-UP CONVERTER (VU)	
CONSTANT-FREQUENCY: (FQ)	$\zeta = \dfrac{2TP_{O,max}(V_O+V_D-V_{I,min})}{JV_O(B_{max}-B_R)^2}$ and $\qquad\qquad \delta = \zeta$	(1,VU)
	$I_{Xe,max} = \dfrac{P_{O,max}(V_O+V_D-V_Q)}{V_O(V_{I,min}-V_Q)}\sqrt{1+\dfrac{1}{12}\left[\dfrac{TV_O(V_{I,min}-V_Q)^2(V_O+V_D-V_{I,min})}{LP_{O,max}(V_O+V_D-V_Q)^2}\right]^2}$	(2)
CONSTANT ON-TIME: (TN)	$\zeta = \dfrac{2t_{on}P_{O,max}(V_O+V_D-V_Q)}{JV_O(B_{max}-B_R)^2}$ and $\qquad \delta = \zeta\,\dfrac{h^2}{2h-1}$ $\text{where } h = \dfrac{V_{I,max}-V_Q}{V_{I,min}-V_Q}$	(3)
	$I_{Xe,max} = \dfrac{P_{O,max}(V_O+V_D-V_Q)}{V_O(V_{I,min}-V_Q)}\sqrt{1+\dfrac{1}{12}\left[\dfrac{t_{on}V_O(V_{I,min}-V_Q)^2}{LP_{O,max}(V_O+V_D-V_Q)}\right]^2}$	(4)
CONSTANT OFF-TIME: (TF)	$\zeta = \dfrac{2t_{off}P_{O,max}(V_O+V_D-V_{I,min})(V_O+V_D-V_Q)}{JV_O(V_{I,min}-V_Q)(B_{max}-B_R)^2}$ and $\qquad \delta = \zeta$	(5)
	$I_{Xe,max} = \dfrac{P_{O,max}(V_O+V_D-V_Q)}{V_O(V_{I,min}-V_Q)}\sqrt{1+\dfrac{1}{12}\left[\dfrac{t_{off}V_O(V_{I,min}-V_Q)(V_O+V_D-V_{I,min})}{LP_{O,max}(V_O+V_D-V_Q)}\right]^2}$	(6)
ALL TYPES: (FQ,TN,TF)	$N = \dfrac{V_O(V_{I,min}-V_Q)(B_{max}-B_R)}{2P_{O,max}(V_O+V_D-V_Q)}\{\tfrac{\ell}{\mu}\}\left[1+\sqrt{1-\dfrac{\zeta}{\{V/\mu\}}}\right]$	(7)

Table 5.1(B) Design Expressions for Single-Winding Current Step-Up Converter

CONTROLLER TYPE	SINGLE-WINDING CURRENT STEP-UP CONVERTER (CU)		
CONSTANT FREQUENCY: (FQ)	$\zeta = \dfrac{2TP_{0,max}(V_{I,max}-V_0-V_Q)(V_0+V_D)}{JV_0(V_{I,max}+V_D-V_Q)(B_{max}-B_R)^2}$ and	$\delta = \zeta$	(1,CU)
	$I_{Xe,max} = \dfrac{P_{0,max}}{V_0}\sqrt{1+\dfrac{1}{12}\left[\dfrac{TV_0(V_{I,max}-V_0-V_Q)(V_0+V_D)}{LP_{0,max}(V_{I,max}+V_D-V_Q)}\right]^2}$		(2)
CONSTANT ON-TIME:	$\zeta = \dfrac{2t_{on}P_{0,max}(V_{I,max}-V_0-V_Q)}{JV_0(B_{max}-B_R)^2}$ and	$\delta = \zeta$	(3)
(TN)	$I_{Xe,max} = \dfrac{P_{0,max}}{V_0}\sqrt{1+\dfrac{1}{12}\left[\dfrac{t_{on}V_0(V_{I,max}-V_0-V_Q)}{LP_{0,max}}\right]^2}$		(4)
CONSTANT OFF-TIME: (TF)	$\zeta = \dfrac{2t_{off}P_{0,max}(V_0+V_D)}{JV_0(B_{max}-B_R)^2}$ and	$\delta = \zeta$	(5)
	$I_{Xe,max} = \dfrac{P_{0,max}}{V_0}\sqrt{1+\dfrac{1}{12}\left[\dfrac{t_{off}V_0(V_0+V_D)}{LP_{0,max}}\right]^2}$		(6)
ALL TYPES: (FQ,TN,TF)	$N = \dfrac{V_0(B_{max}-B_R)}{2P_{0,max}}\{\frac{\ell}{\mu}\}\left[1+\sqrt{1-\dfrac{\zeta}{\{V/\mu\}}}\right]$		(7)

Table 5.1(C) Design Expressions for Single-Winding
Voltage Step-Up/Current Step-Up Converter (UD)

CONTROLLER TYPE	SINGLE-WINDING VOLTAGE STEP-UP/CURRENT STEP-UP CONVERTER (UD)		
CONSTANT FREQUENCY: (FQ)	$\zeta = \dfrac{2^\top P_{0,max}(V_0+V_D)}{JV_0(B_{max}-B_R)^2}$ and	$\delta = \zeta$	(1,UD)
	$I_{Xe,max} = \dfrac{P_{0,max}(V_{I,min}+V_0+V_D-V_Q)}{V_0(V_{I,min}-V_Q)}\sqrt{1+\dfrac{1}{12}\left[\dfrac{TV_0(V_{I,min}-V_Q)^2(V_0+V_D)}{LP_{0,max}(V_{I,min}+V_0+V_D-V_Q)^2}\right]^2}$		(2)
CONSTANT ON-TIME:	$\zeta = \dfrac{2t_{on}P_{0,max}(V_{I,min}+V_0+V_D-V_Q)}{JV_0(B_{max}-B_R)^2}$ and	$\delta = \zeta\,\dfrac{h^2}{2h-1}$	(3)
		where $h = \dfrac{V_{I,max}-V_Q}{V_{I,min}-V_Q}$	
(TN)	$I_{Xe,max} = \dfrac{P_{0,max}(V_{I,min}+V_0+V_D-V_Q)}{V_0(V_{I,min}-V_Q)}\sqrt{1+\dfrac{1}{12}\left[\dfrac{t_{on}V_0(V_{I,min}-V_Q)^2}{LP_{0,max}(V_{I,min}+V_0+V_D-V_Q)}\right]^2}$		(4)
CONSTANT OFF-TIME: (TF)	$\zeta = \dfrac{2t_{off}P_{0,max}(V_{I,min}+V_0+V_D-V_Q)(V_0+V_D)}{JV_0(V_{I,min}-V_Q)(B_{max}-B_R)^2}$ and	$\delta = \zeta$	(5)
	$I_{Xe,max} = \dfrac{P_{0,max}(V_{I,min}+V_0+V_D-V_Q)}{V_0(V_{I,min}-V_Q)}\sqrt{1+\dfrac{1}{12}\left[\dfrac{t_{off}V_0(V_{I,min}-V_Q)(V_0+V_D)}{LP_{0,max}(V_{I,min}+V_0+V_D-V_Q)}\right]^2}$		(6)
ALL TYPES: (FQ,TN,TF)	$N = \dfrac{V_0(V_{I,min}-V_Q)(B_{max}-B_R)}{2P_{0,max}(V_{I,min}+V_0+V_D-V_Q)}\{\tfrac{\ell}{\mu}\}\left[1+\sqrt{1-\dfrac{\zeta}{\{V/\mu\}}}\right]$		(7)

CONTROLLER TYPE	TWO-WINDING VOLTAGE STEP-UP/CURRENT STEP-UP CONVERTER (2UD)	
CONSTANT FREQUENCY (FQ)	$\zeta = \dfrac{2TP_{0,max}(V_0+V_D)}{JV_0(B_{max}-B_R)^2}$ and $\qquad \delta = \zeta$	(1,2UD)
	$I_{Pe,max}=\sqrt{\left[\left[\dfrac{P_{0,max}}{V_0}(\gamma+\dfrac{V_0+V_D}{V_{I,min}-V_Q})\right]^2 + \dfrac{1}{12}\left[\dfrac{(V_0+V_D)T}{L_P(\gamma+\dfrac{V_0+V_D}{V_{I,min}-V_Q})}\right]^2\right]\dfrac{V_0+V_D}{V_0+V_D+\gamma(V_{I,min}-V_Q)}}$	(2P)
	$I_{Se,max}=I_{Pe,max}\sqrt{\dfrac{V_{I,min}-V_Q}{\gamma(V_0+V_D)}}$	(2S)
CONSTANT ON-TIME (TN)	$\zeta = \dfrac{2t_{on}P_{0,max}[V_0+V_D+\gamma(V_{I,min}-V_Q)]}{JV_0(B_{max}-B_R)^2}$ and $\qquad \delta=\zeta\dfrac{h^2}{2h-1}$ where $h = \dfrac{V_{I,max}-V_Q}{V_{I,min}-V_Q}$	(3)
	$I_{Pe}=\sqrt{\left[\left[\dfrac{P_{0,max}}{V_0}(\gamma+\dfrac{V_0+V_D}{V_I-V_Q})\right]^2 + \dfrac{1}{12}\left[\dfrac{(V_I-V_Q)t_{on}}{L_P}\right]^2\right]\dfrac{V_0+V_D}{V_0+V_D+\gamma(V_I-V_Q)}}$ $I_{Pe,max}=I_{Pe}$ at $(P_{0,max},V_{I,min})$ or at $(P_{0,max},V_{I,max})$, whichever is larger	(4P)
	$I_{Se}=I_{Pe}\sqrt{\dfrac{V_I-V_Q}{\gamma(V_0+V_D)}}$ $I_{Se,max}=I_{Se}$ at $(P_{0,max},V_{I,min})$ or at $(P_{0,max},V_{I,max})$, whichever is larger	(4S)
CONSTANT OFF-TIME (TF)	$\zeta = \dfrac{2t_{off}P_{0,max}(V_0+V_D)}{JV_0(B_{max}-B_R)^2}\left[1+\dfrac{V_0+V_D}{\gamma(V_{I,min}-V_Q)}\right]$ and $\qquad \delta=\zeta$	(5)
	$I_{Pe,max}=\sqrt{\left[\left[\dfrac{P_{0,max}}{V_0}(\gamma+\dfrac{V_0+V_D}{V_{I,min}-V_Q})\right]^2 + \dfrac{1}{12}\left[\dfrac{(V_0+V_D)t_{off}}{\gamma L_P}\right]^2\right]\dfrac{(V_0+V_D)}{(V_0+V_D)+\gamma(V_{I,min}-V_Q)}}$	(6P)
	$I_{Se,max}=I_{Pe,max}\sqrt{\dfrac{V_{I,min}-V_Q}{\gamma(V_0+V_D)}}$	(6S)
ALL TYPES (FQ,TN,TF)	$N_P = \dfrac{V_0(V_{I,min}-V_Q)(B_{max}-B_R)}{2P_{0,max}[\gamma(V_{I,min}-V_Q)+V_0+V_D]}\{\dfrac{\ell}{\mu}\}\left[1+\sqrt{1-\dfrac{\zeta}{\{\ell/\mu\}}}\right]$	(7P)
	$N_S = \gamma N_P$	(7S)

Table 5.2 Option Descriptions and Design Equations for Two-Winding Voltage Step-Up/Current Step-Up Converter

OPTION NO	OPTION DESCRIPTION	MODE NO	OPTION CONSTRAINT EQUATION
A	$\dfrac{\alpha_{min}+\alpha_{max}}{2}=U_A$	1	$\dfrac{N_S}{N_P}=\gamma_A=\dfrac{(V_0+V_D)}{2(V_{I,min}-V_Q)(V_{I,max}-V_Q)}\left[-(V_{I,min}+V_{I,max}-2V_Q)(1-\dfrac{1}{2U_A})\right.$ $\left.+\sqrt{(V_{I,min}+V_{I,max}-2V_Q)^2(1-\dfrac{1}{2U_A})^2-4(V_{I,min}-V_Q)(V_{I,max}-V_Q)(1-\dfrac{1}{U_A})}\right]$ (8)
B	$\alpha_{min}=U_B$	1	$\dfrac{N_S}{N_P}=\gamma_B=\dfrac{V_0+V_D}{V_{I,max}-V_Q}(\dfrac{1}{U_B}-1)$ (9)
C	$\alpha_{max}-\alpha_{min}=U_C$	1	$\dfrac{N_S}{N_P}=\gamma_C=\dfrac{-(V_0+V_D)}{2(V_{I,min}-V_Q)(V_{I,max}-V_Q)}\left[(V_{I,min}+V_{I,max}-2V_Q-\dfrac{V_{I,max}-V_{I,min}}{U_C})\right.$ $\left.\pm\sqrt{(V_{I,min}+V_{I,max}-2V_Q-\dfrac{V_{I,max}-V_{I,min}}{U_C})^2-4(V_{I,min}-V_Q)(V_{I,max}-V_Q)}\right]$ (10)
D	$V_{CE_{max}}=U_D$	1 or 2	$\dfrac{N_S}{N_P}=\gamma_D=\dfrac{V_0+V_D}{U_D-V_{I,max}}$ (11)
E	$V_{DR_{max}}=U_E$	1 or 2	$\dfrac{N_S}{N_P}=\gamma_E=\dfrac{U_E-V_0}{V_{I,max}-V_Q}$ (12)
H	$\alpha_{max}=U_H$	1 or 2	$\dfrac{N_S}{N_P}=\gamma_H=\dfrac{V_0+V_D}{V_{I,min}-V_Q}(\dfrac{1}{U_H}-1)$ (13)
J	$\dfrac{N_S}{N_P}=U_J$	1 or 2	$\dfrac{N_S}{N_P}=\gamma_J=U_J$ (14)

Table 5.3 — Expressions for $\Delta W_{m,max}$ for the Twelve Controller-Converter Combinations. Expressions are for Mode 1 operation except for those identified by asterisk (*), which are for Mode 2

CONVERTER TYPE / CONTROLLER TYPE	SINGLE-WINDING VOLTAGE STEP-UP (VU)	SINGLE-WINDING CURRENT STEP-UP (CU)	VOLTAGE STEP-UP/CURRENT STEP-UP SINGLE WDG. (UD) $\gamma=1$; $L_X=L$	TWO WDG. (2UD) $\gamma=N_S/N_P$; $L_X=L_P$
CONSTANT-FREQUENCY (FQ)	$\dfrac{TP_{O,max}(V_O+V_D-V_{I,min})}{V_O}$ (15,VU)	$\dfrac{TP_{O,max}(V_O+V_D)(V_{I,max}-V_O-V_Q)}{V_O(V_{I,max}+V_D-V_Q)}$ (15,CU)	$\dfrac{TP_{O,max}(V_O+V_D)}{V_O}$	(15 ,UD) (15,2UD)
CONSTANT ON-TIME (TN)	$\dfrac{t_{on}^2(V_{I,max}-V_Q)^2}{2L}$ (16)	$\dfrac{t_{on}P_{O,max}(V_{I,max}-V_O-V_Q)}{V_O}$ (16)	$\dfrac{t_{on}^2(V_{I,max}-V_Q)^2}{2L_X}$	(16)
CONSTANT OFF-TIME (TF)	$\dfrac{t_{off}P_{O,max}(V_O+V_D-V_{I,min})(V_O+V_D-V_Q)}{V_O(V_{I,min}-V_Q)}$ (17)	$\dfrac{t_{off}P_{O,max}(V_O+V_D)}{V_O}$ (17)	$t_{off}P_{O,max}\dfrac{(V_O+V_D)}{V_O}\left(1+\dfrac{V_O+V_D}{\gamma(V_{I,min}-V_Q)}\right)$	(17)

Table 5.4(A) — Tables of Parameters for Commercially Available Powder Permalloy Toroidal Magnetic Cores (μ=14 ~ μ=160)

S Core Size No. — {V},m³ / {A_wn},m²	14	26	60	125	147	160
1 1,01E-08 / 1,82E-06				5,35E 01 2,24E-08 / 6,42E-05 2,93E 07	4,55E 01 2,64E-08 / 5,46E-05 2,49E 07	4,18E 01 2,07E-08 / 5,01E-05 2,29E 07
2 1,99E-08 / 2,70E-06	5,35E 02 3,94E-09 / 1,13E-03 1,98E 08	2,88E 02 7,32E-09 / 6,08E-04 1,07E 08	1,25E 02 1,69E-08 / 2,64E-04 4,63E 07	6,02E 01 3,52E-08 / 1,27E-04 2,22E 07	5,10E 01 4,14E-08 / 1,28E-04 1,89E 07	4,69E 01 4,50E-08 / 9,89E-05 1,73E 07
3 3,02E-08 / 2,93E-06	6,03E 02 4,73E-09 / 1,72E-03 2,06E 08	3,24E 02 8,78E-09 / 9,25E-04 1,11E 08	1,41E 02 2,03E-08 / 4,01E-04 4,80E 07	6,75E 01 4,22E-08 / 1,92E-04 2,30E 07	5,74E 01 4,97E-08 / 1,64E-04 1,96E 07	5,27E 01 5,41E-08 / 1,50E-04 1,80E 07
4 6,40E-08 / 4,10E-06	7,74E 02 6,08E-09 / 3,64E-03 1,88E 08	4,17E 02 1,13E-08 / 1,96E-03 1,01E 08	1,81E 02 2,60E-08 / 8,48E-04 4,40E 07	8,66E 01 5,42E-08 / 4,07E-04 2,11E 07	7,37E 01 6,38E-08 / 3,46E-04 1,88E 07	6,77E 01 6,94E-08 / 3,10E-04 1,65E 07
5 6,49E-08 / 4,10E-06	7,75E 02 6,14E-09 / 3,69E-03 1,89E 08	4,17E 02 1,14E-08 / 1,99E-03 1,02E 08	1,81E 02 2,63E-08 / 8,60E-04 4,40E 07	8,68E 01 5,49E-08 / 4,13E-04 2,11E 07	7,39E 01 6,45E-08 / 3,51E-04 1,88E 07	6,78E 01 7,02E-08 / 3,23E-04 1,65E 07
6 1,10E-07 / 9,22E-06	1,02E 03 6,85E-09 / 6,25E-03 1,10E 08	5,47E 02 1,12E-08 / 3,36E-03 5,93E 07	2,37E 02 2,59E-08 / 1,46E-03 2,57E 07	1,14E 02 5,41E-08 / 7,00E-04 1,23E 07	9,67E 01 6,36E-08 / 5,95E-04 1,05E 07	8,89E 01 6,92E-08 / 5,47E-04 9,64E 06
7 1,25E-07 / 3,84E-06	7,75E 02 1,19E-08 / 7,13E-03 2,02E 08	4,17E 02 2,21E-08 / 3,84E-03 1,09E 08	1,81E 02 5,09E-08 / 1,66E-03 4,71E 07	8,68E 01 1,06E-07 / 7,98E-04 2,26E 07	7,38E 01 1,25E-07 / 6,79E-04 1,92E 07	6,78E 01 1,36E-07 / 6,24E-04 1,77E 07
8 1,64E-07 / 1,43E-05	1,24E 03 6,07E-09 / 9,32E-03 8,67E 07	6,67E 02 1,13E-08 / 5,02E-03 4,67E 07	2,89E 02 2,60E-08 / 2,17E-03 2,02E 07	1,39E 02 5,42E-08 / 1,04E-03 9,71E 06	1,18E 02 6,37E-08 / 8,67E-04 8,26E 06	1,08E 02 6,94E-08 / 8,15E-04 7,59E 06
9 2,06E-07 / 1,43E-05	1,24E 03 7,63E-09 / 1,17E-02 8,67E 07	6,67E 02 1,42E-08 / 6,31E-03 4,67E 07	2,89E 02 3,27E-08 / 2,73E-03 2,02E 07	1,39E 02 6,81E-08 / 1,31E-03 9,71E 06	1,18E 02 8,01E-08 / 1,12E-03 8,26E 06	1,08E 02 8,72E-08 / 1,02E-03 7,59E 06
10 2,38E-07 / 1,64E-05	1,35E 03 7,39E-09 / 1,35E-02 8,24E 07	7,28E 02 1,37E-08 / 7,28E-03 4,44E 07	3,16E 02 3,17E-08 / 3,16E-03 1,92E 07	1,52E 02 6,60E-08 / 1,52E-03 9,23E 06	1,29E 02 7,76E-08 / 1,29E-03 7,85E 06	1,18E 02 8,45E-08 / 1,18E-03 7,21E 06
11 2,50E-07 / 2,69E-05	1,56E 03 5,02E-09 / 1,42E-02 5,02E 07	8,42E 02 1,08E-08 / 7,66E-03 3,13E 07	3,65E 02 2,49E-08 / 3,32E-03 1,36E 07	1,75E 02 5,20E-08 / 1,59E-03 6,52E 06	1,49E 02 6,11E-08 / 1,35E-03 5,64E 06	
12 3,56E-07 / 3,83E-05	1,77E 03 6,43E-09 / 2,02E-02 4,63E 07	9,55E 02 1,19E-08 / 1,09E-02 2,49E 07	4,14E 02 2,75E-08 / 4,72E-03 1,08E 07	1,99E 02 5,74E-08 / 2,26E-03 5,19E 06	1,69E 02 6,75E-08 / 1,93E-03 4,41E 06	1,55E 02 7,35E-08 / 1,77E-03 4,05E 06
13 7,89E-07 / 7,12E-05	2,34E 03 8,22E-09 / 4,49E-02 3,28E 07	1,26E 03 1,53E-08 / 2,42E-02 1,77E 07	5,45E 02 3,52E-08 / 1,05E-02 7,65E 06	2,62E 02 7,34E-08 / 5,02E-03 3,67E 06	2,22E 02 8,63E-08 / 4,27E-03 3,12E 06	2,04E 02 9,39E-08 / 3,92E-03 2,87E 06
14 9,77E-07 / 6,38E-05	2,39E 03 9,69E-09 / 5,55E-02 3,75E 07	1,29E 03 1,82E-08 / 2,99E-02 2,02E 07	5,58E 02 4,15E-08 / 1,30E-02 8,75E 06	2,68E 02 8,66E-08 / 6,22E-03 4,20E 06	2,28E 02 1,02E-07 / 5,29E-03 3,57E 06	
15 1,15E-06 / 1,14E-04	2,69E 03 7,81E-09 / 6,54E-02 2,53E 07	1,56E 03 1,45E-08 / 3,52E-02 1,36E 07	6,75E 02 3,35E-08 / 1,53E-02 5,91E 06	3,24E 02 6,97E-08 / 7,32E-03 2,83E 06	2,76E 02 8,20E-08 / 6,23E-03 2,41E 06	2,53E 02 8,93E-08 / 5,72E-03 2,21E 06
16 1,88E-06 / 1,41E-04	3,22E 03 1,03E-08 / 1,07E-01 2,29E 07	1,74E 03 1,91E-08 / 5,74E-02 1,23E 07	7,52E 02 4,40E-08 / 2,49E-02 5,34E 06	3,61E 02 9,17E-08 / 1,19E-02 2,57E 06	3,07E 02 1,08E-07 / 1,02E-02 2,18E 06	2,82E 02 1,17E-07 / 9,33E-03 2,00E 06
17 2,34E-06 / 1,47E-04	3,39E 03 1,16E-08 / 1,33E-01 2,31E 07	1,82E 03 2,15E-08 / 7,17E-02 1,24E 07	7,90E 02 4,97E-08 / 3,11E-02 5,38E 06	3,79E 02 1,04E-07 / 1,49E-02 2,58E 06	3,23E 02 1,22E-07 / 1,27E-02 2,20E 06	2,96E 02 1,33E-07 / 1,16E-02 2,02E 06
18 4,06E-06 / 4,00E-04	5,09E 03 8,92E-09 / 2,31E-01 1,27E 07	2,74E 03 1,66E-08 / 1,24E-01 6,86E 06	1,19E 03 3,82E-08 / 5,39E-02 2,97E 06	5,70E 02 7,97E-08 / 2,59E-02 1,43E 06	4,85E 02 9,37E-08 / 2,20E-02 1,21E 06	4,45E 02 1,02E-07 / 2,02E-02 1,11E 06
19 4,15E-06 / 1,56E-04	3,61E 03 1,81E-08 / 2,36E-01 2,31E 07	1,94E 03 3,37E-08 / 1,27E-01 1,25E 07	8,42E 02 7,77E-08 / 5,51E-02 5,40E 06	4,04E 02 1,62E-07 / 2,64E-02 2,59E 06	3,44E 02 1,90E-07 / 2,25E-02 2,20E 06	3,16E 02 2,07E-07 / 2,07E-02 2,02E 06
20 4,53E-06 / 2,94E-04				5,28E 02 1,03E-07 / 2,89E-02 1,80E 06	4,49E 02 1,22E-07 / 2,45E-02 1,53E 06	
21 5,48E-06 / 2,93E-04	4,63E 03 1,45E-08 / 3,11E-01 1,58E 07	2,49E 03 2,69E-08 / 1,68E-01 8,52E 06	1,06E 03 6,22E-08 / 7,26E-02 3,69E 06	5,19E 02 1,30E-07 / 3,49E-02 1,77E 06	4,41E 02 1,52E-07 / 2,96E-02 1,51E 06	4,05E 02 1,66E-07 / 2,72E-02 1,30E 06
22 5,78E-06 / 2,94E-04	4,72E 03 1,48E-08 / 3,28E-01 1,61E 07	2,54E 03 2,74E-08 / 1,77E-01 8,64E 06	1,10E 03 6,32E-08 / 7,66E-02 3,75E 06			
23 6,09E-06 / 3,64E-04	5,10E 03 1,33E-08 / 3,46E-01 1,40E 07	2,75E 03 2,47E-08 / 1,86E-01 7,54E 06	1,19E 03 5,69E-08 / 8,08E-02 3,27E 06	5,72E 02 1,19E-07 / 3,88E-02 1,57E 06	4,86E 02 1,39E-07 / 3,30E-02 1,33E 06	4,47E 02 1,52E-07 / 3,03E-02 1,23E 06
24 1,05E-05 / 4,27E-04	5,59E 03 1,92E-08 / 6,00E-01 1,31E 07	3,01E 03 3,56E-08 / 3,23E-01 7,05E 06	1,31E 03 8,21E-08 / 1,40E-01 3,06E 06	6,26E 02 1,71E-07 / 6,72E-02 1,47E 06	5,33E 02 2,01E-07 / 5,71E-02 1,25E 06	4,89E 02 2,19E-07 / 5,25E-02 1,15E 06
25 1,56E-05 / 6,11E-04	6,61E 03 2,03E-08 / 8,86E-01 1,08E 07	3,56E 03 3,76E-08 / 4,77E-01 5,82E 06	1,54E 03 8,69E-08 / 2,07E-01 2,52E 06	7,40E 02 1,81E-07 / 9,92E-02 1,21E 06	6,30E 02 2,13E-07 / 8,44E-02 1,03E 06	5,78E 02 2,32E-07 / 7,75E-02 9,47E 05
26 1,59E-05 / 7,52E-04	7,24E 03 1,73E-08 / 9,05E-01 9,62E 06	3,98E 03 3,21E-08 / 4,67E-01 5,18E 06	1,69E 03 7,41E-08 / 2,11E-01 2,25E 06	8,18E 02 1,54E-07 / 1,01E-01 1,08E 06	6,89E 02 1,82E-07 / 8,62E-02 9,16E 05	6,33E 02 1,98E-07 / 7,92E-02 8,42E 05
27 2,06E-05 / 9,48E-04	8,13E 03 1,78E-08 / 1,17E 00 8,57E 06	4,38E 03 3,30E-08 / 6,32E-01 4,62E 06	1,90E 03 7,61E-08 / 2,74E-01 2,00E 06	9,10E 02 1,59E-07 / 1,31E-01 9,60E 05	7,74E 02 1,87E-07 / 1,12E-01 8,17E 05	7,11E 02 2,03E-07 / 1,03E-01 7,50E 05
28 2,14E-05 / 4,27E-04	6,18E 03 3,26E-08 / 1,21E 00 1,43E 07	3,29E 03 6,05E-08 / 6,54E-01 7,72E 06	1,42E 03 1,40E-07 / 2,83E-01 3,34E 06	6,84E 02 2,91E-07 / 1,36E-01 1,60E 06	5,81E 02 3,42E-07 / 1,16E-01 1,36E 06	5,34E 02 3,73E-07 / 1,06E-01 1,25E 06
29 3,54E-05 / 1,82E-03	1,14E 04 1,56E-08 / 2,21E 00 6,23E 06	6,12E 03 2,89E-08 / 1,08E 00 3,36E 06	2,65E 03 6,67E-08 / 4,70E-01 1,45E 06	1,27E 03 1,39E-07 / 2,25E-01 6,98E 05	1,08E 03 1,63E-07 / 1,92E-01 5,94E 05	
30 7,28E-05 / 2,43E-03		7,65E 03 3,82E-08 / 2,23E 00 3,15E 06				
31 8,90E-05 / 2,43E-03				3,32E 03 1,87E-07 / 1,18E 00 1,36E 06	1,59E 03 2,24E-07 / 5,67E-01 6,94E 05	1,35E 03 2,63E-07 / 4,82E-01 5,56E 05
32 1,77E-04 / 4,66E-03	1,89E 04 2,03E-08 / 1,01E 01 4,85E 06	1,02E 04 5,26E-08 / 5,43E 00 2,18E 06	4,40E 03 1,21E-07 / 2,35E 00 9,49E 05	2,11E 03 2,53E-07 / 1,13E 00 4,53E 05	1,86E 03 2,97E-07 / 9,60E-01 3,86E 05	

Tables of Parameters for Commercially
Table 5.4(B) Available Powder Permalloy Toroidal
Magnetic Cores (μ=173 ~ μ=550)
102

| S Core Size No. | {V},m³ | {ℓ/μ},m²/H | {L/N²},H |
| | {A_wn},m² | {V/μ},m⁴/H | {ℓ/uA_wn},1/H |

μr header values: 173, 200, 250, 300, 350, 550

No.	{V}/{A_wn}	173	200	250	300	350	550
1	1.01E-08 / 1.82E-06	3.86E 01 3.11E-08 / 4.64E-05 2.12E 07	3.34E 01 3.59E-08 / 4.01E-05 1.83E 07	2.67E 01 4.49E-08 / 3.21E-05 1.47E 07			
2	1.99E-08 / 2.70E-06	4.33E 01 4.87E-08 / 9.14E-05 1.60E 07	3.75E 01 5.63E-08 / 7.91E-05 1.39E 07	3.00E 01 7.04E-08 / 6.33E-05 1.11E 07	2.50E 01 8.44E-08 / 5.27E-05 9.25E 06		
3	3.02E-08 / 2.93E-06	4.86E 01 5.05E-08 / 1.39E-04 1.66E 07	4.22E 01 6.76E-08 / 1.20E-04 1.44E 07	3.37E 01 8.45E-08 / 9.62E-05 1.15E 07	2.81E 01 1.01E-07 / 8.01E-05 9.60E 06	2.41E 01 1.18E-07 / 6.87E-05 8.23E 06	
4	6.40E-08 / 4.10E-06	6.26E 01 7.51E-08 / 2.94E-04 1.53E 07	5.42E 01 8.68E-08 / 2.55E-04 1.32E 07		3.61E 01 1.30E-07 / 1.70E-04 8.80E 06		1.97E 01 2.39E-07 / 9.26E-05 4.80E 06
5	6.49E-08 / 4.10E-06	6.27E 01 7.59E-08 / 2.98E-04 1.53E 07	5.42E 01 8.78E-08 / 2.58E-04 1.32E 07	4.34E 01 1.10E-07 / 2.07E-04 1.06E 07	3.62E 01 1.32E-07 / 1.72E-04 8.81E 06	3.10E 01 1.54E-07 / 1.48E-04 7.55E 06	1.97E 01 2.41E-07 / 9.39E-05 4.80E 06
6	1.10E-07 / 9.22E-06	8.22E 01 7.48E-08 / 5.06E-04 8.91E 06	7.11E 01 8.65E-08 / 4.37E-04 7.71E 06	5.69E 01 1.08E-07 / 3.50E-04 6.17E 06	4.74E 01 1.30E-07 / 2.92E-04 5.14E 06	4.06E 01 1.51E-07 / 2.50E-04 4.41E 06	2.59E 01 2.38E-07 / 1.59E-04 2.80E 06
7	1.25E-07 / 3.84E-06	6.27E 01 1.47E-07 / 5.77E-04 1.03E 07	5.42E 01 1.70E-07 / 4.99E-04 1.41E 07	4.34E 01 2.12E-07 / 3.99E-04 1.13E 07	3.62E 01 2.54E-07 / 3.33E-04 9.43E 06	3.10E 01 2.97E-07 / 2.85E-04 8.08E 06	1.97E 01 4.67E-07 / 1.81E-04 5.14E 06
8	1.64E-07 / 1.43E-05	1.00E 02 7.50E-08 / 7.54E-04 7.02E 06	8.67E 01 8.67E-08 / 6.52E-04 6.07E 06		5.78E 01 1.30E-07 / 4.35E-04 4.05E 06		3.15E 01 2.38E-07 / 2.37E-04 2.21E 06
9	2.06E-07 / 1.43E-05	1.00E 02 9.42E-08 / 9.48E-04 7.02E 06	8.67E 01 1.09E-07 / 8.20E-04 6.07E 06	6.94E 01 1.36E-07 / 6.56E-04 4.86E 06	5.78E 01 1.63E-07 / 5.46E-04 4.05E 06	4.96E 01 1.91E-07 / 4.68E-04 3.47E 06	3.15E 01 3.00E-07 / 2.98E-04 2.21E 06
10	2.38E-07 / 1.64E-05	1.09E 02 9.13E-08 / 1.09E-03 6.67E 06	9.47E 01 1.06E-07 / 9.47E-04 5.77E 06	7.58E 01 1.32E-07 / 7.58E-04 4.61E 06	6.31E 01 1.58E-07 / 6.31E-24 3.85E 06	5.41E 01 1.85E-07 / 5.41E-04 3.30E 06	3.44E 01 2.90E-07 / 3.44E-04 2.12E 06
11	2.50E-07 / 2.69E-05	1.26E 02 7.19E-08 / 1.15E-03 4.71E 06	1.09E 02 8.32E-08 / 9.96E-04 4.07E 06	8.75E 01 1.04E-07 / 7.97E-04 3.26E 06	7.29E 01 1.25E-07 / 6.64E-04 2.72E 06	6.25E 01 1.46E-07 / 5.69E-04 2.33E 06	
12	3.56E-07 / 3.83E-05	1.44E 02 7.94E-08 / 1.64E-03 3.75E 06	1.24E 02 9.18E-08 / 1.42E-03 3.24E 06	9.93E 01 1.15E-07 / 1.13E-03 2.59E 06	8.28E 01 1.38E-07 / 9.43E-04 2.16E 06	7.09E 01 1.61E-07 / 8.09E-04 1.85E 06	4.51E 01 2.53E-07 / 5.15E-04 1.18E 06
13	7.89E-07 / 7.12E-05	1.89E 02 1.02E-07 / 3.63E-03 2.65E 06	1.64E 02 1.17E-07 / 3.14E-03 2.30E 06	1.31E 02 1.47E-07 / 2.51E-03 1.84E 06	1.09E 02 1.76E-07 / 2.09E-03 1.53E 06	9.34E 01 2.05E-07 / 1.79E-03 1.31E 06	5.95E 01 3.23E-07 / 1.14E-03 8.35E 05
14	9.77E-07 / 6.38E-05	1.94E 02 1.20E-07 / 4.49E-03 3.03E 06	1.68E 02 1.38E-07 / 3.89E-03 2.62E 06	1.34E 02 1.73E-07 / 3.11E-03 2.10E 06	1.12E 02 2.08E-07 / 2.59E-03 1.75E 06	9.57E 01 2.42E-07 / 2.22E-03 1.50E 06	
15	1.15E-06 / 1.14E-04	2.34E 02 9.65E-08 / 5.29E-03 2.85E 06	2.03E 02 1.12E-07 / 4.58E-03 1.77E 06	1.62E 02 1.39E-07 / 3.66E-03 1.42E 06	1.35E 02 1.67E-07 / 3.05E-03 1.18E 06	1.16E 02 1.95E-07 / 2.62E-03 1.01E 06	7.36E 01 3.07E-07 / 1.66E-03 6.44E 05
16	1.88E-06 / 1.41E-04	2.61E 02 1.27E-07 / 8.63E-03 1.85E 06	2.26E 02 1.47E-07 / 7.47E-03 1.60E 06	1.80E 02 1.83E-07 / 5.97E-03 1.28E 06	1.50E 02 2.20E-07 / 4.98E-03 1.07E 06	1.29E 02 2.57E-07 / 4.27E-03 9.16E 05	8.20E 01 4.03E-07 / 2.72E-03 5.83E 05
17	2.34E-06 / 1.47E-04	2.74E 02 1.43E-07 / 1.08E-02 1.87E 06	2.37E 02 1.66E-07 / 9.32E-03 1.61E 06	1.90E 02 2.07E-07 / 7.46E-03 1.29E 06	1.58E 02 2.49E-07 / 6.21E-03 1.06E 06	1.36E 02 2.90E-07 / 5.33E-03 9.22E 05	
18	4.06E-06 / 4.00E-04	4.12E 02 1.18E-07 / 1.87E-02 1.03E 06	3.56E 02 1.27E-07 / 1.62E-02 8.91E 05	2.85E 02 1.59E-07 / 1.29E-02 7.13E 05	2.37E 02 1.91E-07 / 1.08E-02 5.94E 05	2.03E 02 2.23E-07 / 9.24E-03 5.09E 05	1.29E 02 3.51E-07 / 5.86E-03 3.24E 05
19	4.15E-06 / 1.56E-04	2.92E 02 2.24E-07 / 1.91E-02 1.87E 06	2.53E 02 2.59E-07 / 1.65E-02 1.62E 06	2.02E 02 3.24E-07 / 1.32E-02 1.30E 06	1.68E 02 3.88E-07 / 1.10E-02 1.08E 06	1.44E 02 4.53E-07 / 9.44E-03 9.25E 05	9.19E 01 7.12E-07 / 6.01E-03 5.89E 05
20	4.53E-06 / 2.94E-04	3.82E 02 1.43E-07 / 2.08E-02 1.30E 06	3.30E 02 1.65E-07 / 1.80E-02 1.12E 06				
21	6.46E-06 / 2.93E-04	3.75E 02 1.79E-07 / 2.52E-02 1.28E 06	3.24E 02 2.07E-07 / 2.18E-02 1.11E 06	2.59E 02 2.59E-07 / 1.74E-02 8.86E 05	2.16E 02 3.11E-07 / 1.48E-02 7.39E 05	1.85E 02 3.63E-07 / 1.25E-02 6.33E 05	1.18E 02 5.70E-07 / 7.92E-03 4.03E 05
22	5.70E-06 / 2.94E-04						
23	6.09E-06 / 3.64E-04	4.13E 02 1.64E-07 / 2.00E-02 1.13E 06	3.57E 02 1.90E-07 / 2.42E-02 9.81E 05	2.86E 02 2.37E-07 / 1.94E-02 7.84E 05	2.38E 02 2.85E-07 / 1.62E-02 6.54E 05	2.04E 02 3.32E-07 / 1.38E-02 5.60E 05	1.30E 02 5.22E-07 / 8.81E-03 3.57E 05
24	1.05E-05 / 4.27E-04	4.53E 02 2.37E-07 / 4.05E-02 1.06E 06	3.92E 02 2.74E-07 / 4.20E-02 9.17E 05	3.13E 02 3.42E-07 / 3.36E-02 7.34E 05	2.61E 02 4.11E-07 / 2.80E-02 6.11E 05	2.24E 02 4.79E-07 / 2.40E-02 9.24E 05	1.42E 02 7.53E-07 / 1.53E-02 3.33E 05
25	1.56E-05 / 6.11E-04	5.35E 02 2.50E-07 / 7.17E-02 8.75E 05	4.63E 02 2.92E-07 / 6.20E-02 7.57E 05	3.70E 02 3.62E-07 / 4.96E-02 6.06E 05	3.08E 02 4.34E-07 / 4.13E-02 5.05E 05	2.64E 02 8.07E-07 / 3.54E-02 4.33E 05	
26	1.59E-05 / 7.52E-04	5.86E 02 2.14E-07 / 7.33E-02 7.79E 05	5.07E 02 2.47E-07 / 6.34E-02 6.74E 05	4.05E 02 3.09E-07 / 5.07E-02 5.39E 05	3.38E 02 3.70E-07 / 4.22E-02 4.49E 05	2.89E 02 4.32E-07 / 3.62E-02 3.85E 05	
27	2.06E-05 / 9.48E-04	6.58E 02 2.20E-07 / 9.80E-02 6.94E 05	5.69E 02 2.54E-07 / 8.22E-02 6.00E 05	4.55E 02 3.17E-07 / 6.57E-02 4.80E 05	3.79E 02 3.81E-07 / 5.48E-02 4.00E 05	3.28E 02 4.44E-07 / 4.69E-01 3.43E 05	
28	2.14E-05 / 4.27E-04	4.94E 02 4.03E-07 / 9.03E-02 1.16E 06	4.27E 02 4.66E-07 / 8.50E-02 1.00E 06	3.42E 02 5.82E-07 / 6.80E-02 8.01E 05	2.85E 02 6.99E-07 / 5.67E-02 6.67E 05	2.44E 02 8.18E-07 / 4.86E-02 5.72E 05	
29	3.54E-05 / 1.82E-03	9.20E 02 1.92E-07 / 1.63E-01 5.94E 05	7.76E 02 2.28E-07 / 1.37E-01 4.26E 05				
30	7.28E-05 / 2.43E-03						
31	8.09E-05 / 2.43E-03	1.15E 03 3.10E-07 / 4.09E-01 4.73E 05	9.95E 02 3.58E-07 / 3.54E-01 4.09E 05				
32	1.77E-04 / 4.66E-03	1.53E 03 3.59E-07 / 8.15E-01 3.28E 05	1.32E 03 4.04E-07 / 7.65E-01 2.83E 05				

Chapter VI

CONCLUSIONS AND SUGGESTIONS FOR FUTURE RESEARCH

6.1 Conclusions

The research reported in this dissertation provides the designer
with useful analytical guidance and practically usable procedures for
designing the energy-storage reactors for a group of widely used dc-to-dc
converters. Two methodical approaches are presented which eliminate the
conventional cut-and-try design process. One of the approaches is based
on time-domain analyses of the converter circuits, and is well-suited to
computer-aided design procedures. The other approach is based on the
energy transfer equations for the reactor and it depends on a specially
constructed table of magnetic core characteristics. The design calcu-
lations of the latter method are easily made on an electronic pocket
calculator.

Chapters II and III present steady-state time-domain analyses of
the converters which lead to the relationships and procedures for designing
the energy-storage reactors for twelve controller-converter combinations.
The design relationships are presented in tabular format so that they can
be readily used to design practical energy-storage reactors for the various
converters. The design procedures have been automated in digital computer
programs to demonstrate the feasibility of computer-aided design of such
reactors. The presence of two windings on the reactor of the two-winding

converter configuration described in Chapter III provides an additional design freedom which is not available in single-winding converters. By utilizing this extra freedom, ten design options are developed to permit customized design of this configuration with respect to particular performance characteristics.

In Chapter IV, the converters are analyzed from an energy point of view. This analysis provides new insight into the energy transferring process in the converters and leads to a lower-bound condition on the volume of workable reactor cores. Applying this theory to design, use of this lower-bound condition leads to a simple and easily used screening rule for selecting candidate cores from the population of available cores. Using the lower-bound condition in another manner, a comparative evaluation of the various controller-converter combinations is presented. The results of this evaluation provide the designer with information useful in the process of selection of a controller-converter unit from among the various possible combinations.

Making use of the screening rule for workable cores and a specially constructed table of core characteristics, Chapter V presents the second approach for designing reactors for dc-to-dc converters. The most important features of this approach are the straight-forward method for identifying workable cores and the simplicity of the design procedures. With several relatively simple calculations, a workable core can be selected from the special table of core characteristics and the number of turns and the wire size can be determined. This approach does not yield as much information on the predicted performance of a converter as the time-domain approach does, but it does provide the designer with an easy method to quickly reach a workable design, and is particularly useful when the design is to be made by hand calculations or with a calculator.

Although the magnetic cores used in the examples throughout the dissertation and the special table of core characteristics provided in Chapter V are for powder permalloy cores, the design equations and procedures presented are independent of core geometry and magnetic material used and it should be possible to extend them to other geometries and materials. It is believed that the analytical guidance presented in this dissertation enables a better understanding of the converters discussed and the design procedures presented can significantly reduce the time and the effort required to design the energy-storage reactors in dc-to-dc converters.

6.2 Suggestions for Future Research

Two particular areas for future research have suggested themselves during the course of this research effort. The first area is concerned with a configuration of a type of dc-to-dc converter in which a tapped inductor, acting as an autotransformer, serves to store and transfer energy in the circuit [12,13]. The circuit operation of this type of converter is somewhat similar to that of the two-winding voltage step-up/current step-up converter configuration described in this dissertation. It is suggested that the design concepts presented here be investigated for applicability to the tapped-inductor converter configuration.

Secondly, in this dissertation, all of the design procedures require that the converter must operate in Mode 1 at least at the design operating point in the output-power/input-voltage operating range. It recently has been reported that the dynamic response of energy-storage converter is improved if the converter operates in Mode 2 [14]. It is suggested that the advantages and disadvantages of operation of a converter operating entirely in Mode 2 be investigated and that an analysis from which design

equations and design procedures for an all-Mode 2 converter operation be
attempted.

APPENDICES

APPENDIX A

LOCATING $B_{B,max}$ AND $B_{A,min}$ FOR THE
TWELVE CONTROLLER-CONVERTER COMBINATIONS

The converter output power and input voltage conditions for which $B_{B,max}$ and $B_{A,min}$ occur are evaluated for the twelve combinations of converter and controller. The nine single-winding combinations are considered in Appendix A-1, where the equation numbers corresponds to those in Chapter II. The three two-winding combinations are considered in Appendix A-2, where the equation numbers corresponds to those in Chapter III.

Appendix A-1

Voltage Step-up Converter with Constant Frequency Controller

MODE 1, (12,VU)(13,VU)

$$\frac{\partial B_B}{\partial P_0} = \frac{\mu N(V_0 + V_D - V_Q)}{\ell V_0(V_I - V_Q)} > 0 \text{ under assumption (5) in Chapter II.}$$

Therefore, B_B increases monotonically with P_0:

$$\frac{\partial B_B}{\partial V_I} = \frac{-\mu N P_0(V_0 + V_D - V_Q)}{\ell V_0(V_I - V_Q)^2}$$

$$+ \frac{T(V_0 + V_D - V_I)}{2NA(V_0 + V_D - V_Q)} - \frac{T(V_I - V_Q)}{2N A(V_0 + V_D - V_Q)} .$$

The average inductor current I_X is greater than or equal to half of the inductor current excursion $[\ell(B_B - B_A)/2\mu N]$:

$$\frac{P_0}{V_0} \cdot \frac{V_0 + V_D - V_Q}{V_I - V_Q} \geq \frac{\ell T(V_I - V_Q)(V_0 + V_D - V_I)}{2\mu N^2 A(V_0 + V^D - V_Q)}$$

or

$$\frac{\mu N P_0(V_0 + V_D - V_Q)}{\ell V_0(V_I - V_Q)} \geq \frac{T(V_I - V_Q)(V_0 + V_D - V_I)}{2N A(V_0 + V_D - V_Q)} \, .$$

Hence, the sum of the first two terms of the expression for $\partial B_B/\partial V_I$ is zero or negative. Therefore, when the third term which is negative is added, $\partial B_B/\partial V_I$ is less than zero, and $B_{B,max}$ occurs at $P_{0,max}$ and $V_{I,min}$:

$$\frac{\partial B_A}{\partial P_0} = \frac{\mu N(V_0 + V_D - V_Q)}{\ell V_0(V_I - V_Q)} > 0.$$

Therefore, B_A increases monotonically with P_0, and the minimum of B_A with respect to P_0 occurs at $P_{0,min}$.

The cubic equation in (13, VU) is obtained by setting

$$\left(\frac{\partial B_A}{\partial V_I}\right)_{P_0 = P_{0,min}} = 0.$$

At the real root (or roots) of the cubic equation, the curve of B_A versus V_I on the $P_0 = P_{0,min}$ plane has a local extremum. Since there are sign changes in the coefficients of this cubic equation, there is at least one positive real root. But, for the range of $V_I \geq V_Q$,

$$\left(\frac{\partial^2 B_A}{\partial V^2}\right)_{P_0 = P_{0,min}} = \frac{2\mu N P_{0\ min}(V_0 + V_D - V_Q)}{\ell V_0 (V_I - V_Q)^3}$$

$$+ \frac{T}{N\ A(V_0 + V_D - V_Q)} > 0.$$

The curve of B_A versus V_I on the $P_0 = P_{0,min}$ plane is thus concave upward for the range of $V_I > V_Q$. Hence, there cannot be more than one positive real root for this cubic. Thus, there exists one and only one positive real root, say V_R, for this cubic, and at this root, B_A has a local minimum because of the concavity of $B_A(V_I)_{P_0 = P_{0,min}}$. Therefore, if $V_{I,min} < V_R < V_{I,max}$, $B_{A,min}$ occurs at $V_I = V_R$. If $V_R < V_{I,min}$, $B_{A,min}$ occurs at $V_{I,min}$, since B_A must increase monotonically within the input voltage range, due to the concavity of $B_A(V_I)_{P_0 = P_{0,min}}$. If $V_R > V_{I,max}$, $B_{A,min}$ occurs at $V_{I,max}$, since B_A must decrease monotonically within the input voltage range.

MODE 2, (26,VU)

Apparently, $\frac{\partial B_B}{\partial P_0} > 0$; $\frac{\partial B_B}{\partial V_I} < 0$. Therefore, $B_{B,max}$ occurs at $P_{0,max}$ and $V_{I,min}$.

Current Step-Up Converter With Constant Frequency Controller

MODE 1, (12,CU)(13,CU)

$$\frac{\partial B_B}{\partial P_0} = \frac{\mu N}{\ell V_0} > 0$$

$$\frac{\partial B_B}{\partial V_I} = \frac{T(V_0 + V_D)^2}{2N\ A(V_I + V_D - V_Q)^2} > 0.$$

Therefore, B_B increases monotonically with both P_0 and V_I, and $B_{B,max}$ occurs at $P_{0,max}$ and $V_{I,max}$.

$$\frac{\partial B_A}{\partial P_0} = \frac{\partial B_B}{\partial P_0} > 0$$

$$\frac{\partial B_A}{\partial V_I} = -\frac{\partial B_B}{\partial V_I} < 0.$$

Therefore, B_A increases monotonically with P_0, but decreases monotonically with V_I, and $B_{A,min}$ occurs at $P_{0,min}$ and $V_{I,max}$.

MODE 2, (26,CU)

$$\frac{\partial B_B}{\partial P_0} > 0$$

From (26,CU)

$$B_B = B_R + \frac{2\mu TP_0(V_I - V_0 - V_Q)(V_0 + V_D)}{\ell AV_0(V_I + V_D - V_Q)}$$

$$= B_R + \frac{2\mu TP_0(V_0 + V_D)}{\ell AV_0}\left(1 - \frac{V_0 + V_D}{V_I + V_D - V_Q}\right)$$

Apparently, $\frac{\partial B_B}{\partial V_I} > 0$. Therefore $B_{B,max}$ occurs at $P_{0,max}$ and $V_{I,max}$.

Voltage Step-up/Current Step-up Constant Frequency Controller

MODE 1 (12,UD), (13,UD)

$$\frac{\partial B_B}{\partial P_0} = \frac{\mu N(V_I + V_0 + V_D - V_Q)}{\ell V_0(V_I - V_Q)} > 0.$$

Therefore, $B_{B,max}$ occurs at $P_{0,max}$. By argument similar to that in case (12,VU)(13,VU) for $(\partial B_B/\partial V_I)$, $B_{B,max}$ occurs at $V_{I,min}$.

$$\frac{\partial B_A}{\partial P_0} = \frac{\partial B_B}{\partial P_0} > 0$$

$$\frac{\partial B_A}{\partial V_I} = \frac{-\mu N\, P_0 (V_0 + V_D)}{\ell V_0 (V_I - V_Q)^2}$$

$$- \frac{T(V_0 + V_D)^2}{2N\, A(V_I + V_0 + V_D - V_Q)^2} < 0.$$

Thus, B_A increases monotonically with P_0, but decreases monotonically with V_I, and $B_{A,min}$ occurs at $P_{0,min}$ and $V_{I,max}$.

MODE 2, (26,UD)

$$\frac{\partial B_B}{\partial P_0} > 0; \quad \frac{\partial B_B}{\partial V_I} = 0. \quad \text{Therefore, } B_{B,max} \text{ occurs at } P_{0,max} \text{ and is independent}$$

of V_I.

Voltage Step-up Converter With Constant On-Time Controller

MODE 1, (16,VU), (17,VU)

$$\frac{\partial B_B}{\partial P_0} = \frac{\mu N(V_0 + V_D - V_Q)}{\ell V_0 (V_I - V_Q)} > 0.$$

By argument similar to that in case (12,VU) (13,VU) for $(\partial B_B / \partial V_I)$, $B_{B,max}$ occurs at $V_{I,min}$, and from the relationship above must occur at $P_{0,max}$.

$$\frac{\partial B_A}{\partial P_0} = \frac{\partial B_B}{\partial P_0} > 0$$

$$\frac{\partial B_A}{\partial V_I} = - \frac{\mu N P_0 (V_0 + V_D - V_Q)}{\ell V_0 (V_I - V_Q)^2} - \frac{t_{on}}{2NA} < 0.$$

Therefore, $B_{A,min}$ occurs at $P_{0,min}$ and $V_{I,max}$.

MODE 2, (30,VU)

$\frac{\partial B_B}{\partial P_0} = 0$; $\frac{\partial B_B}{\partial V_I} > 0$. Therefore, $B_{B,max}$ occurs at $V_{I,max}$ and is independent of P_0.

Current Step-up Converter With Constant On-Time Controller

MODE 1, (16,CU) (17,CU)

$$\frac{\partial B_B}{\partial P_0} = \frac{\partial B_A}{\partial P_0} = \frac{\mu N}{\ell V_0} > 0$$

$$\frac{\partial B_B}{\partial V_I} = \frac{t_{on}}{2NA} > 0$$

$$\frac{\partial B_A}{\partial V_I} = -\frac{t_{on}}{2NA} < 0.$$

Thus, $B_{B,max}$ occurs at $P_{0,max}$ and $V_{I,max}$; $B_{A,min}$ occurs at $P_{0,min}$ and $V_{I,max}$.

MODE 2, (30,CU)

$\frac{\partial B_B}{\partial P_0} = 0$; $\frac{\partial B_B}{\partial V_I} > 0$. Thus, $B_{B,max}$ occurs at $V_{I,max}$ and is independent of P_0.

Voltage Step-up/Current Step-up Converter With Constant On-Time Controller

MODE 1, (16,UD) (17,UD)

$$\frac{\partial B_B}{\partial P_0} = \frac{\mu N(V_I + V_0 + V_D - V_Q)}{\ell V_0(V_I - V_Q)} > 0.$$

Therefore, $B_{B,max}$ occurs at $P_{0,max}$.

$$\left(\frac{\partial B_B}{\partial V_I}\right)_{P_0 = P_{0,max}} = \frac{-\mu N P_{0,max}(V_0 + V_D)}{\ell V_0(V_I - V_Q)^2} + \frac{t_{on}}{2NA}$$

$$\left(\frac{\partial^2 B_B}{\partial V_I^2}\right)_{P_0 = P_{0,max}} = \frac{2\mu N P_{0,max}(V_0 + V_D)}{\ell V_0(V_I - V_Q)^3} > 0.$$

So, the curve of B_B versus V_I on the $P_0 = P_{0,max}$ plane is concave upward, and $B_{B,max}$ occurs at one of the extremities of the V_I range, i.e., at $V_{I,max}$ or $V_{I,min}$.

$$\frac{\partial B_A}{\partial P_0} = \frac{\partial B_B}{\partial P_0} > 0$$

$$\frac{\partial B_A}{\partial V_I} = \frac{-\mu N P_0(V_0 + V_D)}{\ell V_0(V_I - V_Q)^2} - \frac{t_{on}}{2NA} < 0$$

Therefore, $B_{A,min}$ occurs at $P_{0,min}$ and $V_{I,max}$.

MODE 2, (30,UD)

$$\frac{\partial B_B}{\partial P_0} = 0; \qquad \frac{\partial B_B}{\partial V_I} > 0.$$ Thus, $B_{B,max}$ occurs at $V_{I,max}$ and is independent of P_0.

Voltage Step-up Converter With Constant Off-Time Controller

MODE 1, (20,VU) (21,VU)

$$\frac{\partial B_B}{\partial P_0} = \frac{\mu N(V_0 + V_D - V_Q)}{\ell V_0(V_I - V_Q)} > 0$$

$$\frac{\partial B_B}{\partial V_I} = \frac{-\mu N P_0(V_0 + V_D - V_Q)}{\ell V_0(V_I - V_Q)^2} - \frac{t_{on}}{2NA} < 0.$$

B_B increases monotonically with P_0, but decreases monotonically with V_I. Therefore $B_{B,max}$ occurs at $P_{0,max}$ and $V_{I,min}$.

$$\frac{\partial B_A}{\partial P_0} = \frac{\partial B_B}{\partial P_0} > 0.$$

Therefore, $B_{A,min}$ occurs at $P_{0,min}$.

$$\left(\frac{\partial B_A}{\partial V_I}\right)_{P_0 = P_{0,min}} = \frac{-\mu N P_{0,min}(V_0 + V_D - V_Q)}{\ell V_0 (V_I - V_Q)^2} + \frac{t_{off}}{2NA}$$

$$\left(\frac{\partial^2 B_A}{\partial V_I^2}\right)_{P_0 = P_{0,min}} = \frac{2\mu N P_{0,min}(V_0 + V_D - V_Q)}{\ell V_0 (V_I - V_Q)^2}$$

$$> 0 \quad \text{for } V_I > V_Q.$$

Thus, the curve of B_A versus V_I on the $P_0 = P_{0,min}$ plane is concave upward.

The positive root V_R, found by solving the quadratic equation obtained by setting

$$\left(\frac{\partial B_A}{\partial V_I}\right)_{P_0 = P_{0,min}} = 0,$$

gives the location of the local minimum for B_A. By argument similar to that for (12,VU)(13,VU) concerning the location of $B_{A,min}$ with respect to the input voltage range, if $V_{I,min} < V_R < V_{I,max}$, $B_{A,min}$ occurs at $V_I = V_R$. If $V_R < V_{I,min}$, $B_{A,min}$ occurs at $V_{I,min}$. If $V_R > V_{I,max}$, $B_{A,min}$ occurs at $V_{I,max}$.

MODE 2, (34,VU)

From (34,VU)

$$T_R = t_{off} + \frac{\mu A N^2 P_0 (V_0 + V_D - V_I)}{\ell V_0 (V_I - V_Q)^2}$$

$$+ \sqrt{\left[t_{off} + \frac{\mu A N^2 P_0 (V_0 + V_D - V_I)}{\ell V_0 (V_I - V_Q)^2} \right]^2 - 4 t_{off}^2}$$

$$\frac{\partial T_R}{\partial P_0} > 0; \quad \frac{\partial T_R}{\partial V_I} < 0$$

$$\frac{\partial B_B}{\partial P_0} = \frac{\mu T_R (V_0 + V_D - V_I)}{2 \ell A V_0 P_0} + \frac{2 \mu P_0 (V_0 + V_D - V_I)}{\ell A V_0} \cdot \frac{1}{2} \frac{1}{T_R} \cdot \frac{\partial T_R}{\partial P_0}$$

$$> 0$$

Similarly, $\dfrac{\partial B_B}{\partial V_I} < 0$

Thus $B_{B, max}$ occurs at $P_{0,max}$ and $V_{I,min}$.

Current Step-up Converter With Constant Off-Time Controller

MODE 1, (20,CU) (21,CU)

$$\frac{\partial B_B}{\partial P_0} = \frac{\partial B_A}{\partial P_0} = \frac{\mu N}{\ell V_0} > 0$$

$$\frac{\partial B_B}{\partial V_I} = \frac{\partial B_A}{\partial V_I} = 0.$$

Therefore, $B_{B,max}$ occurs at $P_{0,max}$, and is independent of V_I, and $B_{A,min}$ occurs at $P_{0,min}$, and is independent of V_I.

Mode 2, (34,CU)

From (34,CU)

$$T_R = t_{off} + \frac{\mu AN^2 P_0(V_0+V_D)}{\ell V_0(V_I-V_0-V_Q)(V_I+V_D-V_Q)}$$
$$+ \sqrt{\left[t_{off} + \frac{\mu AN^2 P_0(V_0+V_D)}{\ell V_0(V_I-V_0-V_Q)(V_I+V_D-V_Q)}\right]^2 - t_{off}^2} \qquad [A-1-1]$$

$$\frac{\partial T_R}{\partial P_0} > 0$$

By argument similar to that for (34,VU),

$$\frac{\partial B_B}{\partial P_0} > 0.$$

The sign of $\frac{\partial B_B}{\partial V_I}$ is undetermined. Thus it can only be concluded that $B_{B,max}$ occurs at $P_{0,max}$.

Voltage Step-up/Current Step-up Converter with Constant Off-Time Controller
===

Mode 1 (20,UD), (21,UD)

$$\frac{\partial B_B}{\partial P_0} = \frac{\partial B_A}{\partial P_0} = \frac{\mu N(V_I+V_0+V_D-V_Q)}{\ell V_0(V_I-V_Q)} > 0$$

$$\frac{\partial B_B}{\partial V_I} = \frac{\partial B_A}{\partial V_I} = \frac{-\mu N P_0(V_0+V_D)}{\ell V_0(V_I-V_Q)^2} < 0$$

Thus, $B_{B,max}$ occurs at $P_{0,max}$ and $V_{I,min}$, and $B_{A,min}$ occurs at $P_{0,min}$ and $V_{I,max}$.

Mode 2

From (34,UD)

$$T_R = t_{off} + \frac{\mu AN^2 P_0(V_0+V_D)}{\ell V_0(V_I-V_Q)^2}$$
$$+ \sqrt{t_{off} + \frac{\mu AN^2 P_0(V_0+V_D)}{\ell V_0(V_I-V_Q)^2}}^2 - t_{off}^2$$

$$\frac{\partial T_R}{\partial P_0} > 0 \quad ; \quad \frac{\partial T_R}{\partial V_I} < 0$$

Thus $\dfrac{\partial B_B}{\partial P_0} > 0$ and $\dfrac{\partial B_B}{\partial V_I} < 0$

Therefore, $B_{B,max}$ occurs at $P_{0,max}$ and $V_{I,min}$.

Appendix A-2

Two-Winding Voltage Step-up/Current Step-up Converter With Constant Frequency Controller.

Mode 1, (12,FQ) (13,FQ)

$$\frac{\partial B_B}{\partial P_0} = \frac{\mu}{\ell V_0} \cdot \frac{N_P(V_0+V_D)+N_S(V_I-V_Q)}{V_I-V_Q} > 0$$

$$\frac{\partial B_B}{\partial V_I} = \frac{\mu P_0 N_P(V_0+V_D)}{\ell V_0(V_I-V_Q)^2} + \frac{(V_0+V_D)^2 T N_P}{2A[N_S(V_I-V_Q)+N_P(V_0+V_D)]^2}$$

$$= N_P(V_0+V_D)\left[\frac{-\mu P_0}{\ell V_0(V_I-V_Q)^2} + \frac{(V_0+V_D)T}{2A[N_S(V_I-V_Q)+N_P(V_0+V_D)]^2}\right]$$

For Mode 1 operation, the average flux density $[(B_B+B_A)/2]$ is greater than of equal to the sum of B_R and half of the flux density excursion $[(B_B-B_A)/2]$. Using (12,FQ),

$$\frac{\mu P_0}{\ell V_0} \frac{N_P(V_0+V_D)+N_S(V_I-V_Q)}{V_I-V_Q} \geq \frac{(V_0+V_D)(V_I-V_Q)T}{2A[N_P(V_0+V_D)+N_S(V_I-V_Q)]}$$

$$\text{or} \quad \frac{\mu P_0}{\ell V_0(V_I-V_Q)^2} \geq \frac{(V_0+V_D)T}{2A[N_S(V_I-V_Q)+N_P(V_0+V_D)]^2}$$

Hence $\dfrac{\partial B_B}{\partial V_I} < 0$

Therefore $B_{B,max}$ occurs at $P_{0,max}$ and $V_{I,min}$.

$$\frac{\partial B_A}{\partial P_0} = \frac{\partial B_B}{\partial P_0} > 0$$

$$\frac{\partial B_A}{\partial V_I} = \frac{-\mu P_0 N_P (V_0 + V_D)}{\ell V_0 (V_I - V_Q)^2} - \frac{(V_0 + V_D)^2 T N_P}{2A[N_S(V_I - V_Q) + N_P(V_0 + V_D)]^2} < 0$$

Therefore, $B_{A,min}$ occurs at $P_{0,min}$ and $V_{I,max}$.

Mode 2, (20,FQ)

$$\frac{\partial B_B}{\partial P_0} > 0 \; ; \quad \frac{\partial B_B}{\partial V_I} = 0$$

Thus, $B_{B,max}$ occurs at $P_{0,max}$ and is independent of V_I.

Two-Winding Voltage Step-up/Current Step-up Converter With Constant On-Time Controller.

Mode 1, (12,TN) (13,TN)

$$\frac{\partial B_B}{\partial P_0} > 0 \text{ apparently.}$$

Therefore, $B_{B,max}$ occurs at $P_{0,max}$

$$\frac{\partial B_B}{\partial V_I} = \frac{\mu P_0 (V_0 + V_D) N_P}{\ell V_0 (V_I - V_Q)^2} + \frac{t_{on}}{2AN_P}$$

The sign of $\dfrac{\partial B_B}{\partial V_I}$ is undetermined, but $\left(\dfrac{\partial^2 B_B}{\partial V_I^2}\right)_{P_0 = P_{0,max}} = \dfrac{2\mu P_0 (V_0 + V_D) N_P}{\ell V_0 (V_I - V_Q)^3} > 0$

So, the curve of B_B versus V_I on the $P_0 = P_{0,max}$ plane is concave upward, and

$B_{B,max}$ occurs at either $V_{I,min}$ or $V_{I,max}$.

$$\frac{\partial B_A}{\partial P_0} = \frac{\partial B_B}{\partial P_0} > 0$$

$$\frac{\partial B_A}{\partial V_I} = \frac{-\mu P_0 (V_0 + V_D) N_P}{\ell V_0 (V_I - V_Q)^2} - \frac{t_{on}}{2AN_P} < 0$$

Therefore, $B_{A,min}$ occurs at $P_{0,min}$ and $V_{I,max}$.

Mode 2, (20,FQ)

$$\frac{\partial B_B}{\partial P_0} = 0 \; ; \quad \frac{\partial B_B}{\partial V_I} > 0$$

Therefore, $B_{B,max}$ occurs at $V_{I,max}$ and is independent of P_0.

Two-Winding Voltage Step-up/Current Step-up Converter With Constant Off-Time Controller.

Mode 1 (12,TF) (13,TF)

$$\frac{\partial B_B}{\partial P_0} > 0 \; ; \quad \frac{\partial B_B}{\partial V_I} < 0$$

Thus, $B_{B,max}$ occurs at $P_{0,max}$ and $V_{I,min}$.

$$\frac{\partial B_A}{\partial P_0} > 0; \quad \frac{\partial B_A}{\partial V_I} > 0$$

Thus, $B_{A,min}$ occurs at $P_{0,min}$ and $V_{I,max}$.

Mode 2, (20,TF)

$$\frac{\partial B_B}{\partial P_0} > 0.$$

$$\frac{\partial B_B}{\partial V_I} = \frac{2\mu P_0 (V_0 + V_D)}{\ell A V_0} \cdot \frac{1}{2\sqrt{T_R}} \cdot \frac{\partial T_R}{\partial V_I}$$

From (16,TF), solving for T_R

$$T_R = t_{off} + \frac{N_P^2 \mu A P_0 (V_0 + V_D)}{\ell V_0 (V_I - V_Q)^2}$$

$$+ \sqrt{\left[t_{off} + \frac{N_P^2 \mu A P_0 (V_0 + V_D)}{\ell V_0 (V_I - V_Q)^2} \right]^2 - t_{off}^2}$$

Thus, $\frac{\partial T_R}{\partial V_I} < 0$ obviously , and consequently $\frac{\partial B_B}{\partial V_I} < 0$

Therefore, $B_{B,max}$ occurs at $P_{0,max}$ and $V_{I,min}$.

Appendix B

DERIVATIONS FOR THE EXPRESSIONS FOR THE NUMBER OF TURNS GIVEN IN TABLE 2.3

In this appendix, the single-winding constant frequency voltage step-up converter is taken as an example to illustrate the procedure for deriving the number of turns N [Eq. (14,VU) of Chapter II]. The procedure for deriving the number of turns for the remaining eight single-winding converters is similar to that of this example and will be omitted. All the equation numbers used in this appendix correspond to those used in Chapter II.

By setting $B_B = B_{max}$, and the conditions given in (12,VU), i.e., $P_0 = P_{0,max}$ and $V_I = V_{I,min}$, in (11,VU) and rearranging the resultant equation into a polynomial of variable N:

$$\frac{\mu P_{0,max}(V_0+V_D-V_Q)}{\ell V_0(V_{I,min}-V_Q)} N^2 - (B_{max}-B_R) N + \frac{T(V_{I,min}-V_Q)(V_0+V_D-V_{I,min})}{2A(V_0+V_D-V_Q)} = 0$$

Solving for N from this equation:

$$N_1,N_2 = \frac{\ell V_0(V_{I,min}-V_Q)}{2\mu P_{0,max}(V_0+V_D-V_Q)} \left[(B_{max}-B_R) \pm \sqrt{(B_{max}-B_R)^2 - \frac{2\mu TP_{0,max}}{\ell AV_0}(V_0+V_D-V_{I,min})} \right]$$

Both roots are positive if $(B_{max}-B_R)^2 > \frac{2\mu TP_{0,max}}{\ell AV_0}(V_0+V_D-V_{I,min})$. But the smaller root of the two,

$$N_2 = \frac{\ell V_0(V_{I,min}-V_Q)}{2\mu P_{0,max}(V_0+V_D-V_Q)}[(B_{max}-B_R)$$

$$-\sqrt{(B_{max}-B_R)^2 - \frac{2\mu TP_{0,max}}{\ell AV_0}(V_0+V_D-V_{I,min})}] \qquad [B-1]$$

will, to be proved later, cause the converter to operate in Mode 2 at the point $P_0 = P_{0,max}$ and $V_I = V_{I,min}$, at which the converter is restricted to operate in Mode 1. Consequently, this root should be eliminated from consideration.

To prove that the smaller root will cause the converter to operate in Mode 2 at $(P_{0,max}, V_{I,min})$, let $B_A(P_0 = P_{0,max}, V_I = V_{I,min}, N = N_0) = B_R$. Thus,

$$\frac{\mu N_0 P_{0,max}(V_0+V_D-V_Q)}{\ell V_0(V_{I,min}-V_Q)} = \frac{T(V_{I,min}-V_Q)(V_0+V_D-V_{I,min})}{2N_0 A(V_0+V_D-V_Q)}$$

i.e., $\quad N_0 = \frac{\ell V_0(V_{I,min}-V_Q)}{2\mu P_{0,max}(V_0+V_D-V_Q)}\sqrt{\frac{2\mu TP_{0,max}}{\ell AV_0}(V_0+V_D-V_{I,min})} \qquad [B-2]$

It can be seen from (11,VU) that if $N < N_0$, then $B_A(P_0=P_{0,max}, V_I=V_{I,min}, N=N) < B_R$ and, thus, the converter operates in Mode 2 at this condition. Otherwise, the converter operates in Mode 1 at the same condition. Therefore, it can be proved that N_2 will cause the converter to operate in Mode 2 at $(P_{0,max}, V_{I,min})$ if N_2 can be proved to be less than N_0. In order to prove this, several symbols are defined, which simplify the algebra.

$$a \triangleq \frac{\ell V_0(V_{I,min}-V_Q)}{2\mu P_{0,max}(V_0+V_D-V_Q)}$$

$$b \triangleq (B_{max} - B_R)$$

$$c \triangleq \frac{2\mu T P_{0,max}}{\ell A V_0}(V_0 + V_D - V_{I,min})$$

Using these symbols, $N_2 = a(b - \sqrt{b^2 - c})$

$$\text{and} \quad N_0 = a\sqrt{c}$$

Assume $N_2 < N_0$, and check if the result is contradictory or not. Thus,

$$a(b - \sqrt{b^2 - c}) < a\sqrt{c}$$

Since $a > 0$, $\qquad b - \sqrt{c} < \sqrt{b^2 - c}$

Squaring both sides, $\qquad b^2 + c - 2b\sqrt{c} < b^2 - c$

Rearranging, $\qquad \sqrt{c}(\sqrt{c} - b) < 0$

Thus, $\qquad \sqrt{c} < b$

$\sqrt{c} < b$ is true because $b^2 > c$, which is required by the fact that N_2 has to be a real number.

Therefore, the result is not contradictory, and thus $N < N_0$.

Therefore, N_2 will cause the converter to operate in Mode 2 at $(P_{0,max}, V_{I,min})$, and should be eliminated. By a procedure similar to that just described, N_1 can be proved to be greater than N_0. Thus, N_1 should be used to determine the number of turns, as is given in (14,VU).

Appendix C

DERIVATIONS FOR MODE 2 FLUX-DENSITY AND TIME RELATIONSHIPS FOR THE TWELVE CONTROLLER-CONVERTER COMBINATIONS

In this appendix, the voltage step-up converter with the three types of controller are taken as examples to illustrate the procedures for deriving Mode 2 expressions for flux density and time, which are given in Table 2.5 for single-winding converters, and in Table 3.3-A, B, and C for two-winding converters. For each controller type, the derivation procedures for the other three converter configurations are the same as that of the voltage step-up configuration, and are omitted in this appendix.

Constant Frequency Voltage Step-up Converter

(26,VU), (28,VU) and (29,VU)

From the Mode 2 waveform of the inductor current i_X of the voltage step-up converter as given in Table 2.4 and from (1,VU) and (3,VU),

$$i_B = \frac{(V_I - V_Q)t_{on}}{L} = \frac{(V_0 + V_D - V_I)t'_{off}}{L} \qquad \text{[C-1]}$$

The average output current P_0/V_0 can be expressed in terms of i_B as [C-2] below

$$\frac{P_0}{V_0} = \frac{i_B t'_{off}}{2T} \qquad \text{[C-2]}$$

(125)

Thus, $\qquad i_B = \dfrac{2P_0 T}{V_0 t'_{off}}$ [C-3]

From [C-1] and [C-3], $\qquad \dfrac{(V_0+V_D-V_I)t'_{off}}{L} = \dfrac{2P_0 T}{V_0 t'_{off}}$

Solving t'_{off}: $\qquad t'_{off} = \sqrt{\dfrac{2P_0 TL}{V_0(V_0+V_D-V_I)}}$ [C-4]

Substituting $L = \dfrac{\mu N^2 A}{\ell}$, $\qquad t'_{off} = \sqrt{\dfrac{2\mu TP_0 A}{\ell V_0(V_0+V_D-V_I)}}$ [C-5]

[C-5] is the same as (29,VU).

Substituting [C-4] into [C-1],

$$i_B = \sqrt{\dfrac{2P_0 T(V_0+V_D-V_I)}{LV_0}}$$

Thus, $B_B = B_R + \dfrac{\mu N i_B}{\ell} = B_R + \sqrt{\dfrac{2\mu TP_0(V_0+V_D-V_I)}{\ell AV_0}}$ [C-6]

[C-6] is the same as (26,VU).

From [C-5] and [C-1],

$$t_{on} = \dfrac{N(V_0+V_D-V_I)}{V_I-V_Q)} \sqrt{\dfrac{2\mu TP_0 A}{\ell V_0(V_0+V_D-V_I)}}$$ [C-7]

[C-7] is the same as (28,VU).

Constant On-Time Voltage Step-up Converter

(30,VU), (32,VU) and (33,VU)

All the equations, from [C-1] to [C-7], are true for this case except the fact that T is a specified parameter for the constant frequency case but t_{on} is a specified parameter in this case. Thus, B_B, T, and t'_{off} need to be expressed in terms of the independent variable t_{on}.

From [C-1], and the fact that $B_B = B_R + \dfrac{\mu N i_B}{\ell}$,

$$B_B = B_R + \frac{t_{on}(V_I - V_Q)}{AN} \qquad\qquad [C\text{-}8]$$

[C-8] is the same as (30,VU).

From [C-7], solving for T in terms of t_{on} leads to (32,VU).

From [C-1], solving for t'_{off} in terms of t_{on} leads to (33,VU).

Constant Off-Time Voltage Step-up Converter

(34,VU), (36,VU), (37,VU) and (38,VU)

In this case, t_{off} is a specified parameter. Thus, B_B, T, and t'_{off} need to be expressed in terms of t_{off}.

From [C-7],

$$t_{off} = T - t_{on} = T - \frac{N(V_0 + V_D - V_I)}{V_I - V_Q} \sqrt{\frac{2\mu T P_0 A}{\ell V_0 (V_0 + V_D - V_I)}}$$

Thus, $(T - t_{off})^2 = \left(\dfrac{N(V_0 + V_D - V_I)}{(V_I - V_Q)} \sqrt{\dfrac{2\mu T P_0 A}{\ell V_0 (V_0 + V_D - V_I)}} \right)^2$

i.e., $T^2 - 2\left[t_{off} + \dfrac{\mu A N^2 P_0 (V_0 + V_D - V_I)}{\ell V_0 (V_I - V_Q)^2} \right] T + t_{off}^2 = 0 \qquad [C\text{-}9]$

Solving for T:

$$T_1, T_2 = \tau \pm \sqrt{\tau^2 - t_{off}^2}$$

where $\tau \triangleq t_{off} + \dfrac{\mu A N^2 P_0 (V_0 + V_D - V_I)}{\ell V_0 (V_I - V_Q)^2}$

Since $(\tau - t_{off})^2 < \tau^2 - t_{off}^2$

Thus, $T_2 = \tau - \sqrt{\tau^2 - t_{off}^2} < t_{off}$

which is contradictory to the definition of T and t_{off}.

Therefore, the root T_2 should be eliminated. Denoting the larger root T_1 by T_R, $T = T_1 = T_R$, where T_R is the larger root of the quadratic [C-9]. Substituting $T = T_R$ in [C-6] leads to (34,VU), in [C-7] leads to (37,VU). And (38,VU) is the same as (33,VU), where the t_{on} in (38,VU) is given by (37,VU).

Appendix D

DERIVATIONS FOR RMS REACTOR CURRENTS AND THEIR MAXIMUM

The derivations for RMS reactor currents for the twelve controller-converter combinations are given in Appendix D-1, and Appendix D-2 outlines the steps for locating their maximum values.

Appendix D-1

Single-Winding Converters

Mode 1

From the waveforms for the reactor currents i_X given in Table 2.2,

$$I_{Xe}^2 \triangleq \frac{1}{T} \int_{\text{over } T} i_{Xe}^2(t)dt = \frac{1}{T} [\int_{\substack{\text{over} \\ t_{on}}} i_{Xe}^2(t)dt + \int_{\substack{\text{over} \\ t_{off}}} i_{Xe}^2(t)dt]$$

$$\text{where } \int_{\substack{\text{over} \\ t_{on}}} i_{Xe}^2(t)dt = \int_0^{t_{on}} (i_A + \frac{i_B - i_A}{t_{on}} t)^2 dt$$

$$= i_A^2 t_{on} + (\frac{i_B - i_A}{t_{on}})^2 \frac{t_{on}^3}{3} + i_A \frac{(i_B - i_A)}{t_{on}} t_{on}^2$$

$$= t_{on} [i_A^2 + \frac{(i_B - i_A)^2}{3} + i_A(i_B - i_A)]$$

$$= t_{on} [\frac{(i_B - i_A)^2}{3} + i_A i_B]$$

(129)

Similarly, $\int\limits_{\substack{\text{over} \\ t_{off}}} i_{Xe}^2(t)dt = t_{off}\left[\frac{(i_A - i_B)^2}{3} + i_B i_A\right]$

Thus, $I_{Xe}^2 = \frac{1}{T}\int\limits_{\substack{\text{over} \\ t_{on}}} i_{Xe}^2(t)dt + \int\limits_{\substack{\text{over} \\ t_{off}}} i_{Xe}^2(t)dt$

$= \frac{(i_B - i_A)^2}{3} + i_B i_A$

$= \frac{(i_B + i_A)^2 - i_B i_A}{3}$

$= \frac{\ell^2}{3\mu^2 N^2}\left[(B_B + B_A - 2B_R) - (B_B - B_R)(B_A - B_R)\right]$

Therefore, $I_{Xe} = \frac{\ell}{\mu N}\left[\frac{1}{3}\left[(B_B + B_A - 2B_R)^2 - (B_B - B_R)(B_A - B_R)\right]\right]^{1/2}$

Substituting for B_B and B_A with the appropriate expressions given in Table 2.3-A,B, and C will lead to the Mode 1 expressions for I_{Xe} as given in Table 2.6-A,B, and C.

Take constant frequency voltage step-up converter as an example, From (11,VU)

$$B_B + B_A - 2B_R = \frac{2\mu N P_0(V_0 + V_D - V_Q)}{\ell V_0(V_I - V_Q)}$$

and $$(B_B - B_R)(B_A - B_R) = \left[\frac{\mu N P_0(V_0 + V_D - V_Q)}{\ell V_0(V_I - V_Q)}\right]^2 - \left[\frac{T(V_I - V_0)(V_0 + V_D - V_I)}{2NA(V_0 + V_D - V_Q)}\right]^2$$

Thus, $$I_{Xe} = \frac{P_0(V_0 + V_D - V_Q)}{V_0(V_I - V_Q)}\sqrt{1 + \frac{1}{12}\left[\frac{\ell T V_0(V_I - V_Q)(V_0 + V_D - V_I)}{\mu N^2 A P_0(V_0 + V_D - V_Q)}\right]^2}$$

as given by (39,VU).

For the remaining eight single-winding combinations, the derivation procedures are similar and are omitted.

Mode 2

From the waveforms for the reactor current i_X given in Table 2.4,

$$I_{Xe}^2 \triangleq \frac{1}{T} \int_{\substack{\text{over} \\ T}} i_{Xe}^2(t)dt = \frac{1}{T} \left[\int_{\substack{\text{over} \\ t_{on}}} i_{Xe}^2(t)dt + \int_{\substack{\text{over} \\ t_{off}'}} i_{Xe}^2(t)dt \right]$$

where $\displaystyle \int_{\substack{\text{over} \\ t_{on}}} i_{Xe}^2(t)dt = \int_0^{t_{on}} \left(\frac{i_B t}{t_{on}}\right)^2 dt = \frac{i_B^2 t_{on}}{3}$

Similarly, $\displaystyle \int_{\substack{\text{over} \\ t_{off}}} i_{Xe}^2 dt = \frac{i_B^2 t_{off}'}{3}$

Thus, $\displaystyle I_{Xe} = i_B \left[\frac{(t_{on}+t_{off}')}{3T}\right]^{1/2} = \frac{\ell(B_B - B_R)}{\mu N}\left[\frac{t_{on}+t_{off}'}{3T}\right]^{1/2}$

Substituting B_B and $\dfrac{t_{on}+t_{off}'}{T}$ by the appropriate expressions given in Table 2.5 will lead to the Mode 2 expressions for I_{Xe} as given in Table 2.6-A,B, and C.

Two-Winding Converters

Mode 1

From the Mode 1 waveforms for the primary current i_{Pe} and the secondary current i_S given in Fig. 3.2, the mean square primary current I_{Pe}

$$I_{Pe}^2 = \frac{1}{T} \int_{\substack{\text{over} \\ t_{on}}} i_{Pe}^2(t)dt = \frac{1}{T} \int_0^{t_{on}} \left(i_{PA} + \frac{i_{PB}-i_{PA}}{t_{on}} t\right)^2 dt$$

$$= \frac{t_{on}}{3T} [(i_{PB}+i_{PA})^2 - i_{PB}i_{PA}]$$

$$= \frac{t_{on}\ell^2}{3T\mu^2 N_P^2} [(B_B+B_A-2B_R)^2-(B_B-B_R)(B_A-B_R)]$$

Thus $I_{Pe}= \frac{\ell}{\mu N_S}\left[\frac{t_{off}}{3T}[(B_B+B_A-2B_R)^2-(B_B-B_R)(B_A-B_R)]\right]^{1/2}$ \qquad [D-1-1]

Similarly, $I_{Se}= \frac{\ell}{\mu N_S} \left[\frac{t_{off}}{3T} [(B_B+B_A-2B_R)^2-(B_B-B_R)(B_A-B_R)]\right]^{1/2}$

$$= I_{Pe} \frac{N_P}{N_S} \left(\frac{t_{off}}{t_{on}}\right)^{1/2}$$

From Eq. (8) in Chapter 3, $\quad \frac{t_{on}}{t_{off}} = \frac{N_P(V_0+V_D)}{N_S(V_I-V_Q)}$

Therefore, $I_{Se}= I_{Pe}\sqrt{\frac{N_P(V_I-V_Q)}{N_S(V_0+V_D)}}$ \qquad [D-1-2]

Substituting B_B, B_A, and $\frac{t_{on}}{T}$ in [D-1-1] by the appropriate expressions given in Table 3.2-A,B, and C will lead to Mode 1 expressions for I_{Pe} in Table 3.3-A,B, and C.

Mode 2

From the Mode 2 waveforms for the primary current i_p given in Fig. 3.2,

$$I_{Pe}^2= \frac{1}{T} \int_{over\ t_{on}} i_p^2(t)dt$$

Similar to the procedure for deriving [D-1-1] and [D-1-2],

$$I_{Pe} = \frac{\ell(B_B - B_R)}{\mu N_P} \left(\frac{t_{on}}{3T}\right)^{1/2} \qquad\qquad [D-1-3]$$

and
$$I_{Se} = I_{Pe} \sqrt{\frac{N_P(V_I - V_Q)}{N_S(V_0 + V_D)}}$$

Substituting B_B and $\frac{t_{on}}{T}$ in [D-1-3] by the appropriate expressions given in Table 3.2-A,B, and C will lead to Mode 2 expressions for I_{Pe} in Table 3.3-A,B, and C.

Appendix D-2

LOCATING THE MAXIMUM RMS REACTOR CURRENTS

This appendix outlines the steps leading to the output-power/input-voltage conditions at which the rms reactor currents reach their maxima for the twelve controller-converter combinations. The maximum of I_{Xe} (or I_{Pe} and I_{Se}) is located by evaluating the partial derivatives of the expressions for I_{Xe} (or I_{Pe} and I_{Se}) with respect to P_0 and V_I. For the convenience of algebraic operation, the partial derivatives of I_{Xe}^2 with respect to P_0 and V_I are, for some cases, used to locate the maximum.

Single-Winding Converters

Voltage Step-up Converter With Constant-Frequency Controller

Mode 1 (40,VU)

From (39,VU),

$$I_{Xe}^2 = \left[\frac{P_0(V_0+V_D-V_Q)}{V_0(V_I-V_Q)}\right]^2 + \frac{1}{12}\left[\frac{\ell T(V_I-V_Q)(V_0+V_D-V_I)}{\mu N^2 A(V_0+V_D-V_Q)}\right]^2$$

$$\frac{\partial I_{Xe}^2}{\partial P_0} > 0$$

$$\frac{\partial I_{Xe}^2}{\partial V_I} \doteq \frac{2}{(V_I-V_Q)} \cdot \frac{-P_0^2(V_0+V_D-V_Q)^2}{V_0^2(V_I-V_Q)^2} + \frac{\ell^2 T^2(V_I-V_Q)^2(V_0+V_D-V_I)^2}{12\mu^2 N^4 A^2(V_0+V_D-V_Q)^2}$$

$$- \frac{\ell T^2(V_I-V_Q)^2(V_0+V_D-V_I)}{12\mu^2 A(V_0+V_D-V_Q)^2}$$

By arguments similar to that given in locating $B_{B,max}$ for this controller-converter combination given in Appendix A, for Mode 1 operation,

$$\frac{P_0(V_0+V_D-V_Q)}{V_0(V_I-V_Q)} \geq \frac{\ell T(V_I-V_Q)(V_0+V_D-V_I)}{12\mu N^2 A(V_0+V_D-V_Q)}$$

Thus, $$\frac{P_0^2(V_0+V_D-V_Q)^2}{V_0^2(V_I-V_Q)^2} \geq \frac{\ell^2 T^2(V_I-V_Q)^2(V_0+V_D-V_I)^2}{12\mu^2 N^4 A^2(V_0+V_D-V_Q)^2}$$

Therefore, $$\frac{\partial I_{Xe}^2}{\partial V_I} < 0$$

Consequently, $I_{Xe,max}$ occurs at $P_{0,max}$ and $V_{I,min}$.

Mode 2 (42,VU)

$$\frac{\partial I_{Xe}}{\partial P_0} > 0; \quad \frac{\partial I_{Xe}}{\partial V_I} < 0$$

Therefore, $I_{Xe,max}$ occurs at $P_{0,max}$ and $V_{I,min}$.

Current Step-up Converter With Constant-Frequency Controller

Mode 1 (40,CU)

From (39,CU)

$$I_{Xe}^2 = \frac{P_0^2}{V_0^2} + \frac{\ell^2 (V_I - V_0 - V_Q)^2 (V_0 + V_D)^2 T^2}{12\mu^2 N^4 A^2 (V_I + V_D - V_Q)^2}$$

$$= \frac{P_0^2}{V_0^2} + \frac{\ell^2 (V_0 + V_D)^2 T^2}{12\mu^2 N^4 A^2} \left(1 - \frac{V_0 + V_D}{V_I + V_D - V_Q}\right)^2$$

$$\frac{\partial I_{Xe}^2}{\partial P_0} > 0; \quad \frac{\partial I_{Xe}^2}{\partial V_I} > 0$$

Therefore, $I_{X,max}$ occurs at $P_{0,max}$ and $V_{I,max}$.

Mode 2 (42,CU)

$$\frac{\partial I_{Xe}}{\partial P_0} > 0 \text{ and } \frac{\partial I_{Xe}}{\partial V_I} > 0 \text{ since } \frac{V_I - V_0 - V_Q}{V_I - V_Q + V_D} = 1 - \frac{V_0 + V_D}{V_I + V_D - V_Q}$$

Therefore, $I_{Xe,max}$ occurs at $P_{0,max}$ and $V_{I,max}$.

Voltage Step-up/Current Step-up With Constant-Frequency Controller

Mode 1 (40,UD)

$$\frac{\partial I_{Xe}^2}{\partial P_0} > 0$$

$$\frac{\partial I_{Xe}^2}{\partial V_I} = \frac{V_0 + V_D}{(V_I - V_Q)^2} \quad \frac{P_0^2}{V_0^2} \left(1 + \frac{V_0 + V_D}{V_I - V_Q}\right)^2 + \frac{\ell^2 T^2 (V_0 + V_D)^2}{12\mu^2 N^4 A^2 (1 + \frac{V_0 + V_D}{V_I - V_Q})^2}$$

By arguments similar to that given in locating $I_{Xe,max}$ for Mode 1 operation,

$$\frac{\partial I_{Xe}^2}{\partial V_I} < 0$$

Therefore, $I_{Xe,max}$ occurs at $P_{0,max}$ and $V_{I,min}$.

Mode 2 (42,UD)

$$\frac{\partial I_{Xe}}{\partial P_0} > 0; \quad \frac{\partial I_{Xe}}{\partial V_I} < 0$$

Therefore, $I_{Xe,max}$ occurs at $P_{0,max}$ and $V_{I,min}$.

Voltage Step-up Converter With Constant On-Time Controller

Mode 1 (46,VU)

$$I_{Xe}^2 = \left[\frac{P_0(V_0+V_D-V_Q)}{V_0(V_I-V_Q)}\right]^2 + \frac{1}{12}\left[\frac{\ell t_{on}(V_I-V_Q)}{\mu N^2 A}\right]^2$$

$$\frac{\partial I_{Xe}^2}{\partial P_0} > 0$$

$$\frac{\partial I_{Xe}^2}{\partial V_I} = \frac{-2}{V_I-V_Q}\left[\frac{P_0^2(V_0+V_D-V_Q)^2}{V_0^2(V_I-V_Q)^2} - \frac{\ell^2 t_{on}^2(V_I-V_Q)^2}{12\mu^2 N^4 A^2}\right]$$

By arguments similar to (40,VU) in locating $I_{Xe,max}$ for Mode 1 operation,

$$\frac{P_0(V_0+V_D-V_Q)}{V_0(V_I-V_Q)} \geq \frac{\ell^2 t_{on}^2(V_I-V_Q)^2}{12\mu^2 N^4 A^2}.$$

Therefore, $\frac{\partial I_{Xe}^2}{\partial V_I} < 0$

Consequently, $I_{Xe,max}$ occurs at $P_{0,max}$ and $V_{I,min}$.

Mode 2 (48,VU)

$$\frac{\partial I_{Xe}}{\partial P_0} = 0; \quad \frac{\partial I_{Xe}}{\partial V_I} > 0$$

Therefore, $I_{Xe,max}$ occurs at $V_{I,max}$ and independent of P_0.

Current Step-up Converter With Constant On-Time Controller

Mode 1 (46,CU)

$$\frac{\partial I_{Xe}^2}{\partial P_0} > 0; \quad \frac{\partial I_{Xe}^2}{\partial V_I} > 0$$

Therefore $I_{Xe,max}$ occurs at $P_{0,max}$ and $V_{I,max}$.

Mode 2 (48,CU)

$$\frac{\partial I_{Xe}}{\partial P_0} = 0; \quad \frac{\partial I_{Xe}}{\partial V_I} > 0$$

Therefore $I_{Xe,max}$ occurs at $V_{I,max}$ and is independent of P_0.

Voltage Step-up/Current Step-up Converter With Constant On-Time Controller

Mode 1 (46,UD)

$$\frac{\partial I_{Xe}}{\partial P_0} > 0$$

$$\frac{\partial I_{Xe}^2}{\partial V_I} = \frac{-P_0^2}{V_0^2} \cdot 2 \frac{(V_I + V_0 + V_D - V_Q)}{(V_I - V_Q)} \cdot \frac{V_0 + V_D}{(V_I - V_Q)^2} + \frac{1}{6} \frac{\ell^2 t_{on}^2 (V_I - V_Q)}{\mu^2 {}_N^4 A^2}$$

The sign of $\frac{\partial I_{Xe}^2}{\partial V_I}$ can not be determined, but

$$\frac{\partial^2 I_{Xe}^2}{\partial V_I^2} > 0$$

Thus, $I_{Xe,max}$ occurs at $P_{0,max}$ and $V_I = V_{I,min}$ or $V_I = V_{I,max}$.

Mode 2 (48,UD)

$$\frac{\partial I_{Xe}}{\partial V_I} > 0; \quad \frac{\partial I_{Xe}}{\partial P_0} = 0$$

Therefore, $I_{Xe,max}$ occurs at $V_{I,max}$ and is independent of P_0.

Voltage Step-up Converter With Constant Off-Time Controller

Mode 1 (52,VU)

$$\frac{\partial I_{Xe}^2}{\partial P_0} > 0; \quad \frac{\partial I_{Xe}^2}{\partial V_I} < 0$$

Therefore, $I_{Xe,max}$ occurs at $P_{0,max}$ and $V_{I,min}$.

Mode 2 (54,VU)

From Appendix A, $\dfrac{\partial T_R}{\partial P_0} > 0$ and $\dfrac{\partial T_R}{\partial V_I} < 0$

Therefore, $\dfrac{\partial I_{Xe}}{\partial V_I} < 0$ and $\dfrac{\partial I_{Xe}}{\partial P_0} > 0$

Thus, $I_{Xe,max}$ occurs at $P_{0,max}$ and $V_{I,min}$.

Current Step-up Converter With Constant Off-Time Controller

Mode 1 (52,CU)

$$\frac{\partial I_{Xe}^2}{\partial P_0} > 0; \quad \frac{\partial I_{Xe}}{\partial V_I} = 0$$

Thus, $I_{Xe,max}$ occurs at $P_{0,max}$ and is independent of V_I.

Mode 2 (54.CU)

From (53,CU), and Eq. [A-1-1] in Appendix A-1,

$$\frac{\partial T_R}{\partial P_0} > 0 \text{ and hence } \frac{\partial I_{Xe}}{\partial P_0} > 0$$

Substituting the expression for T_R given in [A-1-1] into (53,CU), it can be seen that I_{Xe} increases with V_I. Therefore, $I_{Xe,max}$ occurs at $P_{0,max}$ and $V_{I,max}$.

Voltage Step-up/Current Step-up Converter With Constant Off-Time Controller

Mode 1 (52,UD)

$$\frac{\partial I_{Xe}^2}{\partial P_0} > 0; \quad \frac{\partial I_{Xe}^2}{\partial V_I} < 0$$

Therefore, $I_{Xe,max}$ occurs at $P_{0,max}$ and $V_{I,min}$.

Mode 2 (54,UD)

$$\frac{\partial I_{Xe}}{\partial P_0} > 0; \quad \frac{\partial I_{Xe}}{\partial V_I} < 0$$

Therefore, $I_{Xe,max}$ occurs at $P_{0,max}$ and $V_{I,min}$.

Two-Winding Converters

Two-Winding Voltage Step-up/Current Step-up Converter With Constant-Frequency Controller

Mode 1 (24,FQ), (30,FQ)

I_{Pe}:

$$\frac{\partial I_{Pe}}{\partial P_0} > 0$$

From (23,FQ),

$$I_{Pe}^2 = \underbrace{\left[\left[\frac{P_0}{V_0}\left(\frac{N_S}{N_P} + \frac{V_0+V_D}{V_I-V_Q}\right)\right]^2 + \frac{1}{12}\left[\frac{\ell(V_0+V_D)(V_I-V_Q)T}{\mu A[N_P^2(V_0+V_D)+N_PN_S(V_I-V_Q)]}\right]^2\right]}_{\triangleq f_1} \cdot \underbrace{\frac{N_P(V_0+V_D)}{N_P(V_0+V_D)+N_S(V_I-V_Q)}}_{\triangleq f_2}$$

$$\triangleq f_1 f_2$$

$$\frac{\partial f_2}{\partial V_I} < 0$$

$$\frac{\partial f_1}{\partial V_I} = 2\left[\frac{P_0}{V_0}\left(\frac{N_S}{N_P} + \frac{V_0+V_D}{V_I-V_Q}\right) + \frac{1}{12}\left[\frac{\ell(V_0+V_D)(V_I-V_Q)T}{\mu A[N_P^2(V_0+V_D)+N_PN_S(V_I-V_Q)]}\right]\right]$$

$$\cdot \underbrace{\left[\frac{-P_0(V_0+V_D)N_P}{V_0(V_I-V_Q)^2} + \frac{1}{12}\frac{\ell(V_0+V_D)T}{\mu N_PA[N_S+\frac{V_0+V_D}{V_I-V_Q}N_P]^2}\right]}_{\triangleq f_3}$$

$$f_3 = \frac{(V_0+V_D)N_P}{(V_I-V_Q)^2}\left[-\frac{P_0}{V_0} + \frac{1}{12}\cdot\frac{\ell(V_0+V_D)T}{\mu N_PA(N_S+\frac{V_0+V_D}{V_I-V_Q}N_P)^2}\right]$$

For Mode 1 operation, the average flux density $\frac{B_B+B_A}{2}$ and B_R. From (12,FQ) and (13,FQ) of Table 3.2-A,

$$\frac{\mu P_0}{\ell V_0} \left(N_S + \frac{V_0 + V_D}{V_I - V_Q} N_P \right) \geq \frac{(V_0 + V_D)(V_I - V_Q)T}{2A[N_S(V_I - V_Q) + N_P(V_0 + V_D)]} \qquad [D\text{-}2\text{-}2]$$

Therefore $\dfrac{P_0}{V_0} \geq \dfrac{\ell(V_0 + V_D)T}{2\mu N_P A \left(N_S + \dfrac{V_0 + V_D}{V_I - V_Q} N_P \right)^2}$

Thus, $f_3 < 0$ and $\dfrac{\partial f_1}{\partial V_I} < 0$

Therefore, $\dfrac{\partial I_P^2}{\partial V_I} = \dfrac{\partial(f_1 f_2)}{\partial V_I} = f_1 \dfrac{\partial f_2}{\partial V_I} + f_2 \dfrac{\partial f_1}{\partial V_I} < 0$

Thus, $I_{pe,max}$ occurs at $P_{0,max}$ and $V_{I,min}$.

I_{Se}:

From (29,FQ)

$$I_{Se}^2 = \left[\left[\frac{P_0}{V_0} \left(\frac{N_S}{N_P} + \frac{V_0 + V_D}{V_I - V_Q} \right) \right]^2 + \frac{1}{12} \left[\frac{\ell(V_0 + V_D)(V_I - V_Q)T}{\mu A[N_P^2(V_0 + V_D) + N_P N_S(V_I - V_Q)]} \right]^2 \right] \cdot \frac{N_P^2(V_I - V_Q)}{N_S^2(V_I - V_Q) + N_S N_P(V_0 + V_D)}$$

$$= N_P \left(\frac{P_0}{V_0} \right)^2 \frac{N_S(V_I - V_Q) + N_P(V_0 + V_D)}{N_S(V_I - V_Q)} + \frac{N_P \ell^2 (V_0 + V_D)^2 T^2}{12\mu^2 A^2 N_S} \left[\frac{V_I - V_Q}{N_P(V_0 + V_D) + N_S(V_I - V_Q)} \right]^3$$

$$\underbrace{\hspace{4cm}}_{\triangleq\, f_4} \qquad \underbrace{\hspace{4cm}}_{\triangleq\, f_5}$$

$$= f_4 + f_5$$

$$\frac{\partial f_4}{\partial V_I} = -\left(\frac{P_0}{V_0} \right)^2 \frac{N_P^2(V_0 + V_D)}{N_S(V_I - V_Q)^2}$$

$$\frac{\partial f_5}{\partial V_I} = \frac{\ell^2(V_0+V_D)^2 T^2}{4\mu^2 A^2 N_S} \left[\frac{(V_I-V_Q)}{N_P(V_0+V_D)+N_S(V_I-V_Q)} \right]^2 \cdot \frac{N_P^2(V_0+V_D)}{[N_P(V_0+V_D)+N_S(V_I-V_Q)]^2}$$

$$= \frac{\ell^2(V_0+V_D)^3 T^2 N_P^2(V_I-V_Q)^2}{4\mu^2 A^2 N_S [N_P(V_0+V_D)+N_S(V_I-V_Q)]^4}$$

From [D-2-2], it can be concluded that $\dfrac{\partial f_4}{\partial V_I} + \dfrac{\partial f_5}{\partial V_I} < 0$

Therefore, $\dfrac{\partial I_{Se}^2}{\partial V_I} = \dfrac{\partial f_4}{\partial V_I} + \dfrac{\partial f_5}{\partial V_I} < 0$

Thus, $I_{Se,max}$ occurs at $P_{0,max}$ and $V_{I,min}$.

Mode 2 (26,FQ), (32,FQ)

I_{pe}: It is apparent from (25,FQ) that

$I_{Pe,max}$ occurs at $P_{0,max}$ and $V_{I,min}$.

I_{Se}: It is apparent from (31,FQ) that

$I_{Se,max}$ occurs at $P_{0,max}$ and is independent of V_I.

Two-Winding Voltage Step-up/Current Step-up Converter With Constant On-Time Controller

Mode 1 (24,TN), (30,TN)

I_{pe}:
$$\frac{\partial I_{pe}}{\partial P_0} > 0$$

From (23, TN)

$$I_{Pe}^2 = \left[\left[\frac{P_0}{V_0} \left(\frac{N_S}{N_P} + \frac{V_0+V_D}{V_I-V_Q} \right) \right]^2 + \frac{1}{12} \left[\frac{\ell(V_I-V_Q)t_{on}}{\mu N^2 A} \right]^2 \right] \cdot \frac{N_P(V_0+V_D)}{N_P(V_0+V_D)+N_S(V_I-V_Q)}$$

$$\underbrace{\qquad\qquad\qquad\qquad}_{\triangleq f_1} \qquad\qquad \underbrace{\qquad\qquad\qquad}_{\triangleq f_2}$$

It can be seen that $f_1 > 0$, and $f_2 > 0$

$$\frac{\partial f_1}{\partial V_I} = 2\left[\frac{P_0}{V_0} \left(\frac{N_S}{V_0} + \frac{V_0+V_D}{V_I-V_Q} \right) + \frac{1}{12} \frac{\ell(V_I-V_Q)t_{on}}{\mu N_P^2 A} \right] \cdot \left[\frac{-P_0(V_0+V_D)}{V_0(V_I-V_Q)^2} + \frac{1}{12} \frac{\ell t_{on}}{\mu N_P^2 A} \right]$$

$$\underbrace{\qquad\qquad\qquad\qquad}_{\triangleq f_3} \qquad\qquad \underbrace{\qquad\qquad\qquad}_{\triangleq f_4}$$

It can be seen that $f_3 > 0$, f_4 may be positive or negative.

$$\frac{\partial f_2}{\partial V_I} = \frac{-N_S N_P(V_0+V_D)}{[N_P(V_0+V_D)+N_S(V_I-V_Q)]^2} < 0$$

$$\frac{\partial^2 f_1}{\partial V_I^2} = f_3 \cdot \frac{2P_0(V_0+V_D)}{V_0(V_I-V_Q)^3} + 2f_4^2 > 0, \text{ because } f_3 > 0.$$

$$\frac{\partial^2 f_2}{\partial V_I^2} = \frac{2N_S^2 N_P(V_0+V_D)}{N_P(V_0+V_D)+N_S(V_I-V_Q)]^3} > 0$$

Since $I_{Pe}^2 \triangleq f_1 \cdot f_2$

$$\frac{\partial I_{Pe}^2}{\partial V_I} = f_1 \frac{\partial f_2}{\partial V_I} + f_2 \frac{\partial f_1}{\partial V_I}$$

$$= f_1 \frac{\partial f_2}{\partial V_I} + f_2 f_3 f_4$$

$$\frac{\partial^2 I_{Pe}^2}{\partial V_I^2} = f_1 \frac{\partial^2 f_2}{\partial V_I^2} + f_2 \frac{\partial^2 f_1}{\partial V_I^2} + 2 \frac{\partial f_1}{\partial V_I} \cdot \frac{\partial f_2}{\partial V_I}$$

$$= f_1 \frac{\partial^2 f_2}{\partial V_I^2} + f_2 \frac{\partial^2 f_1}{\partial V_I^2} + 2 \frac{\partial f_2}{\partial V_I} f_3 f_4$$

From the signs of f_1, f_2, f_3, f_4, $\frac{\partial f_1}{\partial V_I}$, $\frac{\partial f_2}{\partial V_I}$, $\frac{\partial^2 f_1}{\partial V_I^2}$ and $\frac{\partial^2 f_2}{\partial V_I^2}$ as described,

it can be concluded that if $f_4 < 0$, then $\frac{\partial I_{Pe}^2}{\partial V_I} < 0$. Thus, $I_{pe,max}$ occurs

at $P_{0,max}$ and $V_{I,min}$. If $f_4 \geq 0$, then $\frac{\partial^2 I_{Pe}^2}{\partial V_I^2} > 0$. Thus, $I_{Pe,max}$ occurs at

$P_{0,max}$ and $V_I = V_{I,min}$ or $V_{I,max}$. Therefore, $I_{Pe,max}$ occurs at $P_{0,max}$ and

$V_I = V_{I,min}$ or $V_{I,max}$, regardless of the value of f_4.

I_{Se}:

(From 29,TN), $\frac{\partial I_{Se}}{\partial P_0} > 0$

$$I_{Se}^2 = \underbrace{\frac{N_P}{N_S}(\frac{P_0}{V_0})^2(\frac{N_S}{N_P} + \frac{V_0+V_D}{V_I-V_Q})}_{\triangleq f_5} + \underbrace{\frac{1}{12} \cdot \frac{\ell(V_I-V_Q)^3 t_{on}^2}{\mu A N_S} \cdot \frac{1}{N_P(V_0+V_D)+N_S(V_I-V_Q)}}_{\triangleq f_6}$$

$$\frac{\partial^2 f_5}{\partial V_I^2} > 0$$

$$\frac{\partial^2 f_6}{\partial V_I^2} = \frac{6\ell(V_I-V_Q)t_{on}^2}{\mu A N_S} \cdot \frac{1}{[N_P(V_0+V_D)+N_S(V_I-V_Q)]}$$

$$- \frac{6\ell(V_I-V_Q)^2 t_{on}^2}{\mu A[N_P(V_0+V_D)+N_S(V_I-V_Q)]^2} + \frac{\ell(V_I-V_Q)^3 t_{on}^2}{\mu A N_S} \cdot \frac{2N_S^2}{[N_P(V_0+V_D)+N_S(V_I-V_Q)]^3} > 0$$

because the sum of the first two terms is positive and the third terms

is also positive.

Therefore

$$\frac{\partial^2 I_{Se}^2}{\partial V_I^2} = \frac{\partial^2 f_5}{\partial V_I^2} + \frac{\partial^2 f_6}{\partial V_I^2} > 0.$$

Thus, $I_{Se,max}$ occurs at $P_{0,max}$ and $V_I = V_{I,min}$ or $V_{I,max}$

Mode 2   (26,TN), (32,TN)

I_{Pe}: From (25,TN), it is apparent that

$$\frac{\partial I_{Pe}}{\partial P_0} > 0; \quad \frac{\partial I_{Pe}}{\partial V_I} = 0$$

Thus, $I_{Pe,max}$ occurs at $P_{0,max}$ and is independent of V_I.

I_{Se}: From (31,TN), it is apparent that

$$\frac{\partial I_{Se}}{\partial P_0} > 0 \text{ and } \frac{\partial I_{Se}}{\partial V_I} > 0$$

Therefore, $I_{Se,max}$ occurs at $P_{0,max}$ and $V_{I,max}$.

Two-Winding Voltage Step-up/Current Step-up With Constant Off-Time Controller

Mode 1   (24,TF), (30,TF)

I_{Pe}:

From (23,TF),

$$I_{Pe}^2 = \left[\frac{P_0^2}{V_0^2} \left(\frac{N_S}{N_P} + \frac{V_0 + V_D}{V_I - V_Q} \right)^2 + \frac{\ell^2 (V_0 + V_D)^2 t_{off}^2}{12 \mu N_P^2 N_S^2 A^2} \right] \cdot \frac{N_P (V_0 + V_D)}{N_P (V_0 + V_D) + N_S (V_I - V_Q)}$$

Thus, it is apparent that $\frac{\partial I_{Pe}}{\partial P_0} > 0$ and $\frac{\partial I_{Pe}^2}{\partial V_I} < 0$

Therefore, $I_{Pe,max}$ occurs at $P_{0,max}$ and $V_{I,min}$.

I_{Se}:

From (23,TF) and (29,TF)

$$I_{Se}^2 = N_P(\frac{P_0}{V_0})^2 \cdot \underbrace{\frac{N_S(V_I-V_Q)+N_P(V_0+V_D)}{N_S(V_I-V_Q)}}_{\triangleq f_1} + \underbrace{\frac{\ell^2(V_0+V_D)^2 t_{off}^2}{12N_S\mu^2 A^2} \cdot \frac{V_I-V_Q}{N_P(V_0+V_D)+N_S(V_I-V_Q)}}_{\triangleq f_2}$$

$$\frac{\partial f_1}{\partial V_I} = -(\frac{P_0}{V_0})^2 \cdot \frac{N_P^2(V_0+V_D)}{N_S(V_I-V_Q)^2}$$

$$\frac{\partial f_3}{\partial V_I} = \frac{\ell^2(V_0+V_D)^2}{12N_S\mu^2 A^2} \cdot \frac{N_P(V_0+V_D)}{[N_P(V_0+V_D)+N_S(V_I-V_Q)^2}$$

Similar to the procedure for deriving [D-2-2], it can be concluded that

$\frac{\partial f_1}{\partial V_I} + \frac{\partial f_2}{\partial V_I} < 0$. Thus, $I_{Se,max}$ occurs at $P_{0,max}$ and $V_{I,min}$.

Mode 2 (26,TF), (32,TF)

From (16,TF), it can be proved that $\frac{\partial T_R}{\partial V_I} < 0$, and $\frac{\partial T_R}{\partial P_0} > 0$. The

procedure for this proof is similar to that given for the case of voltage

step-up converter with constant off-time controller in Appendix A. From

(25,TF) and the fact that $\frac{\partial T_R}{\partial P_0} > 0$ and $\frac{\partial T_R}{\partial V_I} < 0$, it is apparent that

$\frac{\partial I_{Pe}}{\partial P_0} > 0$ and $\frac{\partial I_{Pe}}{\partial V_I} < 0$. Thus, $I_{Pe,max}$ occurs at $P_{0,max}$ and $V_{I,min}$.

From (31,TF) and (25,TF)

$$I_{Se} = \sqrt{\frac{2P_0 N_P}{3V_0 N_S}} \sqrt{\frac{2\ell P_0(V_0+V_D)T_R}{N_P^2 \mu A V_0}}$$

Since $\dfrac{\partial T_R}{\partial P_0} > 0$ and $\dfrac{\partial T_R}{\partial V_I} < 0$ as described above, it is apparent that

$\dfrac{\partial I_{Se}}{\partial P_0} > 0$ and $\dfrac{\partial I_{Se}}{\partial V_I} < 0$. Therefore, $I_{Se,max}$ occurs at $P_{0,max}$ and $V_{I,min}$.

Appendix E

DERIVATION FOR THE OPTION CONSTRAINT EQUATIONS
GIVEN IN TABLE 3.4

This appendix outlines the steps leading to the option constraint equations given in Table 3.4. All those equation numbers, which are not prefixed by E, correspond to those used in Chapter III. Several symbols need to be reiterated: $V_1 \triangleq V_{I,min}$, $V_2 \triangleq V_{I,max}$, $P_1 \triangleq P_{0,min}$, $P_2 \triangleq P_{0,max}$, and $B_2 \triangleq B_{max}$.

[A] Duty cycle centered at a particular value U_A, Mode 1.

$$\text{From (10),} \quad \alpha_{max} = \frac{N_P(V_0+V_D)}{N_P(V_0+V_D)+N_S(V_1-V_Q)} \tag{E-1}$$

$$\text{and} \quad \alpha_{min} = \frac{N_P(V_0+V_D)}{N_P(V_0+V_D)+N_S(V_2-V_Q)} \tag{E-2}$$

Thus, $\alpha_{max} - U_A = U_A - \alpha_{min}$

i.e.
$$\frac{1}{1+\frac{N_S}{N_P}\cdot\frac{(V_1-V_Q)}{(V_0+V_D)}} + \frac{1}{1+\frac{N_S}{N_P}\cdot\frac{(V_2-V_Q)}{(V_0+V_D)}} = 2U_A$$

Rearrange into polynomial form of variables $\frac{N_S}{N_P}$,

(148)

$$\frac{(V_1-V_Q)(V_2-V_Q)}{(V_0+V_D)^2} \left(\frac{N_S}{N_P}\right)^2 + \frac{(V_1+V_2-2V_Q)}{V_0+V_D} \cdot \left(1 - \frac{1}{2U_A}\right) \cdot \frac{N_S}{N_P} + \left(1 - \frac{1}{U_A}\right) = 0$$

Solve for $\frac{N_S}{N_P}$ from this quadratic equation.

$$\frac{N_S}{N_P} = \frac{-(V_0+V_D)\left[M \pm \sqrt{M^2 - 4(V_1-V_Q)(V_2-V_Q)\left(1 - \frac{1}{U_A}\right)}\,\right]}{2(V_1-V_Q)(V_2-V_Q)}$$

where $M \triangleq (V_1+V_2-2V_Q)\left(1 - \frac{1}{2U_A}\right)$

Since $0 < U_A < 1$; thus $\left(1 - \frac{1}{U_A}\right) < 0$, and the term inside the square root sign is always positive. M may be positive or negative depending on the specification of U_A. But, the term inside the square sign sign

$$M^2 - 4(V_1-V_Q)(V_2-V_Q)\left(1 - \frac{1}{U_A}\right) > |M|$$

Thus, only one of the two roots is positive and should be used, that is

$$\frac{N_S}{N_P} = \frac{(V_0+V_D)\left[-M + \sqrt{M^2 - 4(V_1-V_Q)(V_2-V_Q)\left(1 - \frac{1}{U_A}\right)}\,\right]}{2(V_1-V_Q)(V_2-V_Q)}$$

[B]   Minimum duty cycle $\alpha_{min} = U_B$, Mode 1

From (E-2), $\alpha_{min} = \frac{N_P(V_0+V_D)}{N_P(V_0+V_D) + N_S(V_2-V_Q)} = U_B$

Thus $\frac{N_S}{N_P} = \frac{V_0+V_D}{V_2-V_Q} \left(\frac{1}{U_B} - 1\right)$

[C]   Duty cycle variation = U_C, Mode 1

From (E-1) and (E-2), $\alpha_{max} - \alpha_{min} = U_C$.

i.e. $$\frac{N_P(V_0+V_D)}{N_S(V_1-V_Q)+N_P(V_0+V_D)} - \frac{N_P(V_0+V_D)}{N_S(V_2-V_Q)+N_P(V_0+V_D)} = U_C$$

Rearrange this equation into a quadratic equation of variable $\frac{N_S}{N_P}$, and solve for $\frac{N_S}{N_P}$, similar to that in [A].

$$\frac{N_S}{N_P} = \frac{-(V_0+V_D)(Y \pm Z)}{2(V_1-V_Q)(V_2-V_Q)}$$

where $$Y \triangleq V_1 + V_2 - 2V_Q - \frac{V_2 - V_1}{U_C}$$

$$Z \triangleq \sqrt{Y^2-4(V_1-V_Q)(V_2-V_Q)}$$

The nature of the two roots are discussed in the following:

(a) $Y^2 < 4(V_1-V_Q)(V_2-V_Q)$

Z is a nonreal number, and there is no solution for $\frac{N_S}{N_P}$.

(b) $Y^2 > 4(V_1-V_Q)(V_2-V_Q)$

Since $0 < U_C < 1$,   Y may be positive or negative depending on the specified value of U_C.

(i) $Y > 0$

Both roots are negative because $Y > Z$. Therefore, no solution exists.

(ii) $Y < 0$

Both roots are positive because $|Y| > Z$.

Therefore, both roots are solutions.

[D] Maximum transistor collector-to-emitter voltage = U_D,

$V_{CE,max} = U_D$, Mode 1 or Mode 2

From Fig. 3.1, transistor collector-to-emitter voltage

$= \frac{N_P}{N_S} (V_0 + V_D) + V_I$.

Thus, $U_D = \frac{N_P}{N_S} (V_0 + V_D) + V_2$

Therefore $\frac{N_S}{N_P} = \frac{V_0 + V_D}{U_D - V_2}$

[E] Maximum diode reverse voltage $V_{DR\ max} = U_E$, Mode 1 or Mode 2

From Fig. 3.1, $U_E = V_0 + \frac{N_S}{N_P} (V_2 - V_Q)$

Thus, $\frac{N_S}{N_P} = \frac{U_E - V_0}{V_2 - V_Q}$

[F] Maximum peak transistor current $i_{coll.\ max} = U_F$, Mode 1 or Mode 2

From Fig. 3.1 $i_{coll.} = i_{PB} = \frac{\ell (B_B - B_R)}{\mu N_P}$

Thus, $i_{coll,max} = \frac{\ell (B_2 - B_R)}{\mu N_P} = U_F$

Therefore, $N_P = \frac{\ell (B_2 - B_R)}{\mu U_F}$

[G] Maximum peak diode current $i_{D,max} = U_G$, Mode 1 or Mode 2

From Fig. 3.1 $i_{D,max} = i_{SB,max} = \frac{\ell (B_2 - B_R)}{\mu U_G}$

[H] Maximum duty cycle $\alpha_{max} = U_H$, Mode 1 or Mode 2

From (10) and (18), α_{max} always occurs at $P_{0,max}$ and $V_{I,min}$ no matter whether the converter operates in Mode 1 for the entire range or in Mode 2 for a portion of the range, and since all of the design considered operates at Mode 1 at least at $P_{0,max}$ and $V_{I,min}$. Thus, Mode 1 expression for duty cycle (10) should be used.

$$\alpha_{max} = \frac{N_P(V_0+V_D)}{N_P(V_0+V_D)+N_S(V_1-V_Q)} = U_H$$

$$\text{Therefore,} \quad \frac{N_S}{N_P} = \frac{V_0+V_D}{V_1-V_Q}\left(\frac{1}{U_H} - 1\right)$$

[I] Total number of turns = U_I

[J] Turns ratio = U_J

$$\frac{N_S}{N_P} = U_J$$

Appendix F

DERIVATIONS FOR THE OPTION SOLUTIONS FOR N_P AND N_S GIVEN IN TABLE 3.5-A,B, and C

This appendix outlines the steps leading to the option solutions for N_P and N_S for the two-winding converter with the three controller types.

Constant Frequency Controller

From Eq. (35,FQ) of Chapter III,

$$N_S + \frac{V_0+V_D}{V_1-V_Q} N_P = \frac{\ell V_0}{2\mu P_2} \left[B_2 - B_R + \sqrt{(B_2-B_R)^2 - \frac{2\mu TP_2(V_0+V_D)}{\ell A V_0}} \right] \triangleq K \qquad (35,FQ)$$

Solutions for N_P and N_S for each option are obtained by solving (35,FQ) with the corresponding option constraint equation simultaneously.

Options [A], [B], [C], [D], [E], [H], and [J]

For each of these options, the turns ratio $N_S/N_P = \gamma_y$ is given by the corresponding option constrain equation given in Table 3.4, where the subscript y corresponds to the design options A,B,C,D,E,H, and J. Thus, substituting $N_S = \gamma_y N_P$ into (35,FQ) and solving for N_P, the solutions are written in general form.

$$N_P = \frac{K(V_1-V_Q)}{\gamma_y(V_1-V_Q)+V_0+V_D} \quad ; \quad N_S = \gamma_y N_P$$

Option [F]

From Table 3.4 $N_P = \dfrac{\ell(B_2-B_R)}{\mu U_F}$

From (35,FQ) $N_S = K - \dfrac{V_0+V_D}{V_1-V_Q} \cdot N_P$

Option [G]

From Table 3.4 $N_S = \dfrac{\ell(B_2-B_R)}{\mu U_G}$

From (35,FQ) $N_P = (K - N_S) \cdot \dfrac{V_1-V_Q}{V_0+V_D}$

Option [I]

From Table 3.4 $N_P + N_S = U_I$ (F-1)

From (35,FQ) $N_S + N_P \cdot \dfrac{(V_0+V_D)}{V_1-V_Q} = K$ (F-2)

Solve (F-1), (F-2) simultaneously for N_P and N_S.

$$N_P = (K - U_I) \cdot \dfrac{V_1-V_Q}{V_0+V_D-V_1+V_Q}$$

$$N_S = U_I - N_P$$

Constant On-Time Controller

For options [A], [B], [C], [D], [E], [H], and [J];

$$\dfrac{N_S}{N_P} = \gamma_y, \text{ where } y = A,B,C,D,E,H, \text{ and } J$$

Substitute $N_S = \gamma_y N_P$ into (35,TN) and arrange the resultant equation in a quadratic form of variable N_P.

$$\dfrac{\mu P_2}{\ell V_0}\left[\gamma_y + \dfrac{V_0+V_D}{V_{IO}-V_Q}\right]N_P{}^2 - (B_2-B_R)N_P + \dfrac{(V_{IO}-V_Q)t_{on}}{2A} = 0$$

Solving for N_P leads to the solution expressions for N_p given by Table 3.5-C.

Option [F]:

From option constraint equation given in Table 3.4,

$$N_P = \frac{\ell(B_2 - B_R)}{\mu U_F}$$

From (TN,35), solving for N_S in terms of N_P leads to the solution expression for N_S given in Option [F] of Table 3.5-B.

Option [G]:

From option constraint equation in Table 3.4,

$$N_S = \frac{\ell(B_2 - B_R)}{\mu U_G}$$

Arranging (35,TN) into a polynomial form of variable N_p:

$$\frac{\mu P_2}{\ell V_0} \cdot \frac{(V_0 + V_D)N_P^2}{(V_{IO} - V_Q)} - (B_2 - B_R - \frac{\mu P_2}{\ell V_0} N_S)N_P + \frac{(V_{IO} - V_Q)t_{on}}{2A} = 0$$

Solving this quadratic in terms of N_S leads to the expression for N_P given in Option [G] of Table 3.5-B.

Option [I]

From option constraint equation, $N_P + N_S = U_I$. Substituting $N_S = U_I - N_P$ into (35,TN) and arranging the resultant equation in polynomial form of variable N_P.

$$\frac{\mu P_2}{\ell V_0} \frac{(V_0 + V_D - V_{IO} + V_Q)}{V_{IO} - V_Q} N_P^2 + \frac{\mu P_2}{\ell V_0}(U_I + B_R - B_2) N_P$$

$$+ \frac{(V_{IO} - V_Q)t_{on}}{2A} = 0$$

Solving this quadratic for N_p leads to the expression for N_p given in Option [I] of Table 3.5-B.

Constant Off-Time Controller

From (35,TF) of Chapter III,

$$\frac{\mu P_2}{\ell V_0} \left[\frac{(V_0+V_D)}{V_I-V_Q} N_p N_S + N_S^2 \right] - (B_2-B_R)N_S + \frac{(V_0+V_D)t_{off}}{2A} = 0 \quad (35,TF)$$

For Options [A], [B], [C], [D], [E], [H] and [J]

For each of these options, the turns ratio $\frac{N_S}{N_p} = \gamma_y$ is given by the corresponding constraint equation given in Table 3.4. Substitute $N_S = N_p \cdot \gamma_y$ into (35,TF) and arrange the resultant equation into a polynomial form of variable N_S.

$$\frac{\mu P_2}{\ell V_0} \left[1 + \frac{V_0+V_D}{\gamma_y (V_I-V_Q)} \right] \gamma_y^2 N_p^2 - (B_2-B_R)\gamma_y N_p + \frac{(V_0+V_D)t_{off}}{2A} = 0$$

Solving for N_S from this equation leads to the solution for N_p given for these options in Table 3.5-C.

For Option [F]:

From the constraint equation for option [F] in Table 3.4,

$$N_p = \frac{\ell(B_2-B_R)}{\mu U_F}$$

Arranging (35,TF) in a polynomial form of variable N_S leads to

$$\frac{\mu P_2}{\ell V_0} N_S^2 + \left[\frac{\mu P_2}{\ell V_0} \frac{(V_0+V_D)N_p}{(V_I-V_Q)} - (B_2-B_R) \right] N_S + \frac{(V_0+V_D)t_{off}}{2A} = 0$$

Solving for N_S in terms of N_p leads to the solution for N_S for option [F] in Table 3.5-C.

For Option [G]:

From the constraint equation for option G given in Table 3.4,

$$N_S = \frac{\ell(B_2 - B_R)}{\mu U_G}$$

From (35,TF), solving for N_P in terms of N_S leads to the solution for N_P for Option [G] in Table 3.5-C.

For Option [I]

From the constraint equation, $N_P + N_S = U_I$.

Substituting $N_P = U_I - N_S$ into (35,TF) and arranging the equation into a quadratic equation of variable N_S leads to

$$\frac{\mu P_2}{\ell V_0} N_S{}^2 + \left[\frac{\mu P_2 (V_0 + V_D)}{\ell V_0 (V_I - V_Q)} N_P - B_2 + B_R \right] N_S + \frac{(V_0 + V_D) t_{off}}{2A} = 0$$

Solving for N_S in terms of N_P leads to the solution for N_S in Table 3.5-C.

Appendix G

DERIVATIONS OF EXPRESSIONS FOR ΔW_m

The expressions for ΔW_m for the various controller-converter combinations given are derived in this Appendix. By definition, ΔW_m is equal to the difference between the maximum energy and the minimum energy stored in the magnetic core during a steady-state operating cycle. The amount of energy stored in the converter core increases with time during transistor on-time, reaching its maximum at the instant when transistor is turned off; it then decreases with time until it reaches its minimum value. This value, which may be zero, is the energy stored at the instant when the transistor is turned on again. Thus, ΔW_m is equal to the total energy flowing into reactor during transistor on-time or the total energy released from the reactor during transistor off-time. In other words, for single-winding converters,

$$\Delta W_m = \int_{t_{on}} i_X v_X dt = - \int_{t_{off}} i_X v_X dt \qquad (G-1)$$

For two-winding voltage step-up/current step-up converters,

$$\Delta W_m = \int_{t_{on}} i_p v_p dt = - \int_{t_{off}} i_S v_S dt \qquad (G-2)$$

Using these two equations, the following derivation will be divided into three sections, according to converter configuration type.

(158)

(A) Single-Winding Voltage Step-Up Converter

From Eq. (G-1), $\Delta W_m = - \int_{t_{off}} i_X v_X \, dt$

During t_{off}, $v_X = -(v_0 + V_D - V_I)$, where v_0 is the total output voltage.
Since the ripple voltage is small compared to the average output voltage
V_0, $\Delta W_m \cong (V_0 + V_D - V_I) \int_{t_{off}} i_X dt$. Referring to Fig. 2.1,

$$\int_{t_{off}} i_X dt = \int_{t_{off}} i_D dt = \int_T i_D dt = \int_T (i_C + i_0) dt = \int_T i_0 dt = \frac{P_0 T}{V_0}$$

where the second equality is true because $i_D = 0$ during t_{on}, and the
fourth equality is true because the integration of capacitor current over
a complete switching cycle is zero.

Thus, $\Delta W_m = \dfrac{TP_0(V_0 + V_D - V_I)}{V_0}$ \hfill (G-3)

From Chapter II, T can be expressed in terms of controller time parameters
as follow.

Constant-frequency controller with T specified,

Mode 1 and Mode 2: T = specified value $\hat{T}$

Constant on-time controller with t_{on} specified,

Mode 1: $T = \dfrac{(V_0 + V_D - V_Q)t_{on}}{V_0 + V_D - V_I}$ \qquad [from (8,VU)] \hfill (G-4)

Mode 2: $T = \dfrac{(V_I - V_Q)^2 V_0 \ell t_{on}^2}{2(V_0 + V_D - V_I)P_0 \mu N^2 A}$ \quad [from (32,VU)]

Constant off-time controller with t_{off} specified,

$$\underline{\text{Mode 1:}} \quad T = \frac{(V_0 + V_D - V_Q)t_{off}}{V_I - V_Q} \qquad \text{[from (9,VU)]} \qquad (G-5)$$

$\underline{\text{Mode 2:}} \quad T = T_R$, where T_R is the larger root of quadratic

$$T_R^2 - 2[t_{off} + \frac{\mu A N^2 P_0 (V_0 + V_D - V_I)}{\ell V_0 (V_I - V_Q)^2}] T_R + t_{off}^2 = 0$$

$$\text{[from (36,VU)]}$$

Substituting the appropriate time relationships given above into (G-3), the corresponding expressions for ΔW_m can be obtained.

(B) Single-Winding Current Step-Up Converter

From (G-1),

$$\Delta W_m = \int_{t_{on}} i_X v_X dt = \int_{t_{on}} i_X (V_I - v_0 - V_Q) dt \simeq (V_I - V_0 - V_Q) \int_{t_{on}} i_X dt \qquad (G-6)$$

$$\Delta W_m = - \int_{t_{off}} i_X v_X dt = \int_{t_{off}} i_X (v_0 + V_D) dt \simeq (V_0 + V_D) \int_{t_{off}} i_X dt \qquad (G-7)$$

From (G-6), (G-7), and (G-1),

$$(V_I - V_0 - V_Q) \int_{t_{on}} i_X dt = (V_0 + V_D) \int_{t_{off}} i_X dt$$

$$\text{and} \quad \int_{t_{on}} i_X dt + \int_{t_{off}} i_X dt = \int_T i_X dt = \int_T (i_C + i_0) dt = \int_T i_0 dt = \frac{P_0 T}{V_0} \qquad (G-9)$$

Treating $\int_{t_{on}} i_X dt$ and $\int_{t_{off}} i_X dt$ as unknowns, and solving for the first integral using (G-8) and (G-9),

$$\int_{t_{on}} i_X dt = \frac{(V_0 + V_D) P_0 T}{(V_I + V_D - V_Q) V_0} \tag{G-10}$$

From (G-6) and (G-10), $\Delta W_m = \dfrac{T P_0 (V_I - V_0 - V_Q)(V_0 + V_D)}{(V_I + V_D - V_Q) V_0}$ (G-11)

As in the case of voltage step-up converter in (A), the expressions for ΔW_m for various cases can be obtained by substituting appropriate time relationships for T in (G-1). These time relationships, which are different from those given in (A), can be obtained from Chapter II, and thus, are not repeated here.

(C) Single- and Two-Winding Voltage Step-Up/Current Step-Up Converters

The procedures for deriving ΔW_m for these two configurations are similar to those for the voltage step-up converter given in (A), and are omitted. The time relationships between controller time parameters can be obtained from Chapter II for single-winding configurations, and from Chapter III for two-winding configuration.

APPENDIX H

JUSTIFICATION FOR USING THE MODE 2 ENERGY RELATIONSHIPS FOR CALCULATING $\Delta W_{m,max}$ IN EQUATION (5,19) FOR CONFIGURATIONS TNVU, TNUD AND TN2UD

Examination of the relationships given in Table 4.1 for $(\partial \Delta W_m/\partial P_0)$ and $(\partial \Delta W_m/\partial V_I)$ in Mode 1 and in Mode 2 for the three controller converter combinations TNVU, TNUD and TN2UD shows that, independent of mode, ΔW_m either increases with an increase of P_0 or it is independent of P_0; and, similarly, ΔW_m either increases with or is independent of V_I. It follows that, whether the converter is operating in Mode 1 or in Mode 2, the maximum numerical value for ΔW_m is obtained by using the extreme operating-range condition of $P_0 = P_{0,max}$ and $V_I = V_{I,max}$. It will be shown that, for these three exceptional controller-converter combinations, Mode 2 equations yield the larger value for ΔW_m at this extreme operating point. Consequently, Mode 2 equations evaluated at the point $(P_{0,max}, V_{I,max})$ are used for $\Delta W_{m,max}$ when evaluating the parameter δ which is the right side of inequality (5,19) and the parameter used in searching the special table of core parameters. The TNVU configuration will be taken as an example to prove this assertion. The proofs for the other two cases of TNUD and TN2UD are similar and will not be given.

The first step in showing that for the TNVU converter the larger value of $\Delta W_{m,max}$ at $(P_{0,max}, V_{I,max})$ is obtained with the Mode 2 expression

is to examine the Mode 1 expression for B_A, the minimum value of core flux density over a cycle, given by (15,VU) of Chapter II which is repeated here for convenience

$$B_A = B_R + \frac{\mu N P_0 (V_0 + V_D - V_Q)}{\ell V_0 (V_I - V_Q)} - \frac{t_{on}(V_I - V_Q)}{2NJA} \qquad [H-1]$$

where the total cross-sectional area for a stack of J cores is JA. If the converter is operating in Mode 2 at $(P_{0,max}, V_{I,max})$ then the Mode 1 value of $B_A - B_R$ given by [H-1] evaluated at $(P_{0,max}, V_{I,max})$ will be less than zero, or

$$\frac{t_{on}(V_{I,max} - V_Q)}{2NJA} > \frac{\mu N P_{0,max}(V_0 + V_D - V_Q)}{\ell V_0 (V_{I,max} - V_Q)} \qquad [H-2]$$

Multiplying both sides by $[\ell t_{on}(V_{I,max} - V_Q)/\mu N]$ and recognizing that $L = \mu N^2 JA / \ell$ gives the result

$$\frac{t_{on}^2 (V_{I,max} - V_Q)^2}{2L} > \frac{t_{on} P_{0,max}(V_0 + V_D - V_Q)}{V_0} \qquad [H-3]$$

From (3,TNVU) Table 4.1, the left side is seen to be the Mode 2 expression for ΔW_m at $(P_{0,max}, V_{I,max})$, and from (1,TNVU) of the same table the right side is seen to be the Mode 1 expression for ΔW_m at $(P_{0,max}, V_{I,max})$. Thus, it is proved that the Mode 2 expression will lead to a larger value for ΔW_m.

Continuing with the TNVU configuration to illustrate the derivations, the equation for δ given by (3,VU) is derived. Substitution of the left side of [H-3], which is the same as the expression for $\Delta W_{m,max}$ given by (16,VU) in Table 5.3 into inequality (19) gives

$$\frac{\nu}{\mu} \geq \delta = \frac{t_{on}^2 (V_{I,max} - V_Q)^2}{J(B_{max} - B_R)^2 L} \qquad [H-4]$$

where L is defined as above. Using the expression for N given by (7,VU) and the fact that $\nu = \ell A$, [H-4] can be written as

$$\frac{\nu}{\mu} \geqq \frac{\left[\dfrac{2t_{on}P_{0,max}(V_0+V_D-V_Q)(V_{I,max}-V_Q)}{V_0(B_{max}-B_R)^2(V_{I,min}-V_Q)}\right]^2}{J^2(\frac{\nu}{\mu})\,[1+\sqrt{1-\frac{\zeta}{(\nu/\mu)}}\,]^2} \qquad \text{[H-5]}$$

Multiplying both sides of [H-5] by $(\nu/\mu)[1+\sqrt{1-\zeta/(\nu/\mu)}]^2$ and taking the square root of the resultant inequality leads to the inequality

$$(\frac{\nu}{\mu})[1+\sqrt{1-\frac{\zeta}{(\nu/\mu)}}] \geqq \frac{2t_{on}P_{0,max}(V_0+V_D-V_Q)(V_{I,max}-V_Q)}{JV_0(B_{max}-B_R)^2(V_{I,min}-V_Q)} \qquad \text{[H-6]}$$

Letting $h = (V_{I,max}-V_Q)/(V_{I,min}-V_Q)$ for this case and using the expression for ζ in (3,VU), [H-6] can be rewritten as

$$(\frac{\nu}{\mu})\,[1+\sqrt{1-\frac{\zeta}{(\nu/\mu)}}\,] \geqq \zeta h$$

Solving for (ν/μ) from this inequality,

$$\frac{\nu}{\mu} \geqq \zeta\,\frac{h^2}{2h-1} = \delta, \quad \text{where } h = \frac{V_{I,max}-V_Q}{V_{I,min}-V_Q}$$

LIST OF REFERENCES

LIST OF REFERENCES

[1] T. T. Nisnizaki, R. G. Aiken, and G. J. R. St. Amand, "Computer-aided design and weight estimation of high-power high-voltage power conditioners," _IEEE Trans. Aerospace and Electronic Systems_, Vol. AES-7, pp. 1179-1194, November 1971.

[2] H. A. Owen, Jr., T. G. Wilson, S. Y. Feng, and F. C. Y. Lee, "A computer-aided design procedure for flyback step-up dc-to-dc converters," _IEEE Trans. Magnetics_, Vol. MAG-8, pp. 289-291, September 1972.

[3] D. Y. Chen, H. A. Owen, Jr. and T. G. Wilson, "Computer-aided design and graphics applied to the study of inductor-energy-storage DC-to-DC electronic power converters," _IEEE Trans. on Aerospace and Electronic Systems_, Vol. AES-9, No.4, July 1973, pp. 585-597.

[4] D. Y. Chen, H. A. Owen, Jr. and T. G. Wilson, "Design of two-winding voltage step-up/current step-up constant-frequency DC-to-DC converters," _IEEE Trans. on Magnetics_, Vol. MAG-9, No.3, September 1973, pp. 252-256.

[5] D. Y. Chen, H. A. Owen, Jr. and T. G. Wilson, "Design of energy-storage transformers for two-winding voltage step-up/current step-up converters with constant on-time and constant off-time controllers," Digest of the 1975 IEEE INTERMAG Conference, April 14-17, 1975, London, England.

[6] D. Y. Chen, H. A. Owen, Jr. and T. G. Wilson, "Energy-balance constraints affecting the design of energy-storage DC-to-DC converters," Conference record of the 1975 IEEE Applied Magnetics Workshop, June 1975, Milwaukee, Wisconsin.

[7] D. Y. Chen, H. A. Owen, Jr., and T. G. Wilson, "Table-aided design of the energy-storage reactor in DC-to-DC converters" accepted for publication in the conference proceedings of the 1975 IEEE Power Electronics Specialist Conference, June 1975, Los Angeles.

[8] O. A. Kossov, "Comparative analysis of chopper regulators with LC filter," _IEEE Trans. Magnetics_, Vol. MAG-4, pp. 712-715, December 1968.

[9] E. T. Moore and T. G. Wilson, "Basic considerations for DC-to-DC conversion networks," _IEEE Trans. on Magnetics_, Vol. MAG-2, No. 3, September 1966, pp. 620-624.

(166)

[10]   S. K. Hoo, "On some general laws of DC-DC regulators," IEEE Trans. on
       Magnetics, Vol. MAG-8, No. 3, September 1972, pp. 291-293.

[11]   D. H. Wolaver, "Basic constraints from graph theory for DC-to-DC
       conversion network," IEEE Trans. on Circuit Theory, Vol. CT-19, No.
       6, November 1972, pp. 640-648.

[12]   G.W.Wester, "Linearized stability analysis and design of a flyback
       dc-dc boost regulator" IEEE Power Electronics Specialist Conference
       Record, June 1973, pp. 130-137.

[13]   R. D. Middlebrook, "A continuous model for the tapped-inductor boost
       converter" IEEE Power Electronics Specialist Conference Record,
       June, 1975.

[14]   A. Capel, J. G. Ferrante, R. Prajoux, "Stability analysis of a PWM
       controlled DC/DC regulator with DC and AC feedback loops" IEEE
       Power Electronics Specialist Conference Record, June 1973, pp. 246-
       254.

GLOSSARY OF SYMBOLS

GLOSSARY OF SYMBOLS

A = cross-sectional area of magnetic core, m^2

A_{wn} = area of magnetic core window, m^2

A_{wr} = cross-sectional area of wire, including insulation, m^2

$A_{wr,P}$ = cross-sectional area of wire for primary winding, including insulation, m^2

$A_{wr,S}$ = cross-section area of wire for secondary winding, including insulation, m^2

B_A = minimum value of flux density during a particular cycle, T

B_B = maximum value of flux density during a particular cycle, T

$B_{A,min}$ = minimum value of B_A within operating range, T

$B_{B,max}$ = maximum value of B_B within operating range, T

B_{max} = maximum allowable core flux density, T

B_R = residual core flux density, T

B_S = saturation core flux density, T

$B_2 \triangleq B_{max}$, T

C = filter capacitor for negligible ripple voltage, F

F_W = winding factor, numeric

$F_{W,max}$ = maximum allowable winding factor, numeric

h = coefficient used in calculating ζ, numeric

i_A = minimum value of energy-storage inductor current during a particular cycle, A

(169)

i_B = maximum value of energy-storage inductor current during a particular cycle, A

i_C = total instantaneous capacitor current, A

i_P = total instantaneous primary current, A

i_S = total instantaneous secondary current, A

i_{PA} = mimimum value of the primary current during the transistor on time, A

i_{PB} = maximum value of the primary current, A

i_{SA} = minimum value of the secondary current during the transistor off time, A

i_{SB} = maximum value of the secondary current, A

i_{Pe} = primary winding rms current, A

$I_{Pe,max}$ = maximum value of I_{Pe} within operating range, A

i_{Se} = secondary winding rms current, A

$I_{Se,max}$ = maximum value of I_{Se} within operating range, A

i_X = total instantaneous inductor current, A

I_X = average value of an inductor current, A

I_{Xe} = rms inductor current, A

$I_{Xe,max}$ = maximum value of I_{Xe} within the operating range, A

J = number of cores in stack, numeric

ℓ = mean magnetic path length, m

L = inductance of inductor, H

L_P = inductance of primary winding, H

L_S = inductance of secondary winding, H

P_0 = converter average output power, W

$P_{0,min}$ = minimum value of average output power, W

$P_{0,max}$ = maximum value of average output power, W

$P_1 \triangleq P_{0,min}$, W

$P_2 \triangleq P_{0,max}$, W

R_L = equivalent resistance load, Ω

S = core size number, numeric

t_{off} = transistor cut-off interval, s

t'_{off} = diode conduction interval, s

t''_{off} = interval when $B = B_R$ or $T - t_{on} - t'_{off}$, s

t_{on} = transistor conduction interval, s

T = period of one conversion cycle, s

U_y = option constraint quantity, y = A, B, C, D, E, H, or J; units depend on option

$V = \ell A$ = volume of magnetic core, m^3

$V_{total} = JV$ = total volume of core stack, m^3

V_D = diode forward voltage drop, V

V_I = converter DC input voltage, V

$V_{I,max}$ = maximum converter input voltage, V

$V_{I,min}$ = minimum converter input voltage, V

$V_1 \triangleq V_{I,min}$, V

$V_2 \triangleq V_{I,max}$, V

$V_{IO} = V_{I,min}$ or $V_{I,max}$, V

V_0 = converter output voltage, V

V_Q = transistor saturation voltage drop, V

v_X = total instantaneous voltage across inductor, V

ΔW_m = amount of energy transferred by the energy-storage reactor over a switching cycle, J

$\Delta W_{m,max}$ = maximum amount of energy transferred by core over a switching cycle, J

α_{max} = maximum transistor duty cycle, numeric

α_{min} = minimum transistor duty cycle, numeric

γ = N_S/N_p = turns ratio, numeric

γ_y = turns ratio N_S/N_p for option y wher y = A,B,C,D,E,H, or J, numeric

δ = computed quantity for use in core table search, m^4/H

ζ = computed quantity used in calculating δ, N and N_p, m^4/H

η = computed quantity used in identification of windable cores, $1/H$

μ = $\mu_r\mu_0$ = permeability of magnetic material, H/m

μ_0 = permeability of free space, H/m

μ_r = relative permeability, numeric

$\{\cdot\}$ = identifier of numerical value for core parameter obtained from Table 5.4.

BIOGRAPHY

BIOGRAPHY

Name: De Yu Chen

Date of Birth: ███████████████

Place of Birth: ███████████

Universities Attended:	Dates:	Degrees:	Dates of Degrees:
National Chiao-Tung University	1965-1969	BSEE	June 1969
Duke University	1970-1971	MSEE	May 1971
Duke University	1971-present		

Major: Electrical Engineering

Minor: Mathematics and Physics

Publications:

1. _____,with Harry A. Owen, Jr. and Thomas G. Wilson, "Computer-Aided Design and Graphics Applied to the Study of Inductor-Energy-Storage dc-to-dc Electronic Power Converters" IEEE Power Processing and Electronics Specialists Conference Record IEEE publication 72 CHO 652-8 AES, (May 1972). Also IEEE Transactions on Aerospace and Electronic Systems, Vol. AES-9, No. 4 (July 1973).

2. _____,with Harry A. Owen, Jr. and Thomas G. Wilson, "Design of Two-Winding Voltage Step-Up/Current Step-Up Constant Frequency DC-to-DC Converters". Abstract in 1973 Digest of the INTERMAG Conference, P. 10.1 (April 1973). Text in IEEE Transactions on Magnetics, Vol. MAG-9, No. 3 (September 1973).

3. _____,with Harry A. Owen, Jr., and Thomas G. Wilson, "Design of Energy-Storage Transformers for Two-Winding Voltage-Step-Up/Current-Step-Up Converters with Constant On-Time and Constant Off-Time Controllers" presented in the 1975 IEEE INTERMAG Conference, London, England, April 14-17.

(174)

4. _____,with Harry A. Owen, Jr., and Thomas G. Wilson, "Energy-Balance Constraints Affecting the Design of Energy-Storage DC-to-DC Converters" IEEE Proceedings of APPLIED MAGNETIC WORKSHOP, June 1975.

5. _____,with Harry A. Owen, Jr., and Thomas G. Wilson, "Table-Aided Design of the Energy-Storage Reactors in DC-to-DC Converters" presented in the 1975 IEEE POWER ELECTRONICS SPECIALISTS Conference, Los Angeles, California, June 9-11.

Honor Received:

1974 Barry Carlton Honornable Mention Award (presented by IEEE Aerospace and Electronics System Group for the paper "Computer-Aided Design and Graphics Applied to the Study of Inductor-Energy-Storage dc-to-dc Electronic Power Converters" by De Yu Chen, Harry A. Owen, Jr., and Thomas G. Wilson, published in the IEEE Transactions on Aerospace and Electronic Systems, July, 1973).

Positions held:

1. Part-time Teaching Assistant in the Deparyment of Electrical Engineering, Duke University, September 1971-May 1972.

2. Research Assistant in the Spacecraft Systems Research Lab.,Duke Univ., part-time from June 1972 to September 1973, full-time from October 1973 until present.